SYNTHESIS, STRUCTURE, AND REACTIVITY STUDIES OF KETENYLIDENE, CARBIDE, CARBYNOID, CARBENOID, AND TETRAZOLYL COMPLEXES OF GOLD

A Dissertation
Presented to
The Academic Faculty

by

Nicholas T. Daugherty

In Partial Fulfillment
of the Requirements for the Degree
Doctor of Philosophy in the
School of Chemistry and Biochemistry

Georgia Institute of Technology
August 2018

SYNTHESIS, STRUCTURE, AND REACTIVITY STUDIES OF KETENYLIDENE, CARBIDE, CARBYNOID, CARBENOID, AND TETRAZOLYL COMPLEXES OF GOLD

Approved by:

Dr. Joseph P. Sadighi, Advisor
School of Chemistry and Biochemistry
Georgia Institute of Technology

Dr. Z. John Zhang
School of Chemistry and Biochemistry
Georgia Institute of Technology

Dr. Angus P. Wilkinson
School of Chemistry and Biochemistry
Georgia Institute of Technology

Dr. Carsten Sievers
School of Chemical and Biomolecular Engineering
Georgia Institute of Technology

Dr. Jake D. Soper
School of Chemistry and Biochemistry
Georgia Institute of Technology

Dr. Christopher W. Jones
School of Chemical and Biomolecular Engineering
Georgia Institute of Technology

Date Approved: May 2, 2018

To my wife,

Veronica Daugherty

ACKOWLEDGEMENTS

I thank my research advisor, Professor Joseph Sadighi, for the opportunity to work and learn in his research group. Joseph has taught me a great deal about developing strategies for making and breaking bonds, and he has set an example of honest, responsible, dedicated leadership. Joseph is truly interested in the success of his students, not only in terms of the science, but also at a personal level. I also want to thank Joseph for the occasional cup of coffee and unexpected group-meeting reference to Monty Python. It has truly been a pleasure to work for him.

I thank the members of my thesis committee, Professor Angus Wilkinson, Professor John Zhang, Professor Jake Soper, Professor Carsten Sievers, and Professor Christopher Jones for their mentorship over the years.

I thank Dr. Leslie Gelbaum for his guidance in the NMR lab. I thank Dr. John Bacsa for giving me the opportunity to serve as his assistant in the X-ray diffraction lab for a semester, and for his collaborative efforts. I thank Mr. David Bostwick for his help collecting mass spectral data.

A number of Professors played an important role in my preparation for graduate school. Among them, I thank Professor John Lynch who gave me the opportunity to do undergraduate research in his lab, and offered me much encouragement. I thank Professor Jisook Kim, who recruited me for my first undergraduate teaching experience. I also thank Professor Tom Rybolt, who took the time on several occasions to discuss career paths with me.

There is a great sense of camaraderie between the members of the Sadighi group, and I have been very fortunate to take part in it. I would like to thank all of my fellow group members for their friendship, positivity, and humor. I would like to thank Kevin Omolo for our many stimulating conversations, and for his good advice. I would like to thank Yu Cao

for her cheerfulness and for the occasional reminder to “be positive”. I would like to thank Abe Jordan for his willingness to lend a hand to a friend. And, I would also like to thank Brandon Tate and Chelsea Wyss for their support in getting started in the lab.

I thank my mother, Kim Daugherty, for her love and support and for instilling me with a sense of determination. She is my first teacher, and she worked hard to provide me with plenty of opportunity. She encouraged my curiosity, and ensured that I received a well-rounded education growing up. I can always hear her say, “you can do it.” She is the first in the family to earn a college degree, and did so while working and raising four hard-working, successful children. Her example is always with me.

I thank my grandfather, Tom Daugherty, for teaching me patience, and for teaching me to connect the work of the mind with the work of the hands. We completed a lot of projects together when I was a boy, and these life experiences have been indispensable to me as an experimentalist. I will always remember the sense of accomplishment that he made me feel after we finished solving some problem together.

I thank my grandmother, Barbara Broyles, for her encouragement, and for reminding me that hard work pays off.

I thank my brothers Hunter and Chase Daugherty for always being a phone call away when I need a hand. On a number of occasions, they have driven down to Atlanta to help me move something or pick up a piece of furniture. I can always count on my brothers.

I thank my sister, Mary-Hannah Daugherty, for her encouragement and for always thinking of my family, whether by sending a care package of books to the kids or by making a simple phone call to find out how things are going.

I thank my father-in-law and mother-in-law, Jude and Ivonne Weidner, who have been very supportive and have taught me a great deal about positive thinking, and who recently spent several days helping us move out of a flooded apartment.

I thank my sister-in-law, Maria Weidner, who spent a week with us after my son was born caring for the family. She allowed me to transition back into the lab with ease after some time away, knowing that Veronica, Olivia, and Matthew were in good hands.

I thank my children, Olivia and Matthew Daugherty, for the great joy that I receive from them every day. They are truly a blessing, and watching them grow and learn is a rewarding and uplifting experience.

Finally, I thank my wife, Veronica Daugherty. She has been with me every step of the way through graduate school. The love and friendship that I receive from her are great comforts to me. She waits for me when I have late nights in the lab. She encourages me when experiments have not gone according to plan. When difficult decisions are to be made, I know that I can rely on her support. Her graceful and selfless dedication to our family is unfaltering, and she has worked very hard to allow me to focus much of my attention on earning a PhD.

TABLE OF CONTENTS

LIST OF TABLES

LIST OF FIGURES

produce {[(IDipp)Au]$_2$C($SiMe_3$)(MeCN)}OTf (**4**). Impurities: unlabeled overlapping peaks are attributed to several impurities including {[(IDipp)Au]$_2$CN}OTf and {[(IDipp)Au]$_2$H}OTf. The labelled resonance at δ -0.13 ppm may be attributable to Si(C*H*$_3$)$_3$ in {[(IDipp)Au]$_2$(C_2N_3)($SiMe_3$)(CD_3)}OTf. All other labelled resonances are assigned to **4**.

LIST OF SCHEMES

LIST OF SYMBOLS AND ABBREVIATIONS

β	beta
°	degrees
δ	delta
η	eta
μ	mu
ν	nu
°C	degrees Celsius
[M^+]	molecular ion
^{11}B	boron-11
^{13}C	carbon-13
^{19}F	fluoroine-19
^{1}H	proton
^{31}P	phosphorous-31
Å	Angstroms
ATR	attenuated total reflectance
ca.	circa
CCD	charge coupled device
CCSD	Cambridge Crystallographic Structural Database
cm	centimeters
d	deuterated
d	doublet
DCM	dichloromethane
ESI	electrospray ionization

g	gram
GC-MS	gas chromatography – mass spectrometry
h	hours
HOAc	acetic acid
HSPh	thiophenol
IDipp	1,3-bis(diisopropylphenyl)imidazol-2-ylidene
IMes	1,3-bis(2,4,6-trimethylphenyl)idazol-2-ylidene
IR	infrared spectroscopy
kV	kilovolts
L	ligand
M	metal
M	molar
m	multiplet
m/z	mass to charge ratio
mA	milliamperes
Me	methyl
mg	milligram
MHz	megahertz
mL	milliliter
mmol	millimole
MS	mass spectrometry
NHC	N-heterocyclic carbene
NMR	nuclear magnetic resonance
OAc^-	acetate
OAc_2	acetic anhydride
OTf	trifluoromethanesulfonate

Ph	phenyl
ppm	parts per million
S	seconds
s	singlet
SIMes	1,3-bis(2,4,6-trimethylphenyl)imidazolidin-2-ylidene
T	temperature
t	triplet
tBu	tert-butyl
THF	tetrahydrofuran
wt%	weight percent
XRD	X-ray diffraction

SUMMARY

Chapter 1 contains a brief description of aurophilic interactions and their role in the formation of high order gold clusters. The isolobal analogy is applied to trigold(I) clusters. In particular, an analogy is drawn between the sigma- and pi-bonding interactions in $[Au_3C]^+$, $[AuCR_2]^+$, CR_3^+ (R = Aryl), and CO_3^{2-}. This analogy leads into a discussion of the recent gold(I) carbenoid literature, and the rationale for the pursuit of an NHC-supported trigold(I) carbido cation. Finally, bond metrics corresponding to observed close Au-Au contacts reported in the literature are compared with their corresponding calculated and measured interaction energies. From this analysis, the energetic contribution of the Au-Au interactions observed for the compounds described herein are estimated.

Chapter 2 describes the synthesis, structure, and reactivity studies of a SIMes-supported trigold(I) cluster. This species was initially prepared as a potential precursor to a trigold(I) carbido cation; however, the stronger than expected Au_3C-CO bond, exemplified by a short crystallographic C-CO bond distance, and suggestive of net double bond character, precludes such reactivity. The CCO moiety exhibited neither appreciable nucleophilic, nor electrophilic behavior. However, the lability of the three Au_3-CCO bonds was exploited for ketene transfer reactivity.

Chapter 3 describes the exploration of other routes to an NHC-supported trigold(I) carbido cation by reaction of gold(I) diazoalkanes with suitable gold(I) precursors. Solvent adducts of digold(I) silylmethylidyne cations, a digold(I) methylidyne cation, and a trigold(I) carbido cation were prepared. A gold(I) methoxymethyl carbenoid complex was also prepared. Diffraction studies reveal weak aurophilic interactions between the Au centers in these species. The trigold(I) carbido cation exhibited electrophilic behavior at the bridging carbon, reacting with CO to give the trigold(I) ketenylidene cation. Reaction with stronger nucleophiles resulted in deauration.

Chapter 4 describes the synthesis of an isomeric mixture of 1-auro(tetrazolate) and 2-auro(tetrazolate). Addition of a gold triflate to the isomeric mixture resulted in a fluxional diauro(tetrazolate) cation. Attempts to deprotonate the tetrazole derived CH proton of this species led to deauration, regenerating the monoauro(tetrazolate). I envisioned circumventing this problem by carrying out 1,3-dipolar cycloaddition between a terminal gold azide with a terminal gold cyanide to form a 1,5-diauoro(tetrazolate). Little evidence of reactivity was observed between (IDipp)AuN_3 and (IDipp)AuCN when they were combined in THF or DCM, even with heating. In CD_3CN solution at 60°C, however, (IDipp)AuN_3 underwent cycloaddition with the nitrile solvent to give the (IDipp)Au(CD_3CN_4).

CHAPTER 1

INTRODUCTION

1.1 Aurophilic Interactions in the Formation of High Order Gold Clusters

Organophosphine-supported gold clusters bridged by main group elements are stabilized by an attractive interaction between closed-shell metal centers termed aurophilicity, or more generally metallophilicity.[1-4] These clusters have the general formula $[(LAu)_nX^m]^{(n+m)}$, where X is a single bridging atom or a bridging moiety and L is the ancillary organophosphine ligand. The effects of aurophilic interactions manifest in these clusters as close Au-Au contacts even for those having classical coordination numbers at the bridging ligand, but are particularly apparent in the hypercoordinate clusters of interstitial main group elements. Such elements include, but are not limited to, the smaller main group elements B, C, N, and O, as well as larger main group elements including P, S, and Se. Selected examples of these species are represented in Scheme 1.1.

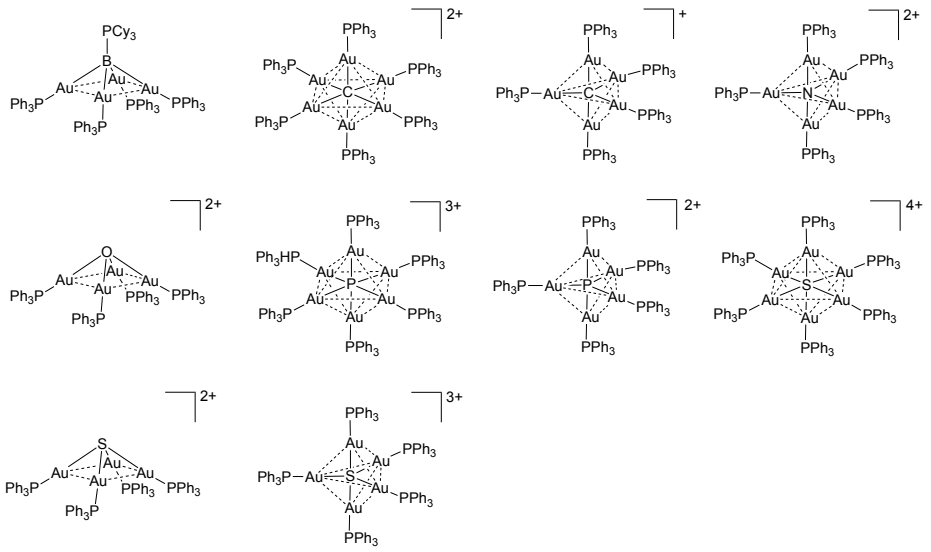

Scheme 1.1. Selected hypercoordinate gold(I) clusters bridged by main group elements. $\{[(Ph_3P)Au]_4B(PCy_3)\}^+$,[5] $\{[(Ph_3P)Au]_6C\}^{2+}$,[6] $\{[(Ph_3P)Au]_5C\}^+$,[7] $\{[(Ph_3P)Au]_4N\}^+$, $\{[(Ph_3P)Au]_5N\}^{2+}$,[8-9] $\{[(Ph_3P)Au]_4O\}^{2+}$,[10] $\{[(Ph_3P)Au]_3O\}^+$,[11] $\{[(Ph_3P)Au]_6P\}^{3+}$,[12] $\{[(Ph_3P)Au]_5P\}^{2+}$,[13] $\{[(Ph_3P)Au]_3P(o\text{-Tol})\}^+$,[13] $\{[(Ph_3P)Au]_6S\}^{4+}$, $\{[(Ph_3P)Au]_5S\}^{3+}$, $\{[(Ph_3P)Au]_4S\}^{2+}$,[14-15] $\{[(Ph_3P)Au]_4Se\}^{2+}$, $\{[(Ph_3P)Au]_3Se\}^+$.[16]

In fact, hypercoordination of main group elements by LAu^+ often occurs despite reaction conditions that could be readily expected to result in lower-nuclearity species. For example, even under stoichiometric conditions, the phosphine-supported tetragold(I) methane $[(o\text{-Tol}_3P)Au]_4C$ was isolated only after employing sterically bulky tri(*ortho*-tolyl)phosphines to suppress the tendency of LAu^+ to aggregate and form the penta- or hexa-aurated species.[17] Similarly, when $\{[(Ph_3P)Au]_3O\}^+$[11] reacts with a large excess of ammonia, the resulting product is not a mixture of mono-, di-, or even triaurated species. Instead, the tetraurated ammonium cation is isolated in 72% yield $\{[(Ph_3P)Au]_4N\}^+$.[9] Likewise, when $(Ph_3P)AuCl$ reacts with an excess of Ag_2O, not the di- but the triaurated oxonium $\{[(Ph_3P)Au]_3O\}^+$ is formed in 90% yield[11] (Scheme 1.2).

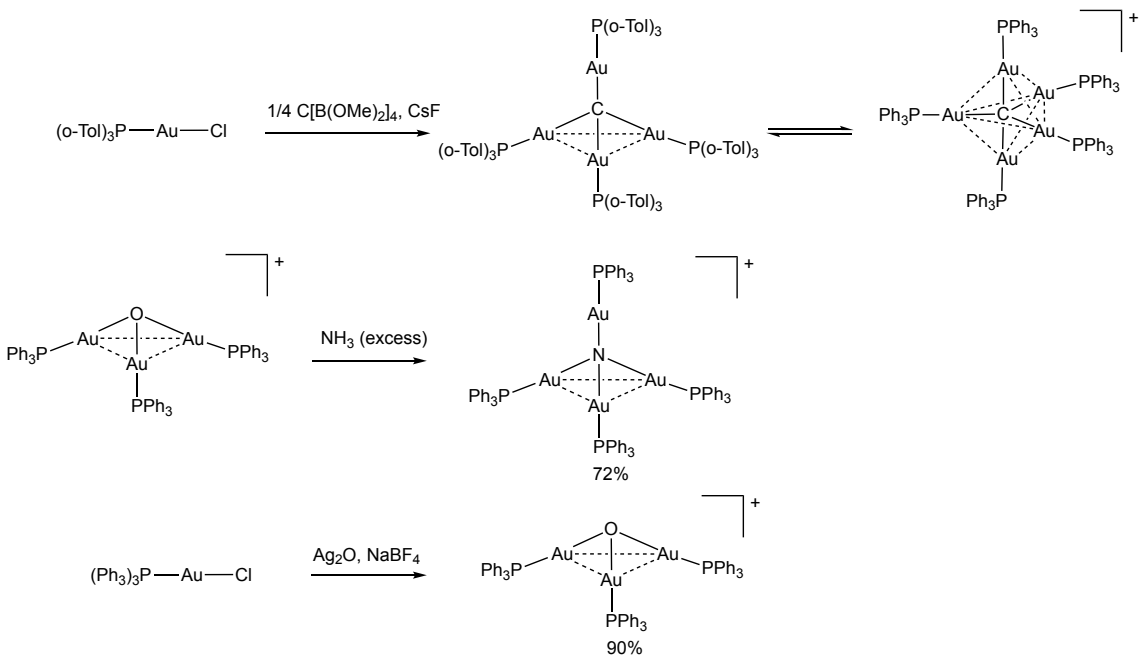

Scheme 1.2. Cluster syntheses leading to higher than expected auration.[9,11,17]

1.2 Description of Aurophilic Interactions

Aurophilic interactions are counterintuitive if one expects coulombic repulsion between neighboring LAu^+ fragments to overwhelm attractive van der Waals forces. The situation becomes clearer when electron-correlation and relativistic effects are considered, but the precise origin of aurophilic interactions are not fully understood.[18] Relativistic effects become non-negligible for heavier ions bearing large nuclear charge and reach a maximum for gold (Z=79). Aurophilic interactions are much weaker than ionic interactions, but can approach the strength of a hydrogen-bond with energies in the range of 20-50 kJ/mol and bond lengths in the range of 2.8-3.5 Å.[19-30]

1.3 Main Group Element Bridged Trigold(I) Clusters. Isolobal Analogues of $[Au_3C]^+$ and Its Adducts.

Pyramidal bridged trigold(I) clusters bearing capping ligands or organic moieties in the apical position of the bridging atom include, for example, the trigold(I) phosphonium boride complex $\{[(o\text{-}Tol_3P)Au]_3B(P(Cy)_3)\}$,[31] the trigold(I) phosphonium carbide cation $\{[(Ph_3P)Au]_3C(P(Me)_3)\}^+$,[32] the trigold(I) methyl(dimethylsulfoxonium) cation $\{[(Ph_3P)\text{-}Au]_3C(S(O)(CH_3)_2)\}^+$, the trigold(I) phosphonium nitride dication $\{[(Ph_3P)Au]_3N\text{-}(P(Ph)_3)\}^{2+}$,[33] and the trigold(I) *o*-tolylphosphide cation $\{[(Ph_3P)Au]_3P(o\text{-}Tol\}^+$ (Scheme 1.3).[34] Examples of trigold(I) clusters bridged by uncapped atoms include for example those of O, S, and Se with the formulae $[(LAu)_3O]^+$,[35] and $[(LAu)_3S]^+$, $[(LAu)_3Se]^+$.[19-21] To date, there have been no reports on members of the isolobal series consisting of the uncapped open shell trigold(I) boride $[(LAu)_3B]$, carbide $[(LAu)_3C]^+$, and nitride $[(LAu)_3N]^{2+}$ clusters. The trigold(I) carbide and nitride species in this series would be fundamentally different than existing higher nuclearity examples[19-21] with respect to formal oxidation state at the bridging ligand. To illustrate this point, consider tetranuclear, pentanuclear, and hexanuclear gold carbides bearing $[Au_4C]$, $[Au_5C]^+$, and $[Au_6C]^{2+}$ cores. In each case, the gold atoms are assigned an oxidation state of 1+, which when balanced with the overall charge of the core gives a formal oxidation state of 4- at the bridging carbide ligand. Using the same approach, one arrives at a oxidation state of 2- for the bridging carbide ligand in $[Au_3C]^+$. A lower coordination number at the bridging carbide of $[Au_3C]^+$ coupled with its open-shell electronic structure is expected to impart reactivity at the carbide carbon not observed in the higher-nuclearity closed-shell gold(I) carbide clusters.[6,7-17]

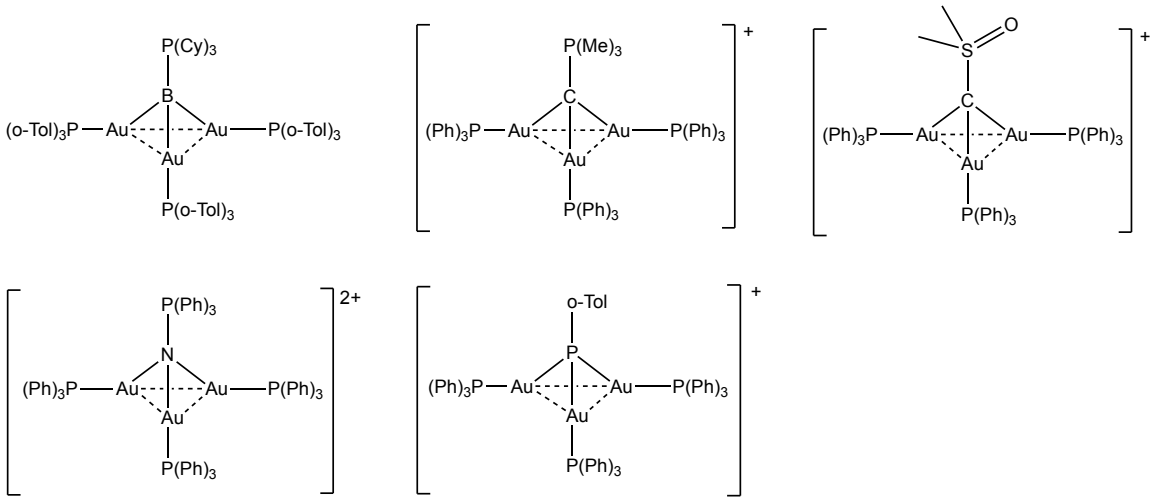

Scheme 1.3. Main group element bridged trigold(I) clusters bearing capping substitutents.[31-34]

The isolobal analogy[36-38] has been applied to the LAu^+ fragment allowing various useful chemical comparisons between the empty Au^+ frontier σ-orbitals and the empty H^+ 1s orbital.[39] Another less obvious comparison using a special case of Hoffman's isolobal analogy termed autogenic isolobality by Pyykö relates $[Au_3C]^+$ to CO_3^{2-}.[40] Under these circumstances, an analogy is drawn between the empty $2p_z$ orbital of singlet activated oxygen and the empty 6s orbital of Au^+, both of which may behave as σ-acceptor orbitals. Additionally, an analogy is drawn between the filled $2p_x$ orbital of oxygen and the filled d_{xz} orbital of Au^+, both of which may behave as π-donors to the empty carbon $2p_x$ orbital. Using this approach, the isolobal analogy may be drawn between CO_3^{2-}, $[(R_3C]^+$ (R = Aryl), $[(LAu)CR_2]^+$ (R = Aryl), and $[(LAu)_3C]^+$.

1.4 Contribution of Au-to-Carbon d_π-p_π Back Bonding to the Stabilization of Gold(I) Carbenes. Rationale for the Efficacy of $[(LAu)_3C]^+$.

Mechanisms assigned to a number of gold-catalyzed transformations require cationic gold intermediates coordinated by formally divalent carbon.[41-42] The extent to which the carbons of these gold-bound intermediates bear formal carbenoid ($Au^+=CR_2$) or carbenium ($Au-CR_2^+$) character depends on the degree of stabilizing Au-to-carbon d_π-p_π back-donation, which has been highly debated.[43] The Toste-Goddard model describes orbital interactions in complexes of the form $[(L)Au(CR_2)]^+$, where L is a 2-electron donor and CR_2 is a carbene fragment. This description includes one 3-center 4-electron σ-bonding interaction, and two separate orthogonal π-boding interactions (Scheme 1.4).[44]

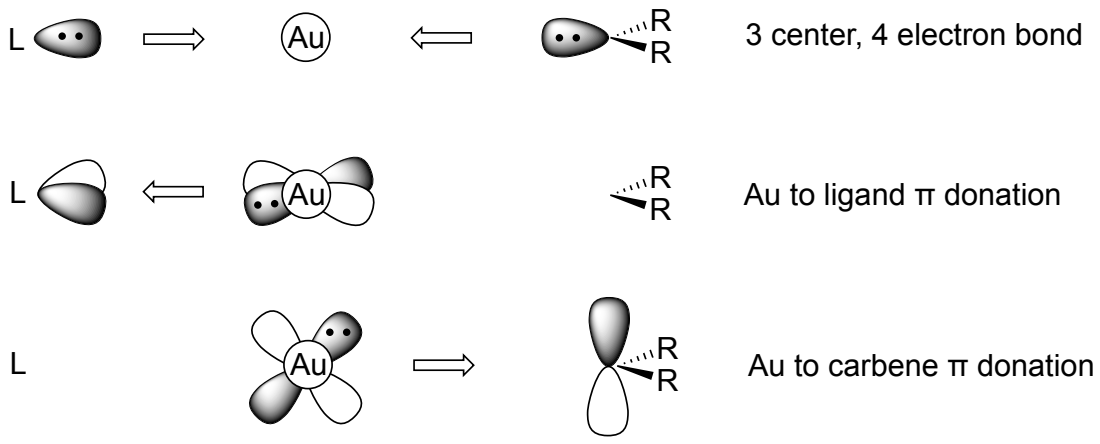

Scheme 1.4. Toste-Goddard model for $(L)Au(CR_2)$ frontier orbital interactions.[42,44]

According to this model, increasing the electrophilicity of the carbene carbon should decrease its ability to σ-donate to the metal, while simultaneously increasing its π-acidity. Therefore, representation of the gold-carbene interaction in these complexes as $Au=CR_2$ is accurate to the extent that it represents the combined σ and π contribution to the overall bonding situation, but it is not necessarily representative of bond order.[45] Brooner and

Wiedenhoefer conducted the first experimental determination of the π-donating ability of LAu^+ into the empty p_z orbital of a gold-bound carbene carbon using the cyclopropyl(methoxy)carbene complex $[(Johnphos)AuC(OMe)(c\text{-}Pr)]^+$ (Johnphos = (2-biphenylyl)di-*tert*-butylphosphine. They concluded, based on comparison of bond metrics in the cyclopropyl ring of the gold-bound carbene with organic analogues containing cyclopropyl rings bound to a π-acceptor group, that the carbocation-stabilizing ability of $(Johnphos)Au^+$ by π-donation exceeds that of a methyl or phenyl group, but is similar to that of a cylclopropyl group (Scheme 1.5).[46]

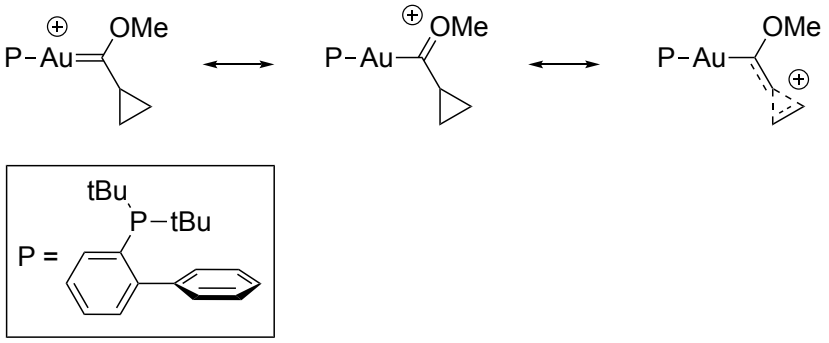

Scheme 1.5. Resonance contributors for $[(Johnphos)AuC(OMe)(c\text{-}Pr)]^+$.[46]

The Au-CR_2 bond lengths in a series of bis(4-methoxyphenyl)carbene gold complexes $(P)Au(C(p\text{-}C_6H_4OCH_3)_2)$ (P = phosphine) described by Fürstner, bearing electronically different phosphine supporting ligands, were responsive to phosphine donor strength, but ranged narrowly (**a**, 2.039(5) Å; **b**, 2.028(4) Å; **c**, 2.039(5) Å) (Scheme 1.6).[47] Fürstner argues that this limited effect, taken together with pronounced shortening of the bonds from the carbene carbon to *ipso*-carbons, indicates dominant contribution from the anisyl substituents in stabilizing the electron-deficient carbene carbon by π-interaction. He also argues that, in contrast to Straub's non-heteroatom-stabilized gold carbene,[48] the narrow range of carbene ^{13}C NMR chemical shifts is further evidence of electronic

communication between the empty carbene p_z orbital and the anisyl π-system, which is free to rotate at -50°C as demonstrated by a single set of NMR signals.

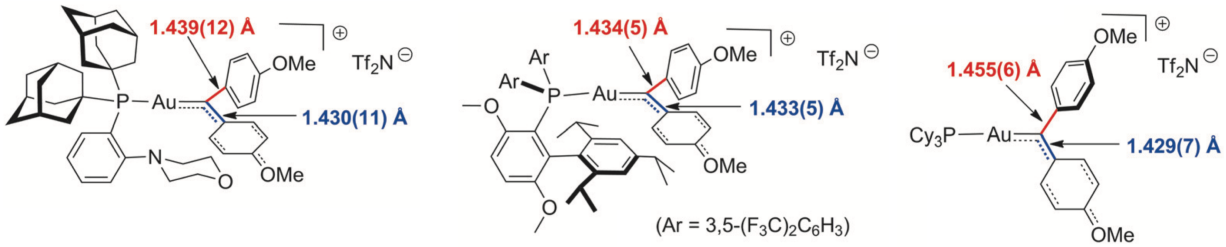

a **b** **c**

Scheme 1.6. Resonance stabilization of the carbene carbon in (P)Au(C(*p*-$C_6H_4OCH_3)_2$) (P = phosphine).[47]

Straub described the first isolable non-heteroatom-stabilized gold diarylcarbene complex (IPr**)Au(CMes)$_2$ (Scheme 1.7).[48] The authors point out that the Au-CMes$_2$ bond was slightly longer (Δd = 1.6 pm) than the Au-IPr** bond, which was attributed to a greater degree of π-back bonding in the Au-CMes$_2$ interaction. This was rationalized with the argument that the greater degree of s-character on the carbene carbon of IPr** compared with CMes$_2$ should contribute to a shorter Au-IPr** bond length in a σ-only description of both interactions.

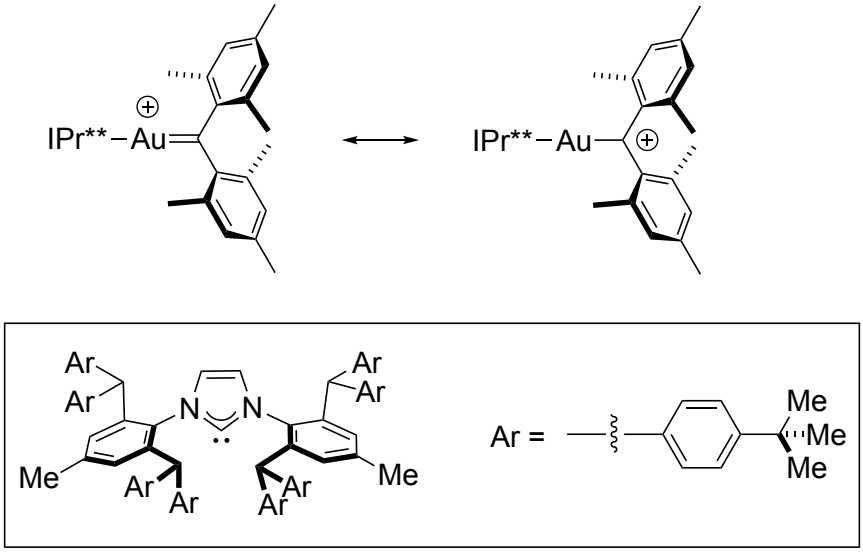

Scheme 1.7. The first isolated complex of gold(I) with a non-heteroatom-stabilized diarylcarbene.[48]

Based in part on the above reports and using the isolobal analogy, I hypothesized that a trigonal planar N-heterocyclic carbene-supported trigold(I) carbido cation $\{[(NHC)Au]_3C\}^+$ might be stabilized sufficiently by gold-to-carbon d_π-p_π back bonding to permit its isolation. It was envisaged that the reaction of suitable gold(I) precursors with gold(I) diazoalkanes to afford digold(I) carbynoid and trigld(I) carbide species might be achieved. Relevant organogold species resulting from the synthetic approaches explored include the NHC-supported trigold(I) ketenylidene cation (NHC = SIMes, IMes) (*see* Chapter 2), the acetonitrile and pyridine adducts of the NHC-supported trigold(I) trimethylsilyl(methylidyne) cation (NHC = IDipp, SIMes) (*see* Chapter 3), the pyridine adduct of SIMes-supported digold(I) methylidyne cation (*see* Chapter 3), the IDipp-supported gold(I) methoxymethyl complex (*see* Chapter 3), and the labile SIMes-supported *N*-(triauromethyl)pyridinium cation (*see* Chapter 3). The SIMes-supported *N*-(triauromethyl)pyridinium cation exhibited net electrophilic reactivity at the carbide carbon, supporting its description as the labile pyridine adduct of a trigold(I) carbido cation.

1.5 The Contribution of Aurophilic Interactions to Triauration in the Formation of Trigold(I) Ketenylidene and *N*-(triauromethyl)pyridinium Cations.

In this work, the tendency of gold(I) to hypercoordinate carbon resulted in the trigold(I) ketenylidene cation[49] and *N*-(triauromethyl)pyridinium cation under conditions that might have resulted instead in digold(I) ketene and digold(I) diazomethane respectively (Scheme 1.8). This observation may be attributable to the effects of aurophilic interactions. Aurophilic interactions are not essential to the bonding description of either compound however, several points of comparison make a compelling case for involvement of aurophilic interactions in their formation.

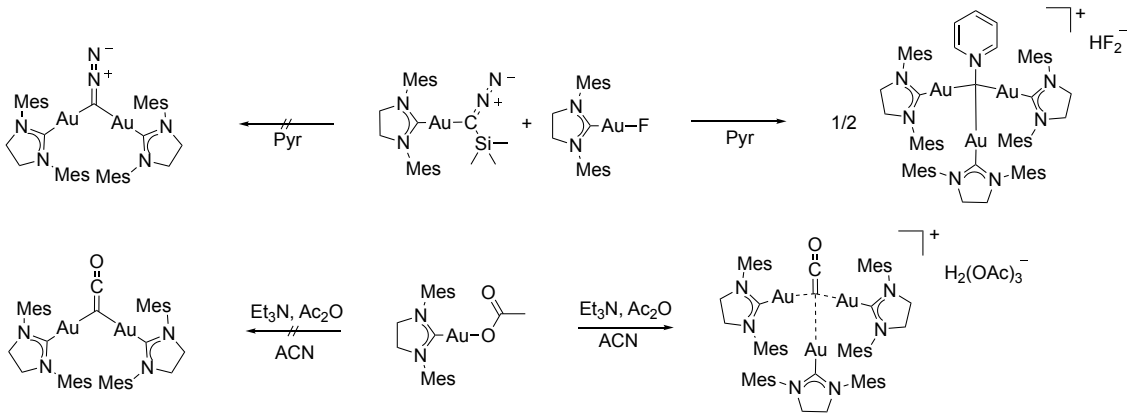

Scheme 1.8. Reactions leading to an *N*-(triauromethyl)pyridinium cation and a trigold(I) ketenylidene cation[49] rather than plausible digold(I) species.

Aurophilic interactions have been investigated in compounds with Au-Au distances mostly ranging from about 2.8-3.5 Å. Aurophilic attractions at longer distances are contentious; however, there is some evidence to suggest that energetic contributions resulting from long-distance aurophilic interactions may be non-negligible. A particularly surprising example of weak aurophilic interaction with a long crystallographic Au-Au separation of 3.746(1) Å was studied computationally for the IDipp-supported digold(I)

hydroxide {[(IDipp)Au]$_2$OH}BF_4.[50] The Au-Au separation in this compound falls well outside of the sum of van der Waals radii for two gold atoms, yet the Mayer bond order was determined to be 0.14 with a calculated energetic contribution of 8.7 kcal/mol.[51] In a less extreme example, the intermolecular Au-Au distance between monomers in the solid-state structure of (triethylphosphine)gold(I) chloride was crystallographically determined to be 3.615(2) Å.[52] The Au-Au distance was calculated in good agreement with this measurement, and the energetic contribution was determined to be 9.5 kcal/mol.[53] The crystallographic intermolecular Au-Au separation of 3.414(1) Å between [Au(NH_3)$_2$]Br monomers[54] was calculated in good agreement with this measurement, and the energetic contribution of the Au-Au interaction was computationally determined to be 9.4 kcal/mol.[55] The intramolecular Au-Au separation in [Au_2(*p*-tc)$_2$(dpppn)] (*p*-tc = *para*-thiocresol, dpppn = 1,5-bis(diphenylphosphino)pentane) was crystallographically determined to be 3.200(1) Å. The energetic contribution of this interaction was determined to be 10 kcal/mol by NMR line broadening experiments.[56] The intramolecular Au-Au separation in [Au_2(μ-xantphos)$_2$](NO_3)$_2$ was crystallographically determined to be 2.858(1) Å. The energetic contribution of this interaction was determined to be 11.7 kcal/mol by NMR line broadening experiments.[57] These data (Table 1.1, Plot 1.1) taken together suggest an estimated stabilization resulting from two additional Au-Au interactions in SIMes-supported trigold(I) ketenylidene tetrafluoroborate {[(SIMes)Au]$_3$CCO}BF_4 (Au1-Au2 3.528(1), Au2-Au3 3.3878(9), Au3-Au1 3.2904(8)) (*see* Chapter 2) on the order of *ca.* 19-20 kcal/mol compared with its hypothetical digold(I) ketenide {[(SIMes)Au]$_2$CCO} congener. Similarly, these data suggest a stabilization resulting from two additional Au-Au interactions in IDipp-supported *N*-(triauromethyl)pyridinium trifluoromethanesulfonate {[(SIMes)Au]$_3$C(NC_5H_5}-OTf (Au1-Au2 3.4836(5), Au2-Au3 3.1129(6), Au3-Au4 3.1048(6)) (*see* Chapter 3) on the order of *ca.* 20-21 kcal/mol compared with its plausible digold(I) diazomethane intermediate.

Table 1.1. Selected experimentally determined intra- and intermolecular Au-Au interaction distances and their associated experimentally or computationally determined energetic contribution.

Compound	Au-Au (Å)	D (kcal/mol)
$\{[(IDipp)Au]_2OH\}BF_4$	3.746(1) [49]	8.7 [50]
$(Et_3P)AuCl$	3.615(2) [52]	9.5 [52]
$[Au(NH_3)_2]Br$	3.414(1) [53]	9.4 [54]
$[Au_2(p\text{-tc})_2(dpppn)]$	3.200(1) [55]	10 [55]
$[Au_2(\mu\text{-xantphos})_2](NO_3)_2$	2.858(1) [56]	11.7 [56]

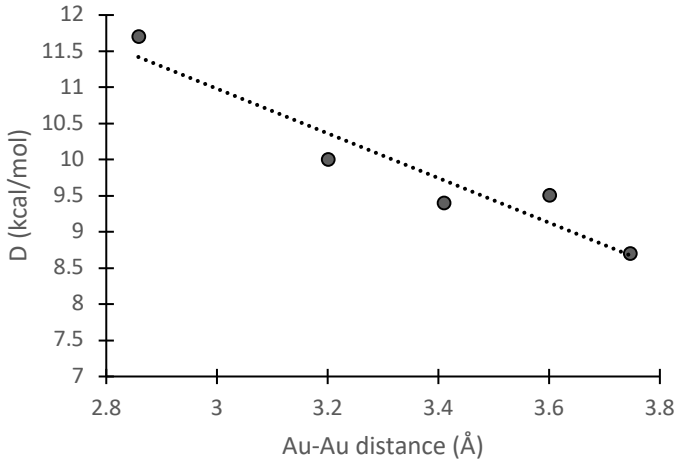

Figure 1.1. Plot of Au-Au interaction distances and their associated energetic contributions (see Table 1.1).[50-51,53-57]

1.6 Concluding Remarks

The chapters that follow describe the synthesis, characterization, and reactivity of low nuclearity NHC-supported gold(I) clusters in pursuit of a trigold(I) carbido cation. Chapter 2 describes the synthesis of a trigold(I) ketenylidene cation with an unexpectedly strong Au_3C-CO bond, and its ketene transfer reactivity. Chapter 3 describes the reactivity of NHC-supported gold(I) (trimethylsilyl)diazomethyl complexes to form solvent adducts of digold(I) trimethylsilyl(methylidyne), digold(I) methylidyne, and trigold(I) carbido cations,

as well as a gold(I) methoxymethyl complex. The pyridine adduct of the trigold(I) carbido cation exhibits electrophilic reactivity toward CO to form a trigold(I) ketenylidene cation. Finally, trapping experiments are described that suggest the transient formation of a free trigold(I) carbido cation in non-coordinating solvents. Chapter 4 describes the auration of tetrazole to form an isomeric mixture of 1-auro(tetrazolate) and 2-auro(tetrazolate). Addition of a gold(I) triflate to the mixture affords a fluxional cationic *N,N'*-diauro(tetrazolate). 1,3-Dipolar cycloaddition of a terminal gold(I) azide with a terminal gold(I) cyanide in CD_3CN solution was attmpted. Cycloaddition of the gold(I) azide with the nitrile solvent occurred instead to form the neutral 1-auor(5-methyltetrazolate)-d_3.

1.7 References

1. Schmidbaur, H.; Schier, A. Aurophilic interactions as a subject of current research: an up-date. *Chem. Soc. Rev.,* **2012**, 41, 370-412.

2. Schmidbaur, H.; Schier, A. A Briefing on aurophilicity. *Chem. Soc. Rev.* **2008**, 37, 1931-1951.

3. Schmidbaur, H. The Aurophilicity Phenomenon: A Decade of Experimental Findings, Theoretical Concepts and Emerging Applications. *Gold Bull*. **2000**, 33, 3-10.

4. Bardaji, M.; Laguna, A. Heteronuclear Metal-Metal Contacts between Gold(I) and Group-11, 12, and 13 Centers. *Eur. J. Inorg. Chem.* **2003**, 3069-3079.

5. Blumenthal, A.; Beruda, H.; Schmidbaur, H. Tetrakis[(triphenylphosphine)-gold(I)](tricyclohexylphosphine)boronium tetrafluoroborate, a Novel Boron-centered Gold Cluster. *J. Chem. Soc., Chem. Commun*. **1993**, 1005-1006.

6. Scherbaum, F.; Grohmann, A.; Huber, B.; Krüger, C.; Schmidbaur, H. "Aurophilicity" as a Consequence of Relativistic Effects: The Hexakis(triphenyl-phosphaneaurio)methane Dication $[Ph_3PAu)_6C]^{2+}$. *Angew. Chem. Int. Ed. Engl.* **1988**, 27, 1544-1546.

7. Scherbaum, F.; Grohmann, A.; Müller, G.; Schmidbaur, H. Synthesis, Structure, and Bonding of the Cation $[\{C_6H_5)_4PAu\}_5C]^{+}$. *Angew. Chem. Int. Ed. Engl.* **1989**, 463-465.

8. Grohmann, A.; Riede, J.; Schmidbaur, H.; Electron-deficient bonding at pentacoordinate nitrogen. *Nature* **1990**, 345, 140-142.

9. Schier, A.; Grohmann, A.; López-de-Luzuriaga, J. M.; Schmidbaur, H. The Elusive Structures of Pentakis[(triphenylphonspine)gold]ammonium(2+)Bis[tetrafluoro-borate(1-)]. *Inorg. Chem.* **2000**, 39, 547-554.

10. Nomiya, K.; Takuya, Y.; Sakai, Y.; Nanba, A.; Tsuruta, S. Intercluster Compound between a Tetrakis{triphenylphosphinegold(I)}oxonium Cation and a Keggin Polyoxometalate (POM): Formation during the Course of Carboxylate Elimination of a Monomeric Triphenylphosphinegold(I) Carboxylate in the Presence of POMs. *Inorg*. *Chem.* **2010**, 49, 8247-8254.

11. Nesmeyanov, A. N.; Perevalova, E. G.; Struchkov, Yu. T.; Antipin, M. Yu.; Grandberg, K. I.; Dyadchenko, V. P. Tris(triphenylphosphoniumgold)oxonium Salts. *J. Organomet. Chem.* **1980**, 201, 343-349.

12. Zeller, E.; Schmidbaur, H. Hypercoordinate Phosphorous in Gold Clusters: Novel Species $[P(AuL)_6]^{3+}(BF_4^-)_3$. *J. Chem. Soc., Chem. Commun.* **1993**, 0, 69-70.

13. Schmidbaur, H.; Weidenhiller, G.; Steigelmann, O. Triaurated Phosphonium Cations $[RP(AuPPh)_3]^+$ and the Electron-deficient, Hypercoordinated Phosphonium Dication $[P(AuPPh_3)_5]^{2+}$. *Angew. Chem. Int. Ed.* **1991**, 30, 433-435.

14. Canales, F.; Gimeno, M. C.; Jones, P. G.; Laguna, A. Aurophilicity at Sulfur Centers: Synthesis and Structure of the Tetragold(I) Species $[(Ph_3PAu)_4S](SF_3SO_3)_2 \bullet 2CH_2Cl_2$. *Angew. Chemie. Int. Ed.* **1994**, 33, 769-770.

15. Canales, F.; Gimeno, C.; Laguna, A.; Villacampa, M. D. Aurophilicity at Sulfur centers. Synthesis of the polyaurated species $[S(AuPR_3)_n]^{(n-2)+}$ (n = 2-6). *Inorg. Chim. Act.* **1996**, 244, 95-103.

16. Cannales, S.; Crespo, O.; Gimeno, C.; Jones, P. G.; Laguna, A. Synthesis of the first gold complex with a central μ_4-selenido ligand. *Chem. Commun.* **1999**, 679-680.

17. Schmidbaur, H.; Steigelmann, O. The First Complexes of Tetragoldmethane CAu_4. *Z. Naturfosch.* **1992**, 47b, 1721.

18. Kaltsoyannis, N. Relativistic effects in inorganic and organometallic chemistry. *J. Chem. Soc. Dalton Trans.* **1996**, 1-11.

19. Schmidbaur, H.; Schier, A. Aurophilic interactions as a subject of current research: an up-date. *Chem. Soc. Rev.,* **2012**., 41, 370.

20. Schmidbaur, H.; Schier, A. A Briefing on aurophilicity. *Chem. Soc. Rev.* **2008**, 37, 1931.

21. Schmidbaur, H. The Aurophilicity Phenomenon: A Decade of Experimental Findings, Theoretical Concepts and Emerging Applications. *Gold Bull*. **2000**, 33, 3.

22. Bardaji, M.; Laguna, A. Heteronuclear Metal-Metal Contacts between Gold(I) and Group-11, 12, and 13 Centers. *Eur. J. Inorg. Chem.* **2003**, 3069.

23. Pyykö, P.; Runeberg, N.; Medizabal, F. Theory of the d^{10}-d^{10} Closed-Shell Attraction: 1. Dimers Near Equilibrium. *Chem. Eur. J.* **1997**, 3, 1451.

24. Pyykö, P.; Medizabal, F. Theory of the d^{10}-d^{10} Closed-Shell Attraction: 2. Long-Distance Behaviour and Nonadditive Effects in Dimers and trimers of Type $[(X\text{-}Au\text{-}L)_n]$ (n=2, 3; X=Cl, I, H; L=PH_3, PMe_3, -N≡CH). *Chem. Eur. J.* **1997**, 3, 1458.

25. Pyykö, P.; Medizabal, F. Theory of the d^{10}-d^{10} Closed-Shell Attraction: III. Rings. *Inorg. Chem.* **1998**, 37, 3018.

26. Pyykö, P.; Tamm, T. Theory of the d^{10}-d^{10} Closed-Shell Attraction: 4. $X(AuL)_n^{m+}$ Centered Systems. *Organometallics*. **1998**, 17, 4842.

27. Pyykö, P. Strong Closed-Shell Interactions in Inorganic Chemistry. *Chem. Rev.* **1997**, 97, 597.

28. Raubenheimer, H. G.; Schmidbaur, H. The Late Start and Amazing Upswing in Gold Chemistry. *J. Chem. Ed.* **2014**, 91, 2024.

29. Bardahi, M.; Laguna, A. Gold chemistry: The Aurophilic Attraction. *J. Chem. Ed.* **1999**, 76, 201.

30. McKelvey, D. R. Relativistic Effects on Chemical Properties. *J. Chem. Ed.* **1983**, 60, 112.

31. Schmidbaur, H.; Blumenthal, M. A.; Kraus, F. Synthesis of a Tri(gold)boride Complex $(Cy_3P)B[AuP(o\text{-}Tol)_3]_3$. *Z. Naturforsch.* **2013**, 68b, 1321.

32. Schmidbaur, H.; Scherbaum, F.; Huber, B.; Müller, G. Polyauriomethane Compounds. *Angew. Chem. Int. Ed. Engl.* **1988**, 27, 419.

33. Pivoriunas, G.; Maichle-Mössmer, C.; Schwarz, S.; Strähle, J. Synthesis and Crystal Structure of $[(PPh_3PAu)_3NPPh_3NPPh_3][PF_6]_2$, a Gold Phosphoraneiminato Complex. *Z. Anorg. Allg. Chem.* **2005**, 631, 1743-1745.

34. Schmidbaur, H.; Weidenhiller, G.; Steigelmann, O. Triaurated Phosphonium Cations $[RP(AuPPh)_3]^+$ and the Electron-deficient, Hypercoordinated phosphonium Dication $[P(AuPPh_3)_5]^{2+}$. *Angew. Chem. Int. Ed. Engl.* **1991**, 30, 433-435.

35. Nesmeyanov, A. N.; Perevalova, E. G.; Struchkov, Yu. T.; Antipin, M. Yu.; Grandberg, K. I.; Dyadchenko, V. P. Tris(triphenylphosphoniumgold)oxonium Salts. *J. Organomet. Chem.* **1980**, 201, 343-349.

36. Hoffman, R. Building Bridges Between Inorganic and Organic Chemistry. *Angew. Chem. Int. Ed.* **1982**, 21, 711.

37. Elian, M.; Chen, M. M. L.; Mingos, D. M. P.; Hoffman, R. Comparative Bonding Study of Conical Fragments. *Inorg. Chem.* **1976**, 15, 1148.

38. Hoffman, R. Theoretical Organometallic Chemistry. *Science* **1981**, 211, 995.

39. Raubenheimer, H. G.; Schmidbaur, H. Gold Chemistry Guided by the Isolobality Concept. *Organometallics* **2012**, 31, 2507.

40. Pyykkö, P.; Patzscheke, M.; Suurpere, J. Calculated structures of $[Au=C=Au]^{2+}$ and related systems. *Chem. Phys. Lett.* **2003**, 381, 45.

41. Quian, D.; Zhang, J. Gold-catalyzed cyclopropation reactions using a carbenoid precursor toolbox. *Chem. Soc. Rev.* **2015**, 44, 677.

42. Harris, R. J.; Widenhoefer, R. A. Gold carbenes, gold-stabilized carbocations, and cationic intermediates relevant to gold-catalyzed enyne cycloaddition. *Chem. Soc. Rev.* **2016**, 45, 4533.

43. Wang, Y.; Muratore, M. E.; Echavarren, A. M. Gold Carbene or Carbenoid: Is There a Difference? *Chem. Eur. J.* **2015**, 21, 7332-7339.

44. Benitez, D.; Shapiro, N. D.; Tkatchouk, E.; Yiming, W.; Goddard, W. A.; Toste, F. D. A Bonding Model for gold(I) carbene complexes. *Nat. Chem.* **2010**, 482-486.

45. Benitez, D.; Shapiro, N. D.; Tkatchouk, E.; Wang, Y.; Goddard, W. A.; Toste, F. D. A bonding model for gold(I) carbene complexes. *Nat. Chem.*, **2009**, 1, 482-486.

46. Brooner, R. E. M.; Widenhoefer, R. A. Experimental evaluation of the electron donor ability of a gold phosphine fragment in a gold carbene complex. *Chem. Commun.* **2014**, 50, 2420.

47. Werlé, C.; Goddard, R.; Fürstner, A. The First Crystal Structure of a Reactive Dirhodium Carbene Complex and a Versatile Method for the Preparation of Gold Carbenes by Rhodium-to-Gold Transmetalation. *Angew. Chem. Int. Ed.* **2015**, 54, 15452-15456.

48. Hussong, M. W.; Rominger, F.; Krämer, P.; Straub, B. F. Isolation of a Non-Heteroatom-Stabilized Gold-Carbene Complex. *Angew. Chem. Int. Ed.* **2014**, 53, 9372-9375.

49. Daugherty, N. T.; Bacsa, J.; Sadighi, J. P. A Trigold(I) Ketenylidene Cation. *Organometallics* **2017**, 36, 3171-3174.

50. Gaillard, S.; Bosson, J; Ramón, R. S.; Nun, P.; Slawin, A. M. Z.; Nolan, S. P. Development of Versatile and Silver-Free Protocols for Gold(I) Catalysis. *Chem. Eur. J.* **2010**, 16, 13729- 13740.

51. Ramón, R. S.; Gailard, S.; Poater, A.; Cavallo, L.; Slawin, A. M. Z.; Nolan, S. P. $[\{Au(IPr)\}_2(\mu\text{-OH})]X$ Complexes: Synthetic, Structural and Catalytic Studies. *Chem. Eur. J.* **2011**, 17, 1238-1246.

52. Tiekink, E. R. T. Chloro(triethylphosphine)gold(I). *Acta Cryst.* **1989**, C45, 1233-1234.

53. Kang, J.; Jeong, Y.; Oh, S.; Kim, H.; Park, C.; Tiekink, E. R. R. Photophysical Properties of Chlorotriethylphosphinegold(I). *Bull. Korean Chem. Soc.* **2010**, 31, 2151-2157.

54. Mingos, D. M. P; Menzer, S.; Williams, D. J. Synthesis of $[Au(NH_3)_2]^+$ Salts and the Crystal Structure of $[Au(NH_3)_2]Br$. *J. Chem. Soc. Dalton Trans.* **1995**, 319.

55. Ionov, S. P.; Kuznetsov, N. T. Energetics of Long-Range Coordination Interactions of Gold Atoms in Inorganic Complexes. *Russ. J. Coord. Chem.* **2001**, 27, 628-631.

56. Narayanaswamy, R.; Young, M. A.; Parkhurst, E.; Ouellette, M.; Kerr, M. E.; Ho, D. M.; Elder, R. C.; Bruce, A. E.; Bruce, M. R. M. *Inorg. Chem.* **1993**, 32, 2506-2517.

57. Deák, A.; Megyes, T.; Tárkányi, G.; Király, P.; Biczók, L.; Pálinkás, G.; Stang, P. J. Synthesis and Solution- and Solid-State Characterization of Gold(I) Rings with Short Au···Au Interactions. Spontaneous Resolution of a Gold(I) Complex. *J. Am. Chem. Soc.* **2006**, 128, 12668-12670.

58. Ponomarev, S. V. Silyl-, Germyl-, and Stannyl-substituted Ketenes. *Angew. Chem. Int. Ed. Engl.* **1973**, 12, 675.

59. Lappert, M. F.; Lorberth, J.; Poland, J. S. Organometallic Diazoalkanes. Part I. Synthesis and Characterization of Simple Group IVB Organometallic Diazomethanes, and the Tin-Carbon Cleavage Reactions of Bis(trimethyl-stannyl)diazomethane. *J. Chem. Soc. (A)* **1970**, 2954-2959.

60. Glozbach, E.; Lorbeth, J. Metallorganische Diazoalkane XVI*. Synthese Von Silyldiazoalkanen $Me_3Si(L_nM)CN_2$. *J. Organometallic. Chem.*, **1980**, 191, 371-379.

CHAPTER 2

A TRIGOLD(I) KETENYLIDENE CATION

2.1 Background

Transition metal ketenides and ketenylidenes have been studied as models for plausible intermediates in carbon monoxide chemistry[1]. The first molecular trimetalloketenylidene cluster $[[(CO)_3Co]_3CCO]^+$, a highly electrophilic compound, was reported by Seyferth *et. al.* in 1974[2-4]. Subsequently, Shapley *et. al.* reported $[H_2Os_3(CO)_9(\mu_3\text{-}1,2\text{-}\eta^1\text{-}CCO)]$ [5-6] and $[H_2Ru_3(CO)_9(CCO)]$[7], and Shriver and coworkers studied a series of generally nucleophilic, anionic ketenylidenes,[8-13] including one featuring a mixed-metal $[Fe_3Cu]$ core.[14] Several of these complexes display remarkable C–C coupling and cleavage reactions.[15] Vahrenkamp reported the mixed metal Fe/Co ketenylidene $(PPN)[Fe_2Co(CO)_9(\mu_3\text{-}CCO)]$, as well as the Fe/Au ketenylidene cluster $[(PPh_3Au)_2Fe_3(CO)_9(\mu_3\text{-}CCO)]$ bearing LAu^+ fragments as charge balancing equivalents[16]. Low-valent early metals such as Zr and Hf can convert coordinated CO to a doubly bridging ketenide fragment.[17-18] Mononuclear ketenylidenes are formed from Ta(III) via reductive coupling of CO[19] and from W(II), transiently, by reaction with carbon suboxide (C_3O_2).[20] In the early 1970's, Blues *et. al.* reported the coinage meatal ketenides prepared by a general procedure involving deprotonation of ketene $H_2C{=}C{=}O$ generated *in situ* from a tertiary amine and acetic anhydride, followed by coordination of the terminal carbon with 2 equivalents of M^+ (M = Cu, Ag, Au) to give the sparingly soluble, mildly explosive gold(I) ketenide $Au_2C{=}C{=}O$, silver(I) ketenide $Ag_2C{=}C{=}O$, and copper(I) ketenide $Cu_2C{=}C{=}O$ coordination polymers. In each case, either endogenous acetate or excess tertiary amine deprotonate an activated side-on complex of ketene by M^+.[21-23]

These compounds were characterized by infrared spectroscopy, which revealed distinctively strong absorbances near 2,000 cm^{-1} arising from the ketenide. X-ray powder diffraction studies on the silver complex indicated a μ_4-ketenide in a two-dimensional coordination polymer.[24] The copper and silver ketenides serve as precatalysts for olefin oxidation reactions,[25-28] and a surface-bound ketenylidene has been observed in the growth of thin copper films from β-diketonates.[29] Fürstner et al. have described a neutral gold(I) chloride complex of Ph_3PCCO, in which the Lewis-basic ylide carbon acts as a donor to gold.[30] Recently, Yates and coworkers have identified and studied surface-bound [Au_2CCO] as a reactive intermediate in the aerobic oxidation of acetic acid and related species on Au/TiO_2 surfaces[31-33]. In this chapter, the synthesis and structure of a stable trigold ketenylidene cation is described. Reaction of this cation with soft Lewis bases leads to Au–C bond cleavage.

2.2 Results and Discussion

Initially the digold(I) ketenide $\{[(SIMes)Au]_2(\mu_2\text{-}CCO)$ was sought as a precursor to the trigold ketenylidene cation $\{[(SIMes)Au]_3(\mu_3\text{-}CCO)\}^+$. Reaction of (SIMes)gold(I) acetate [SIMes = 1,3-bis(2,4,6-trimethylphenyl)imidazolin-2-ylidene] with excess acetic anhydride and triethylamine, under conditions that generate ketene at equilibrium,[34] afforded a product that precipitated upon addition of diethyl ether to a concentrated acetonitrile solution. The infrared spectrum of this product displayed a strong absorbance at 2,000 cm^{-1}, which was initially attributed to the doubly bridging ketenide of the expected product. The ^1H NMR spectrum of the product in CD_3CN solution appeared consistent with this assignment, except for an additional broad singlet at δ 1.88 ppm. This resonance appeared acetate-derived, and integration suggested the presence of one acetate per SIMes ligand.

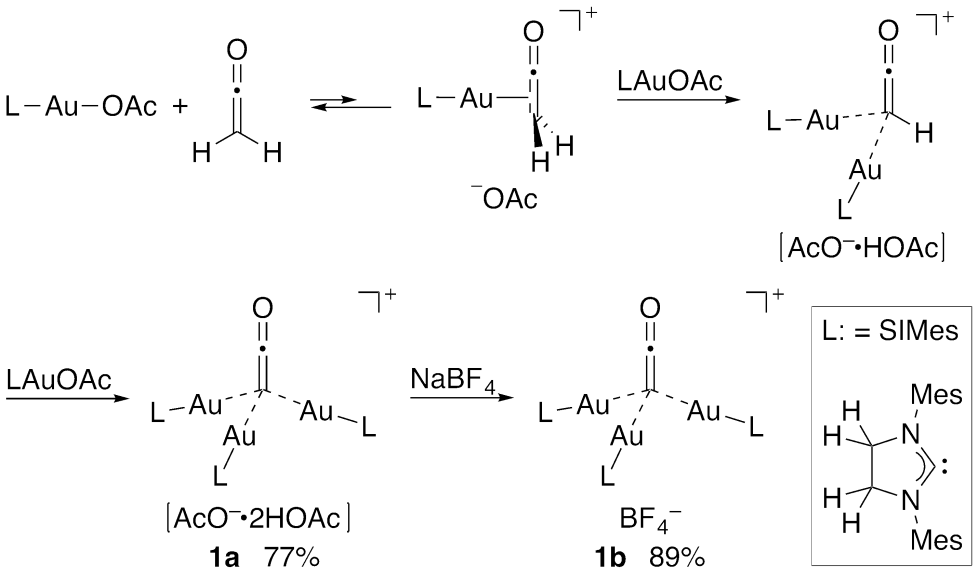

Scheme 2.1. Proposed sequence for $[Au_3CCO]^+$ formation.

The ESI mass spectrum of the isolated complex displayed a strong parent ion peak at m/z = 1549.4, corresponding to the trigold(I) ketenylidene cation $\{[(SIMes)Au]_3(\mu_3\text{-}CCO)\}^+$. Because the formation of this cation from (SIMes)gold(I) acetate and ketene requires liberation of two equivalents of acetic acid plus acetate anion, the isolated product was initially formulated as $\{[(SIMes)Au]_3(\mu_3\text{-}CCO)\}^+$ $[AcO•2HOAc]^-$ (**1a**), consistent with the ^1H NMR signals observed for both SIMes and acetate. The IMes-supported analogue of **1a** [IMes = 1,3-dimesitylimidazol-2-ylidene] may be similarly prepared, but is accompanied by a significant fraction of homoleptic $[(IMes)_2Au]^+$,[35] which proved impractical to remove. Use of the more sterically encumbering IDipp[36] [Dipp = 2,6-diisopropylphenyl] did not give rise to clean product formation. Scheme 2.1 depicts a plausible sequence leading to **1a**, similar to that invoked for the formation of binary silver ketenide $[Ag_2CCO]_n$.[24]

Complex **1a** proved slightly unstable on prolonged standing in the solid form, or in the course of repeated manipulations in solution. Reasoning that this instability might arise

from the protic and potentially nucleophilic anion, anion exchange was carried out with sodium tetrafluoroborate to obtain the stable $\{[(SIMes)Au]_3(\mu_3\text{-}CCO)\}^+ BF_4^-$ (**1b**).

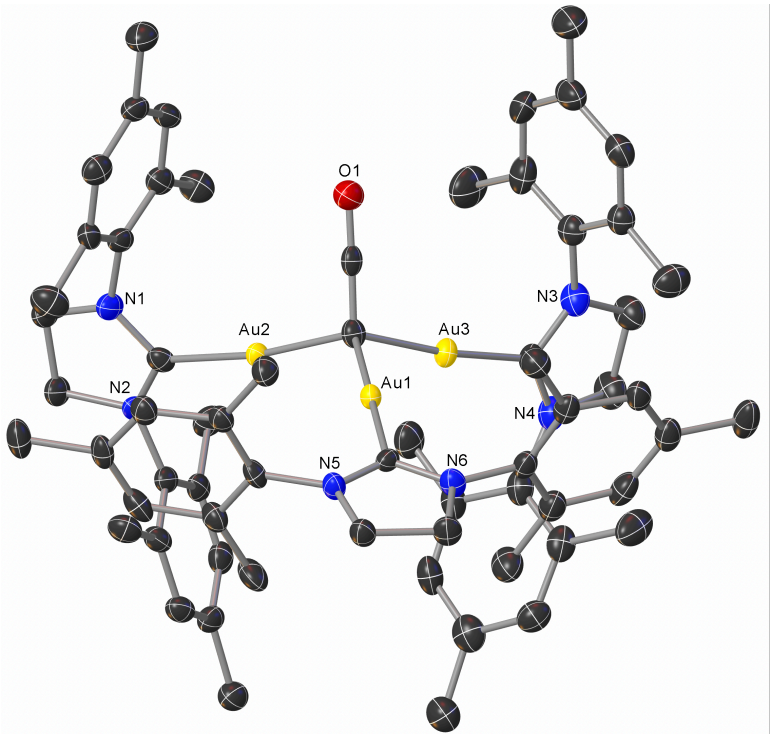

Figure 2.1. Solid-state structure of **1b** (50% probability ellipsoids). H atoms, BF_4 anion, and co-crystallized CH_2Cl_2 omitted for clarity. Selected interatomic distances (Å) and angles (°): C1–C2, 1.318(8); C2–O1, 1.183(7); Au1–C1, 2.062(6); Au2–C1, 2.080(6); Au3–C1, 2.075(6); Au1–C2, 2.903(6); Au2–C2, 2.704(6); Au3–C2, 2.733(6); C1–C2–O1, 178.5(6); Au1–C1–C2, 116.6(4), Au1-Au2 3.528(1), Au1-Au3 3.2904(8), Au2-Au3 3.3878(9); Au2–C1–C2, 103.2(4); Au3–C1–C2, 105.0(4); C45–Au1–C1, 178.8(2); C3–Au2–C1, 171.5(2); C24–Au3–C1, 172.5(2).

Careful layering of hexanes onto a solution of **1b** in CH_2Cl_2 afforded crystals suitable for X-ray diffraction. The solid-state structure (Figure 2.1) revealed a linear ketenylidene moiety bridging three gold centers in a cation distorted from threefold symmetry. The plane of the heterocycle bound to Au1 forms a torsion angle of 87.9(5)° with respect to the ketenylidene C–C vector, compared to 18.2(5)° and 18.0(5)° for the

other two NHC ligands. The Au–C–C angle is significantly larger for Au1 than for Au2 or Au3, placing Au1 further from the carbonyl carbon C2, 2.903(6) Å versus 2.704(6) Å for Au2 and 2.733(6) Å for Au3. The Au–C1 distances range narrowly from 2.062(5) to 2.080(6) Å. The Au–C_{NHC} distances are likewise quite similar, ranging from 1.998(5) to 2.007(5) Å. The shortest Au•••Au distance is just within two van der Waals radii[37] at 3.2904(8) Å, suggestive of a weak aurophilic interaction.[38]

In solution, all three SIMes ligands are symmetric and equivalent on the ^{1}H NMR timescale, suggesting small energy differences both for distortion from threefold symmetry, and for rotation of the NHC about the C–Au bond. Table 1 compares key metrics and stretching frequencies for **1b** to those of selected transition metal ketenylidenes and a ketenide, of the main group ketenylidene Ph_3PCCO,[39] of the acetylium ion and of ketene itself. Although in idealized threefold symmetry the trigold(I) ketenylidene cation is isolobal to acetylium,[40] the bond metrics and infrared stretching frequency for the ketenylidene are closer to those of neutral ketene than of acetylium ion. These data suggest an arrangement closer to net double bonds than to a single and a triple bond.

Table 2.1. Key metrics, IR data in ketenylidene-related species. [a] PF_6^- counterion; Refs. [2-3]. [b] $[Ph_4As]^+$ salt; Ref. [9]. [c] Ref. [18]. [d] Refs. [39, 41]. [e] Ref. [42]. [f] Derived from microwave rotational spectroscopy; Ref. [43].

Compound	C–C (Å)	C–O (Å)	ν (cm^{-1})
1b (this work)	1.318(8)	1.183(7)	2013
$[(OC)_9Co_3(CCO)]^+$ [a]			2260
$[(OC)_9Fe_3(CCO)]^{2-}$ [b]	1.28(3)	1.18(3)	1924
$\{Cp_2Zr_3(\mu_2\text{-CCO})(\mu_3\text{-O})[O_2CN(i\text{-Pr})_2]_6\}$ [c]	1.31(2)	1.24(1)	2016
Ph_3PCCO [d]	1.210(10)	1.185(9)	2110
$H_3CCO^+ SbF_6^-$ [e]	1.419(4)	1.108(4)	2302
H_2CCO [f]	1.3165(15)	1.1614(14)	2152

Consistent with this interpretation, the carbonyl carbon of the $[(LAu)_3(\mu_3\text{-}CCO)]^+$ cation showed no electrophilic behavior toward a range of Lewis bases. Treatment with sodium azide or sodium trimethylsiloxide, in attempts to produce triaurated acetyl derivatives, gave little apparent reaction after several hours as judged by ^{1}H NMR spectroscopy. Attempted aza-Wittig reactions[44] to form the complexes $[(LAu)_3(\mu_3\text{-}CCNR)]^+$, using *N*-phenyl or *N*-benzyliminotriphenylphosphorane, led to some phosphine oxide formation as judged by ^{31}P NMR spectroscopy, in addition to a number of yet-unidentified byproducts. Treatment with a solution of the Tebbe reagent $[(\eta^5\text{-}C_5H_5)_2Ti(\mu\text{-}Cl)(\mu\text{-}CH_2)Al(CH_3)_2]$,[45] in the hope of forming the allenylidene $[(LAu)_3(\mu_3\text{-}CCCH_2)]^+$,[46-47] gave complex product mixtures.

The reaction of **1b** with excess sodium borohydride in THF suspension, did not lead to C–H bond formation, but led instead to the formation of (SIMes)AuH (**2**), reflecting nucleophilic addition of boron hydrides to gold rather than to carbon. This reaction proceeds rather cleanly, with a single set of SIMes resonances in the ^{1}H NMR spectrum, and a singlet resonance integrating to one hydrogen for the hydride. Like that of (IDipp)AuH,[48] the hydride resonance for **2** exhibits large solvent shifts, appearing at δ 3.79 ppm in THF-d_8, but δ 5.28 ppm in C_6D_6 solution. The yield was assessed at 88% relative to an internal standard (4,4'-dimethylbiphenyl), and a preparative-scale reaction starting from **1a** afforded the hydride in 81% isolated yield, ruling out the possibility that only one or two of the three gold centers is converted to hydride (Scheme 2.2).

The fate of the ketenylidene fragment in this reaction could not be accounted for by IR, ^{1}H or ^{11}B NMR spectroscopy. The reaction between equimolar **1b** and $NaBH_4$ would afford three (SIMes)AuH plus [HBCCO], not expected to persist in solution. With excess borohydride, anionic ketenide-borane adducts or their decomposition products might be expected. A reaction was chosen to give both gold–carbon bond cleavage and conversion

of the ketenide to a readily identifiable product (Scheme 2.2). The reaction of **1b** in CD_2Cl_2 solution with a mixture of thiophenol and sodium thiophenolate resulted in the clean formation of three equivalents of (SIMes)AuSPh and one equivalent of *S*-phenyl thioacetate[49] as judged by ^{1}H NMR spectroscopy. The identity of the thioacetate ester was confirmed by GC-mass spectrometry.

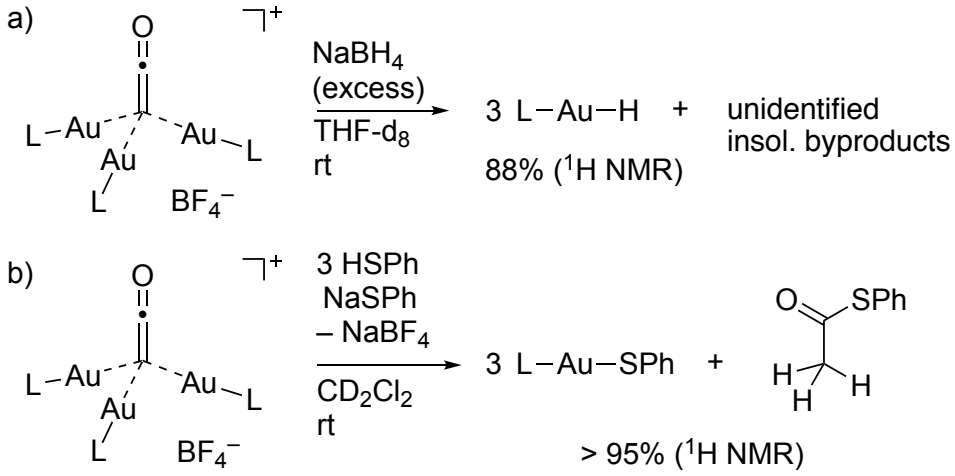

Scheme 2.2. Reactions of $[(LAu)_3CCO]BF_4$ with Lewis Bases.

2.3 Conclusion

In summary, the reaction of an (NHC)gold(I) acetate with ketene and base leads directly to a trigold ketenylidene cation, rather than to neutral monogold ketenyl or digold ketenide. Paired with a suitable anion, this cation is stable, permitting spectroscopic and structural characterization. Reaction with soft Lewis bases leads to facile gold–carbon bond cleavage and, in the case of a protic substrate, to conversion of the ketenylidene fragment to an acetyl group.

2.4 Experimental

2.4.1 General Considerations

Unless otherwise indicated, manipulations were performed in an MBraun glovebox under nitrogen atmosphere, or using standard Schlenk techniques under argon atmosphere. Glassware was dried in a ventilated oven at 160 °C and allowed to cool under vacuum. Molecular sieves (Alfa Aesar) and Celite (EMD 545) were dried under vacuum for at least twelve hours at 160°C. Dichloromethane (EMD Millipore Omnisolv), hexanes EMD Millipore Omnisolv), diethyl ether (EMD Millipore Omnisolv), and tetrahydrofuran (EMD Millipore Omnisolv) were sparged with ultra-high purity argon for 30 minutes and dried using an MBraun solvent purification system, then transferred to resealable Straus flasks and taken into the glove box where they were stored over 3Å molecular sieves. Acetonitrile (EMD HPLC) was stirred over calcium hydride (Alfa Aesar) in a sealed flask for at least twelve hours and degassed by several freeze-pump-thaw cycles, then vacuum-transferred to a resealable Straus flask and taken into the glove box, where it was stored over 3Å molecular sieves. Methanol (BDH), acetone (BDH), and hexanes used in benchtop work (BDH) were used as received.

Benzene-d_6 and THF-d_8 (Cambridge Isotope Laboratories) were dried over sodium benzophenone ketyl, degassed by several freeze-pump-thaw cycles, and vacuum-transferred into oven-dried resealable flasks. Dichloromethane-d_2 and acetonitrile-d_3 (Cambridge Isotope Laboratories) were dried over calcium hydride for at least twelve hours, degassed by several freeze-pump-thaw cycles, and vacuum-transferred into oven-dried resealable flasks.

Tetrachloroauric acid (Strem), dimethyl sulfide (Alfa Aesar), potassium carbonate (Alfa Aesar), silver acetate (Sigma-Aldrich), 2,4,6-trimethylaniline (Alfa Aesar), acetic

anhydride (Sigma Aldrich), triethylamine (J.T. Baker), sodium metal (Alfa Aesar), benzophenone (Alfa Aesar), 1,2-dichloroethane (EMD Millipore Omnisolv), 1,4-dimethoxybenzene (Alfa Aesar), nitrogen (NexAir), and argon (both industrial and ultra-high purity grades, NexAir) were used as received. *N*,*N*′-Bis(2,4,6-trimethylphenyl)imidazolium chloride,[50] *N*,*N*′-bis(2,4,6-trimethylphenyl)imidazolinium chloride,[51] (IMes)AuCl,[52] and (SIMes)AuCl[52] were prepared according to literature protocol and were characterized by ^{1}H NMR spectroscopy.

2.4.2 Analytical Measurements

^{1}H and ^{13}C spectra were obtained using a Varian Vx 400 MHz spectrometer. ^{1}H and ^{13}C NMR chemical shifts are referenced with respect to solvent signals and reported relative to tetramethylsilane. Infrared spectra were collected from neat solid samples using a Bruker Alpha-P infrared spectrometer equipped with an attenuated total reflection (ATR) attachment. Samples were exposed to air as briefly as possible prior to data collection. Elemental analyses were performed by Atlantic Microlab, Inc. in Norcross, Georgia.

2.4.3 Synthetic Procedures

2.4.3.1 (SIMes)AuOAc

(SIMes)AuCl (0.300 g, 0.557 mmol) was combined with silver acetate (0.139 g, 0.833 mmol) in a 20-mL scintillation vial. Dichloromethane (15 mL) was added and the suspension was stirred in the dark for 29 hours. The mixture was then filtered through a plug of Celite and evaporated *in vacuo* to afford the title complex as a white solid (0.310 g, 99%). ^{1}H NMR (400 MHz, CD_3CN): δ (ppm) 7.03 (s, 4H, CH_{Ar}), 4.03 (s, 4H, NCH_2), 2.32 (s, 12, *ortho*-CH_3), 2.31 (s, 6H, *para*-CH_3), 1.58 (s, 3H, OC(O)CH_3). ^{13}C{^{1}H} NMR (100 MHz,$CDCl_3$): δ (ppm) 189.00 (N*C*Au), 175.76 (O*C*(O)CH_3), 139.84 (C_{Ar}), 137.03 (C_{Ar}),

136.16 (C_{Ar}), 136.16 (C_{Ar}), 130.36 (C_{Ar}), 51.52 (NCH_2), 23.76 ($OC(O)CH_3$), 21.16 (CH_3),18.20 (CH_3. IR: $\nu(cm^{-1})$ 1629, 1497, 1440, 1357, 1307, 1273, 1032, 1008, 854, 681, 625, 575. Anal. Calcd for $C_{23}H_{29}N_2O_2Au$: C, 49.11; H, 5.20; N, 4.98. Found C, 48.84; H, 5.14; N, 4.96.

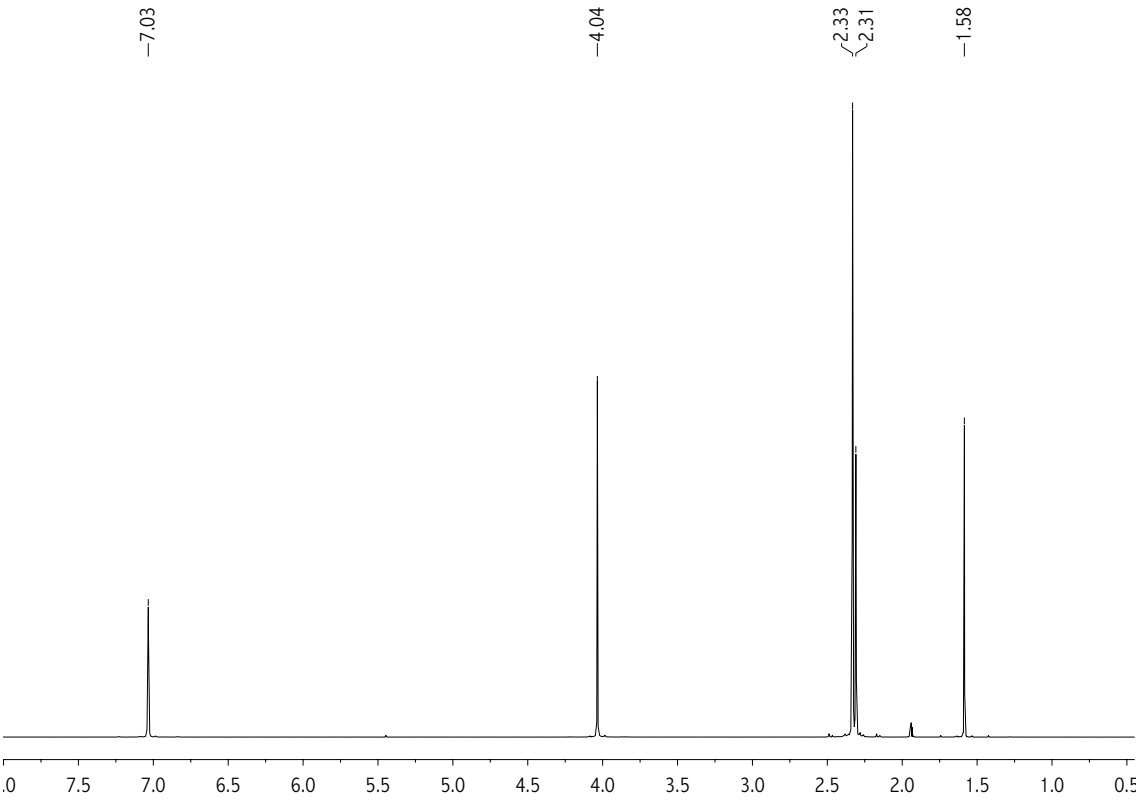

Figure 2.2. ^1H NMR spectrum of (SIMes)AuOAc in CD_3CN.

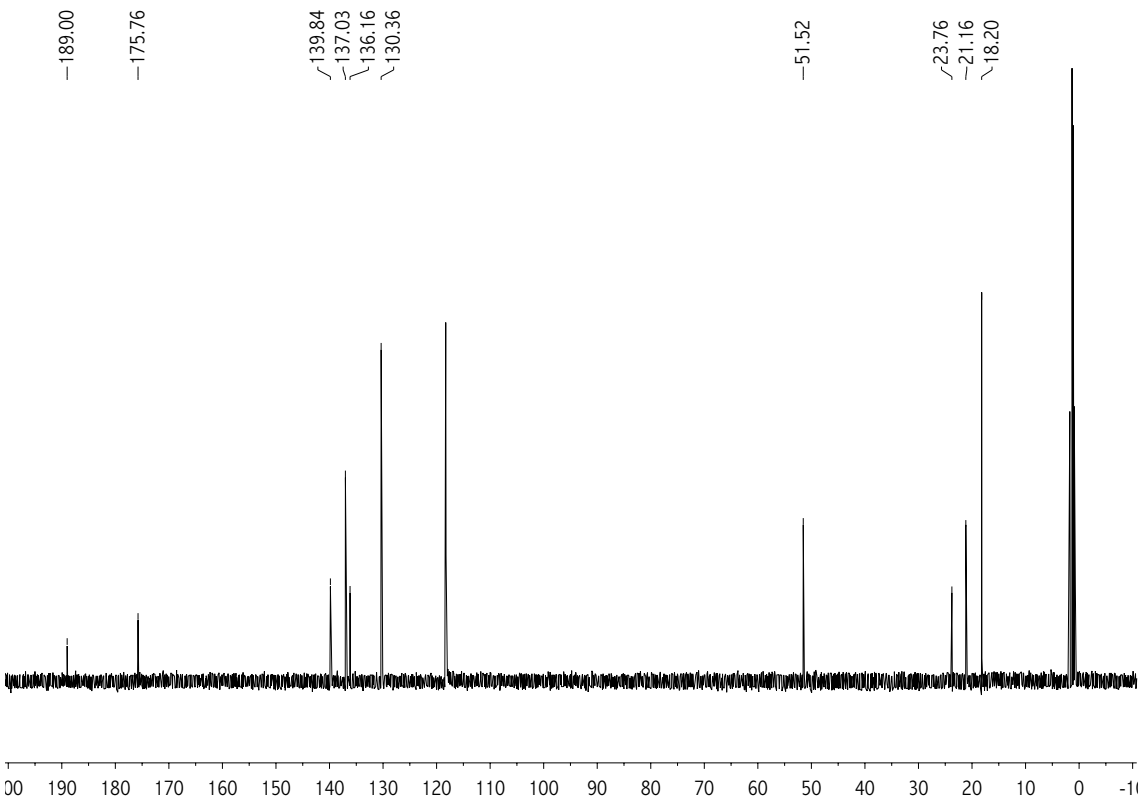

Figure 2.3. ^{13}C NMR spectrum of (SIMes)AuOAc in CD_3CN.

2.4.3.2 $\{[(SIMes)Au]_3(\mu_3\text{-}CCO)\}^+$ $[AcO{\bullet}2HOAc]^-$

(SIMes)AuOAc (0.106 g, 0.187 mmol) was dissolved in acetonitrile (2 mL) in a 10-mL Schlenk flask. Triethylamine (0.52 mL, 3.7 mmol) was added by syringe, and the reaction mixture was stirred for ten minutes. Acetic anhydride (0.18 mL, 1.9 mmol) was then added by syringe. The flask was covered in aluminum foil to exclude light, and stirring was continued for 16 hours. Volatiles were then removed *in vacuo* to give an oily residue. The flask was brought into the glovebox, the residue was dissolved in minimal acetonitrile (less than 1 mL), and the product was precipitated as a white solid by addition of cold diethyl ether. The precipitate was collected by vacuum filtration and washed with a small quantity of cold diethyl ether. Drying under vacuum afforded the title complex (0.108 g, 77%). ^1H NMR (400 MHz, CD_3CN): δ (ppm) 7.00 (s, 12H, *meta*-C*H*), 3.89 (s, 12H, NCH_2),

2.35 (s, 18H, *para*-CH_3), 2.19 (s, 36H, *ortho*-CH_3), 1.88 (s, 9H, OC(O)CH_3). $^{13}C\{^1H\}$ NMR (100 MHz, CD_3CN): δ (ppm) 203.8 (N*C*Au), 175.1 (OC(O)*C*H_3), 158.1 (C*C*O), 139.3 (C_{Ar}), 136.6 (C_{Ar}), 136.0 (C_{Ar}), 130.3 (C_{Ar}), 51.57 (N*C*H_2), 22.97 (O*C*(O)CH_3), 21.32 (CH_3),18.33 (CH_3), 5.09 (*C*CO). IR: ν (cm^{-1}) 2000, 1491, 1439, 1373, 1304, 1269, 1180, 1028, 849, 573. Anal. Calcd for $C_{71}H_{89}N_6O_7Au_3$: C, 49.31; H, 5.19; N, 4.86. Found C, 48.63; H, 5.20; N, 4.91.

Note: We have not obtained a satisfactory analysis for the above compound; however, it is suitable for use in the preparation of the analytically pure BF_4^- salt (*vide infra*).

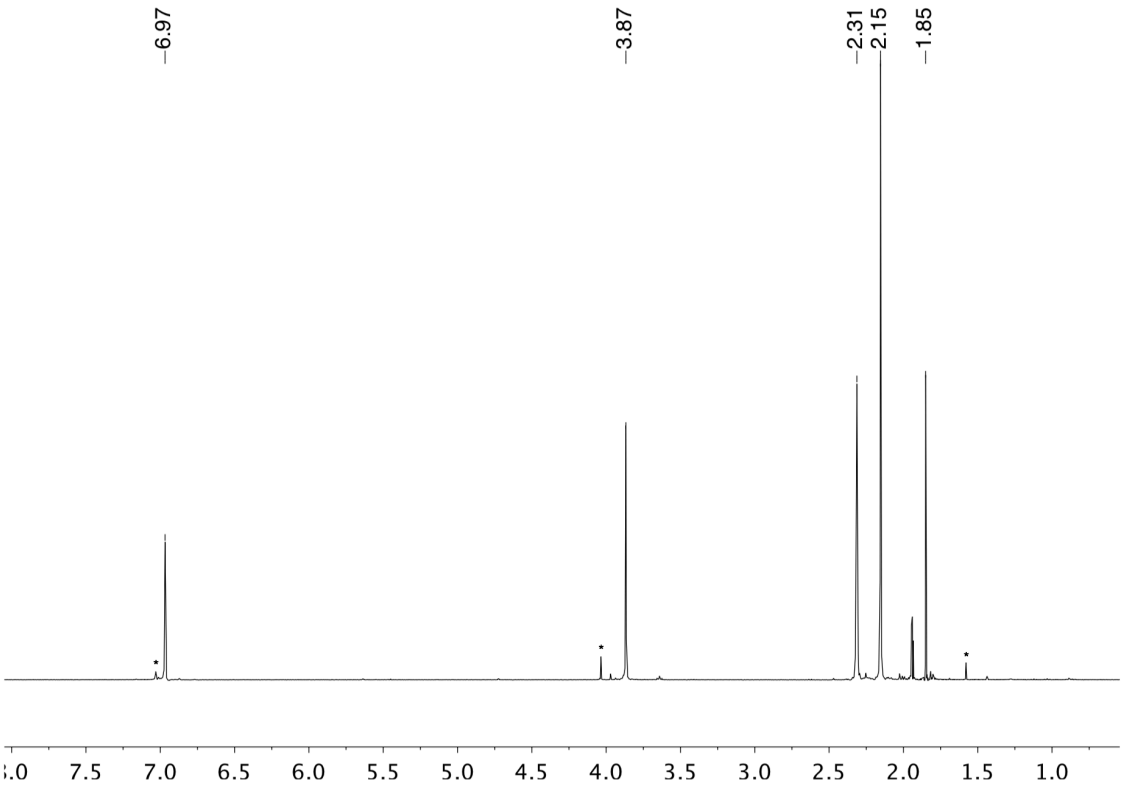

Figure 2.4. ^1H NMR spectrum of **1a** in CD_3CN solution. Asterisks denote residual (SIMes)Au(OAc), *ca.* 5 wt% calculated from integration.

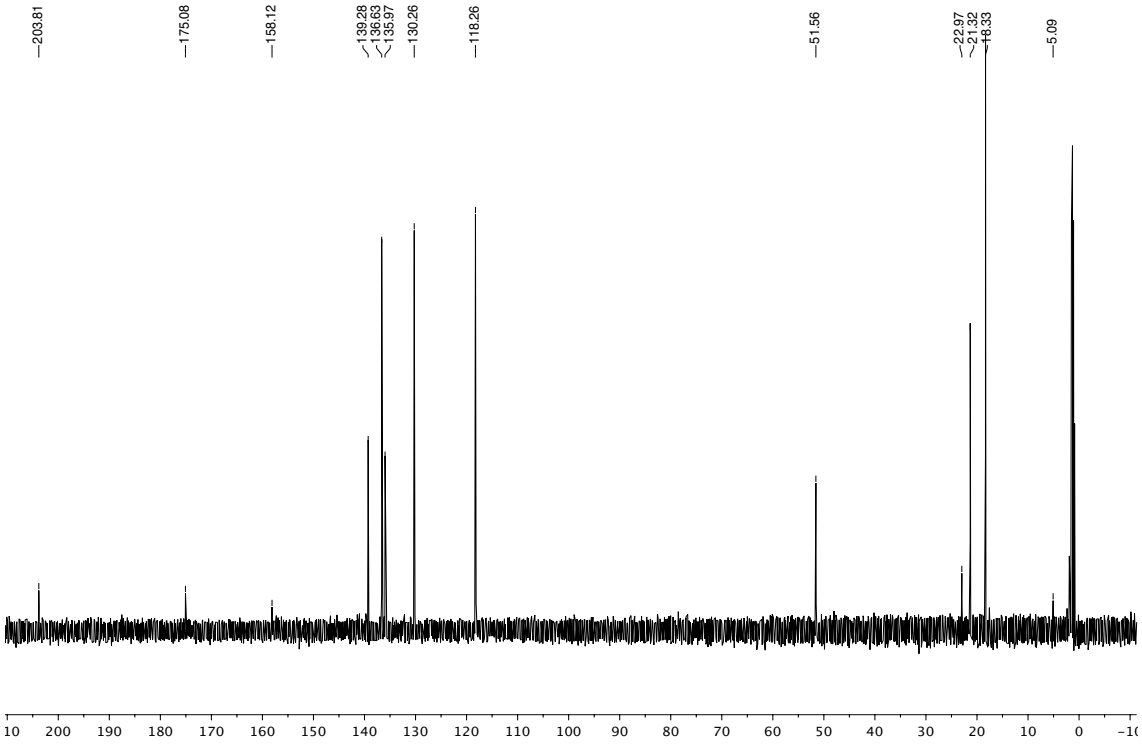

Figure 2.5. ^{13}C NMR spectrum of **1a** in CD_3CN solution.

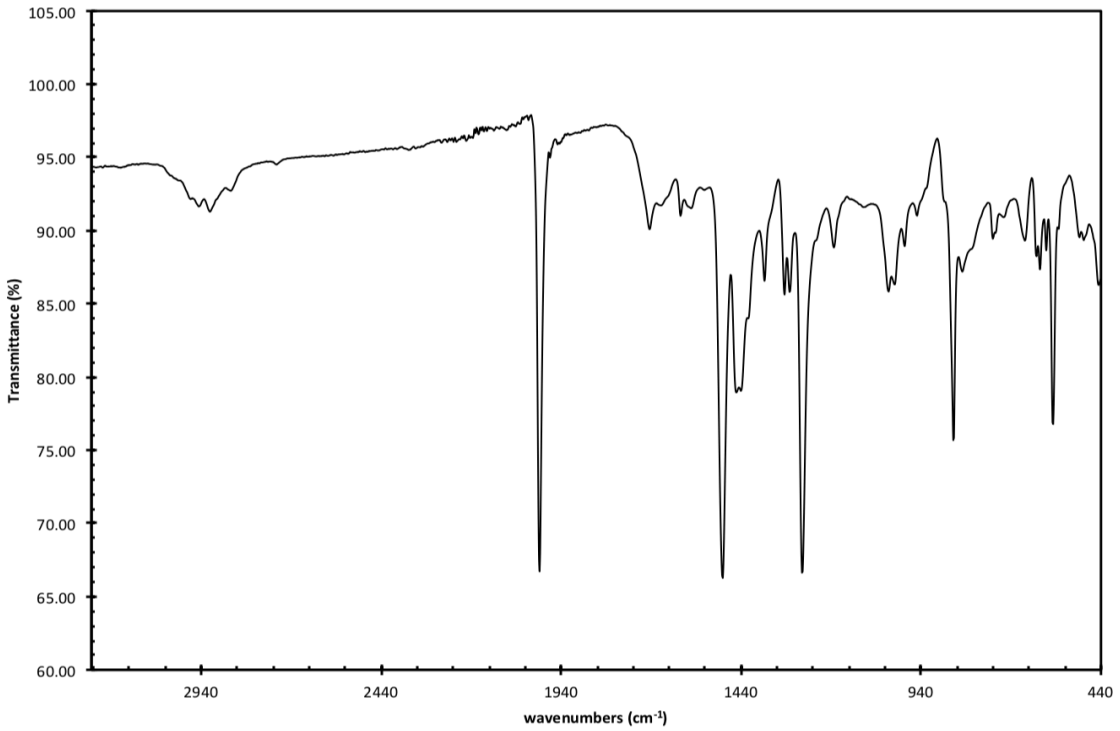

Figure 2.6. IR spectrum of spectrum of **1a**.

2.4.3.3 $\{[(SIMes)Au]_3(\mu_3\text{-}CCO)\}^+ [BF_4]^-$ (**1b**)

$\{[(SIMes)Au]_3(\mu_3\text{-}CCO)\}^+ [AcO{\bullet}2HOAc]^-$ (0.451 g, 0.261 mmol) was combined with sodium tetrafluoroborate (0.100 g, 0.91 mmol) in a 250-mL round bottom flask. THF (125 mL) was added and the suspension was stirred for 16 hours in the dark. The reaction mixture was then filtered twice through a plug of Celite into a 500-mL Schlenk flask, and the solvent was evaporated *in vacuo*. The resulting off-white solid was suspended in THF (*ca.* 4 mL) and a minimal volume of CH_2Cl_2 was added to achieve dissolution. The product was precipitated by addition of cold hexanes, collected by vacuum filtration and dried *in vacuo* to afford the title complex as a white solid (0.458 g, 89%). ^{1}H NMR (400 MHz, CD_2Cl_2): δ (ppm) 6.88 (s, 12H, *meta*-C*H*), 3.84 (s, 12H, NCH_2), 2.31 (s, 18H, *para*-CH_3), 2.12 (s, 36H, *ortho*-CH_3). ^{13}C{^{1}H} NMR (100 MHz, CD_2Cl_2): δ (ppm) 204.8 (N*C*Au), 158.2 (C*C*O), 138.6 (C_{Ar}), 136.0 (C_{Ar}), 136.0 (C_{Ar}), 135.4 (C_{Ar}), 51.35 (NCH_2)), 21.42 (CH_3), 18.34 (CH_3), 4.04 (*C*CO). IR: ν (cm^{-1}) 2912, 2013, 1608, 1489, 1452, 1373, 1317, 1267, 1028, 852, 577. ESI-MS(+): 1549.4 [M^+]. Anal. Calcd for $C_{65}H_{78}Au_3BF_4N_6O$: C, 47.69; H, 4.80; N, 5.13. Found C, 47.86; H, 4.67; N, 5.23.

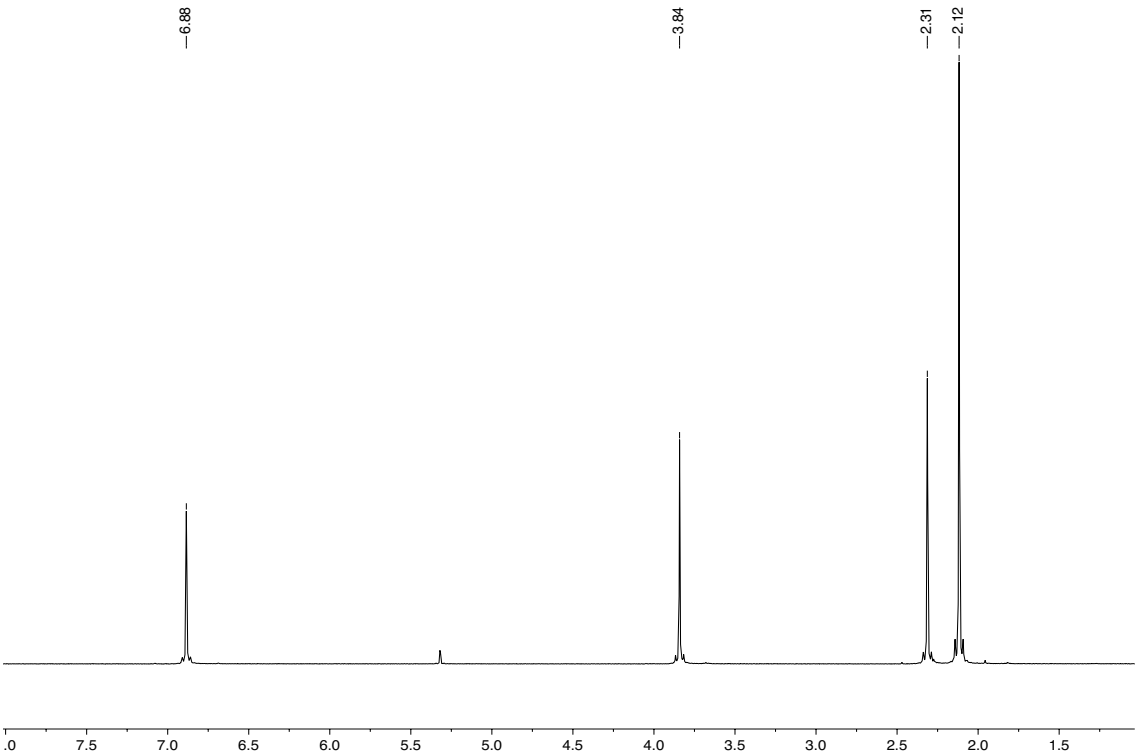

Figure 2.7. ^{1}H NMR spectrum of $\{[(SIMes)Au]_3(\mu_3\text{-}CCO)\}^+ [BF_4]^-$ in CD_2Cl_2.

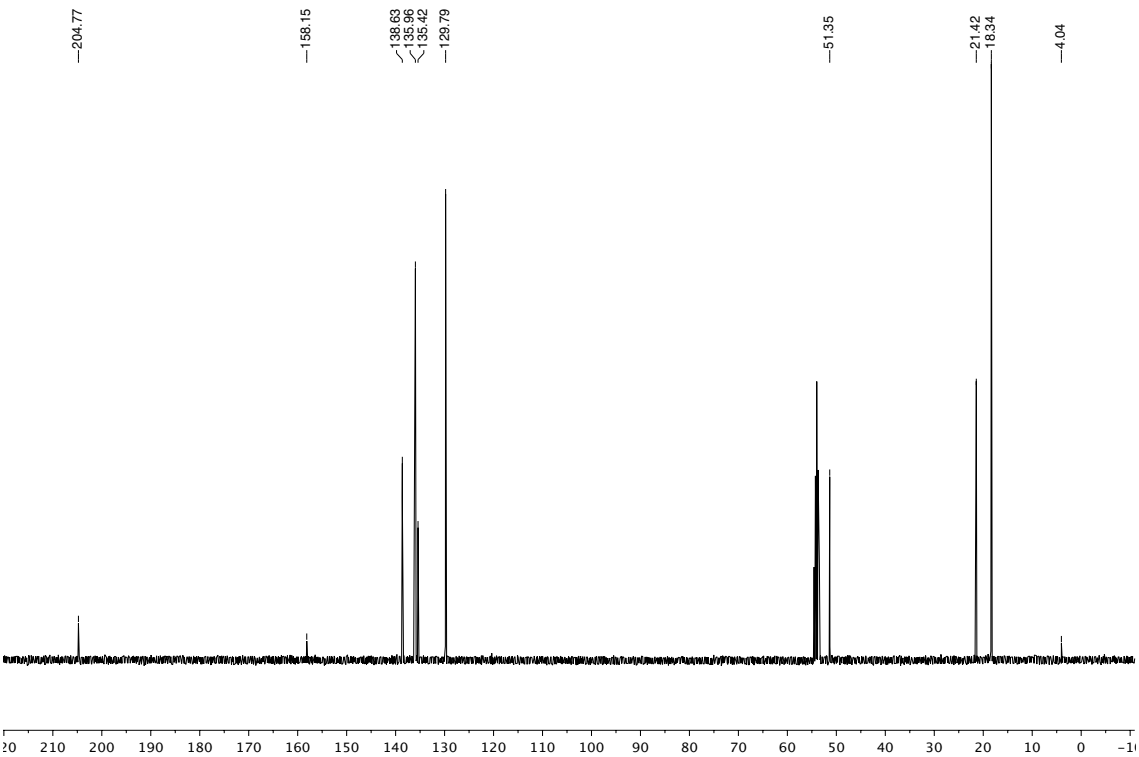

Figure 2.8. ^{13}C NMR spectrum of $\{[(SIMes)Au]_3(\mu_3\text{-}CCO)\}^+ [BF_4]^-$ in CD_2Cl_2.

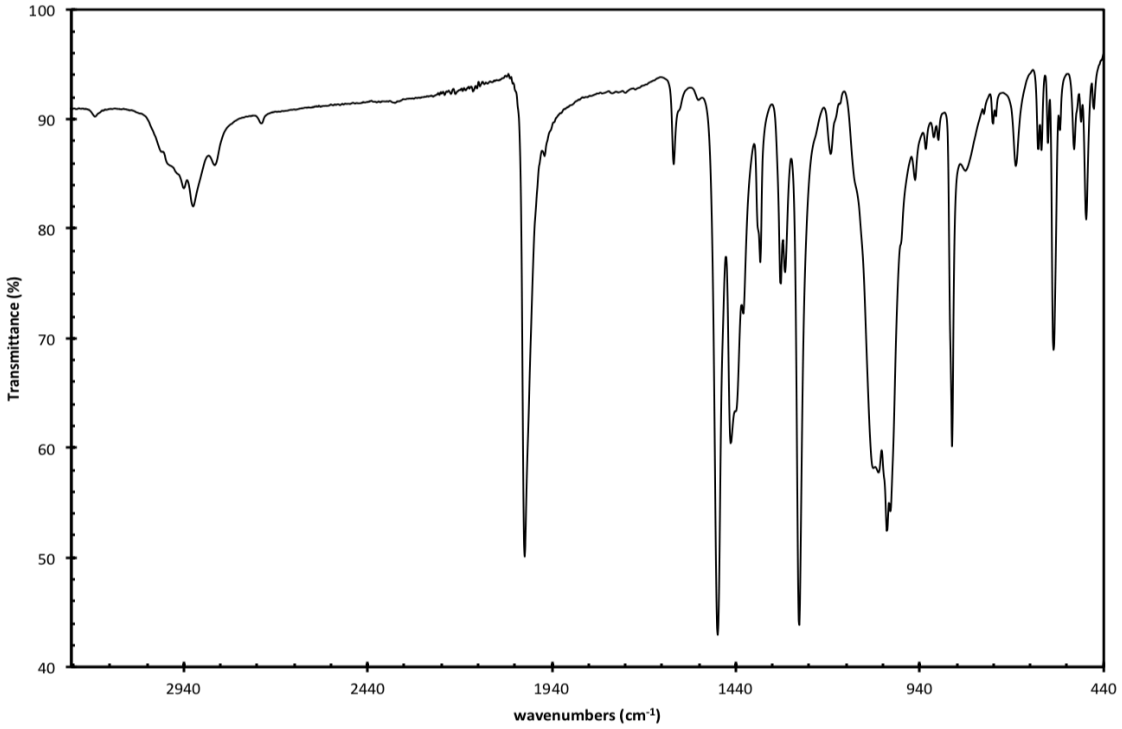

Figure 2.9. IR spectrum of $\{[(SIMes)Au]_3(\mu_3\text{-}CCO)\}^+ [BF_4]^-$.

2.4.3.4 (SIMes)AuH

Method A. $\{[(SIMes)Au]_3(\mu_3\text{-}CCO)\}^+ [AcO{\bullet}2HOAc]^-$ in CD_3CN. (0.299 g, 0.174 mmol) and $NaBH_4$ (0.029 g, 0.264 mmol) were combined in a 20-mL scintillation vial. THF (15 mL) was added and the suspension was stirred overnight. The reaction mixture was filtered through Celite to give a clear colorless solution. The solvent was evaporated *in vacuo* to give a white solid (0.212 g, 81%). ^{1}H NMR (400 MHz, THF-d_8): δ (ppm) 6.72 (s, 4H, *meta*-C*H*), 5.28 (s, 1H, Au-*H*), 2.99 (s, 4H, NCH_2), 2.20 (s, 12H, *ortho*-CH_3), 2.08 (s, 6H, *ortho*-CH_3). ^{13}C{^{1}H} NMR (100 MHz, THF-d_8): δ (ppm) 222.5 (N*C*Au), 138.6 (C_{Ar}), 136.8 (C_{Ar}), 130.2 (C_{Ar}), 129.2 (C_{Ar}), 51.80 (NCH_2), 21.35 (CH_3), 18.45 (CH_3). IR: ν (cm^{-1}) 2915, 1991, 1488, 1452, 1375, 1265, 1017, 851, 636, 576, 504, 487. Anal. Calcd for $C_{21}H_{27}AuN_2$: C, 50.01; H, 5.40; N, 5.55. Found C, 50.00; H, 5.48; N, 5.45.

Method B. $\{[(SIMes)Au]_3(\mu_3\text{-}CCO)\}^+ [BF_4]^-$ (0.015 g, 9.1 μmol) and $NaBH_4$ (0.025 g, 0.66 mmol) were combined in a 20-mL scintillation vial. THF-d_8 (1 mL) was added and the vial was capped and sealed with Parafilm. The vial was taken outside of the glove box and sonicated for 4.5 hours, resulting in a yellow solution. The vial was brought back into the glovebox, opened, and a solution of 4,4'-dimethylbiphenyl (0.010 g, 0.055 mmol) in THF-d_8 (0.5 mL) was added as internal standard. The yield of gold hydride, as determined by integration of its ^{1}H NMR signals relative to those of 4,4'-dimethylbiphenyl, was 88%.

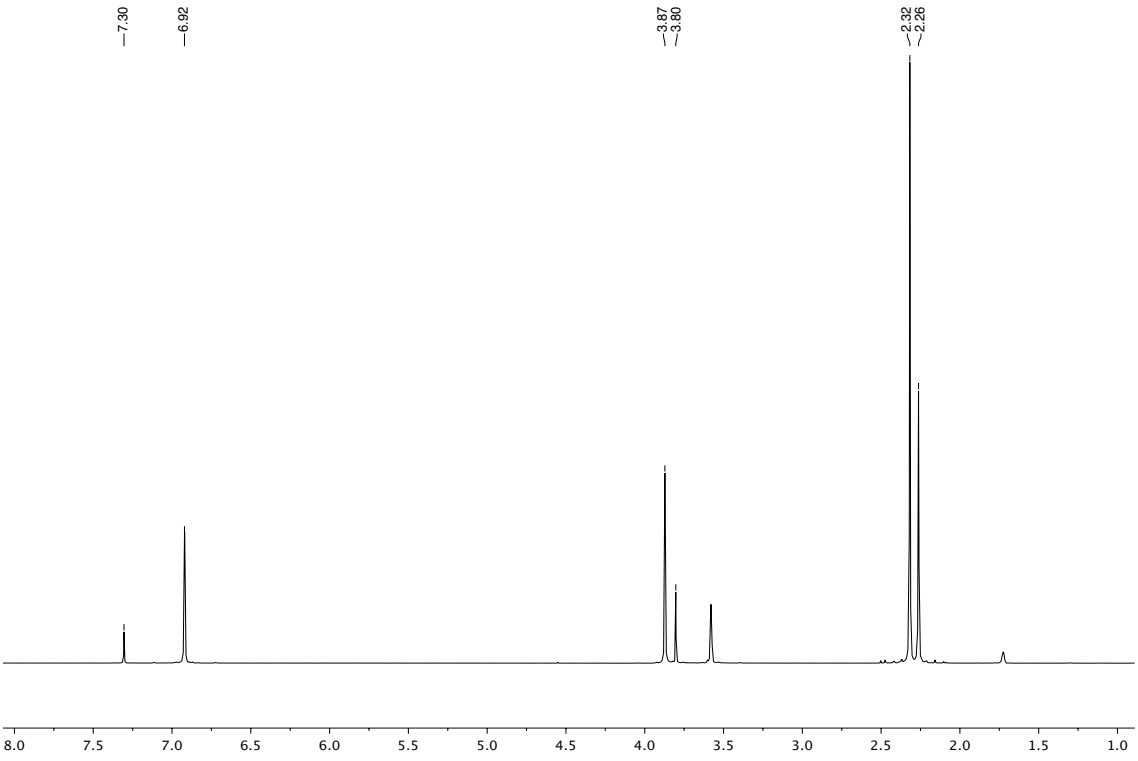

Figure 2.10. ^{1}HNMR spectrum of (SIMes)AuH in THF-d_8.

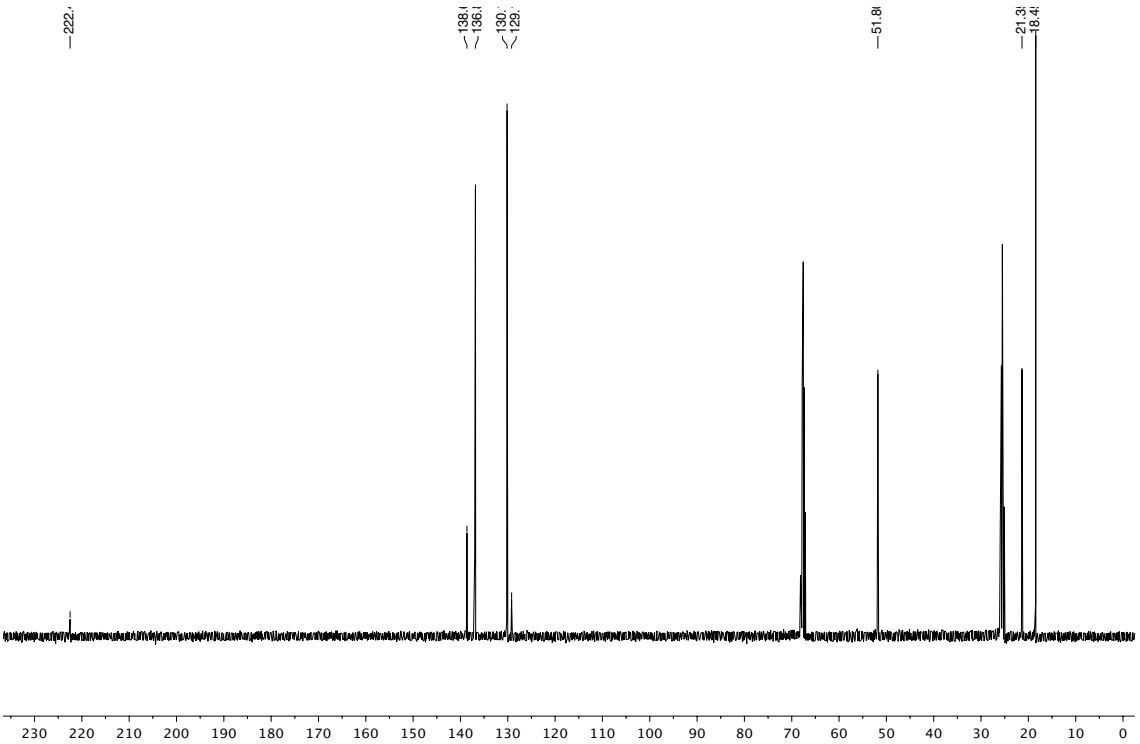

Figure 2.11. ^{1}HNMR spectrum of (SIMes)AuH in THF-d_8.

2.4.3.5 (SIMes)AuSPh

Method A. (SIMes)AuCl (0.100 g, 0.19 mmol) and K_2CO_3 (0.060 g, 0.43 mmol) were combined in a 20-mL scintillation vial. Acetone (15 mL) and thiophenol (0.019 mL, 0.19 mmol) and the reaction mixture was stirred and heated to 60°C for 15 hours. The solvent was removed *in vacuo* and the residue was dissolved again in DCM and filtered through Celite. The resulting clear, colorless solution was concentrated in vacuo to less than 1 mL. The product was precipitated by addition of hexanes and collected by vacuum filtration, affording the title complex as a white solid (0.116 g, 100%). ^{1}H NMR (400 MHz, CD_2Cl_2): δ (ppm) 7.03 (s, 4H, *meta*-C*H*), 6.76 (m, SC_6H_5), 4.01 (s, 4H, NCH_2), 2.37 (s, 12H, *ortho*-CH_3), 2.35 (s, 6H, *ortho*-CH_3). ^{13}C{^{1}H} NMR (100 MHz, CD_2Cl_2): δ (ppm) 204.85 (N*C*Au), 144.43 (C_{Ar}), 139.26 (C_{Ar}), 136.47 (C_{Ar}), 135.39 (C_{Ar}), 131.76 (C_{Ar}), 129.98 (C_{Ar}), 127.78 (C_{Ar}), 122.45 (C_{Ar}), 51.37 (NCH_2), 21.45 (CH_3), 18.31 (CH_3). IR: ν (cm^{-1}) 2917,

1578, 1495, 1470, 1457, 1376, 1321, 1181, 1086, 1024, 858, 736, 690, 613, 572, 479. Anal. Calcd for $C_{27}H_{31}AuN_2S$: C, 52.94; H, 5.10; N, 4.57. Found C, 52.45; H, 5.01; N, 4.56.

Method B. $\{[(SIMes)Au]_3(\mu_3\text{-}CCO)\}^+ [BF_4]^-$ (0.025 g, 0.015 mmol) was combined with 1,4-dimethoxybenzene (2.4 mg, 0.017 mmol) as an integration standard in a 20-mL scintillation vial. The solids were dissolved in CD_2Cl_2 (1.2 mL) and combined with thiophenol (5.0 µL, 0.049 mmol) and finely divided sodium thiophenolate (3 mg, 0.02 mmol). The vial was capped and sonicated for 15 minutes, then left to stand for 1.5 h. The ^1H NMR spectrum was acquired, and integration relative to 1,4-dimethoxybenzene indicated quantitative formation of both *S*-phenyl thioacetate and (SIMes)AuSPh. Volatiles were separated from the reaction mixture by vacuum transfer and the formation of *S*-phenyl thioacetate was confirmed by GC-MS: 152 $[M^+]$.

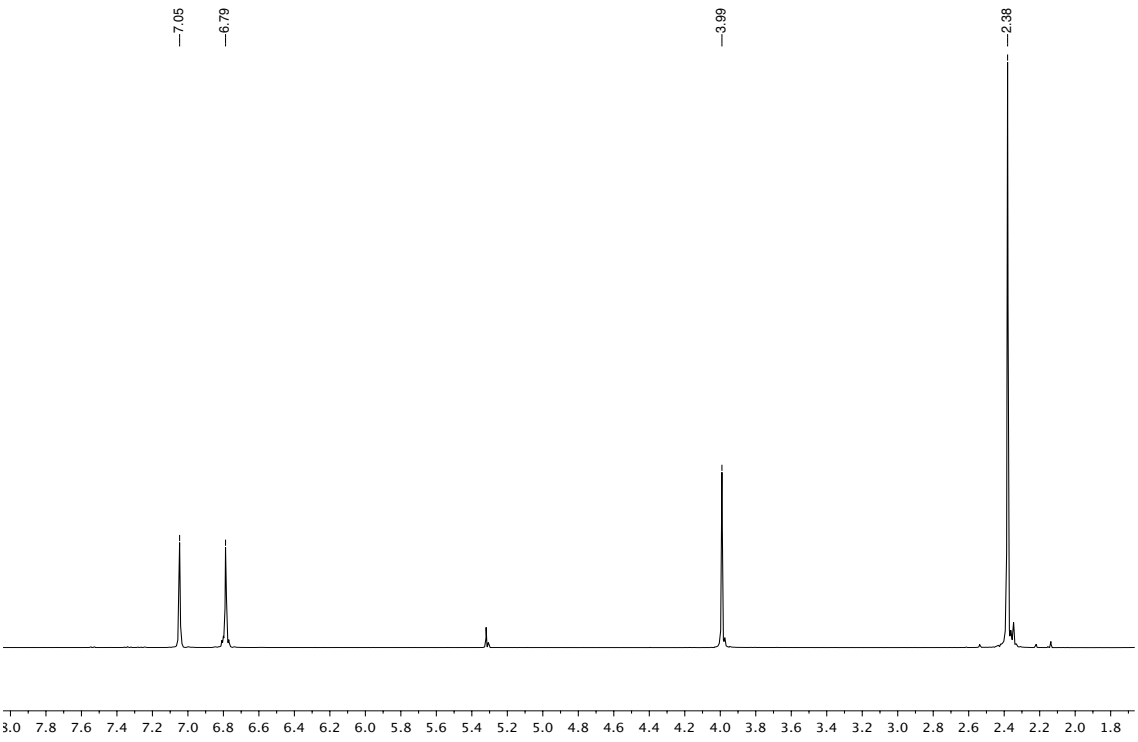

Figure 2.12. ^1H NMR spectrum of (SIMes)AuSPh in CD_2Cl_2.

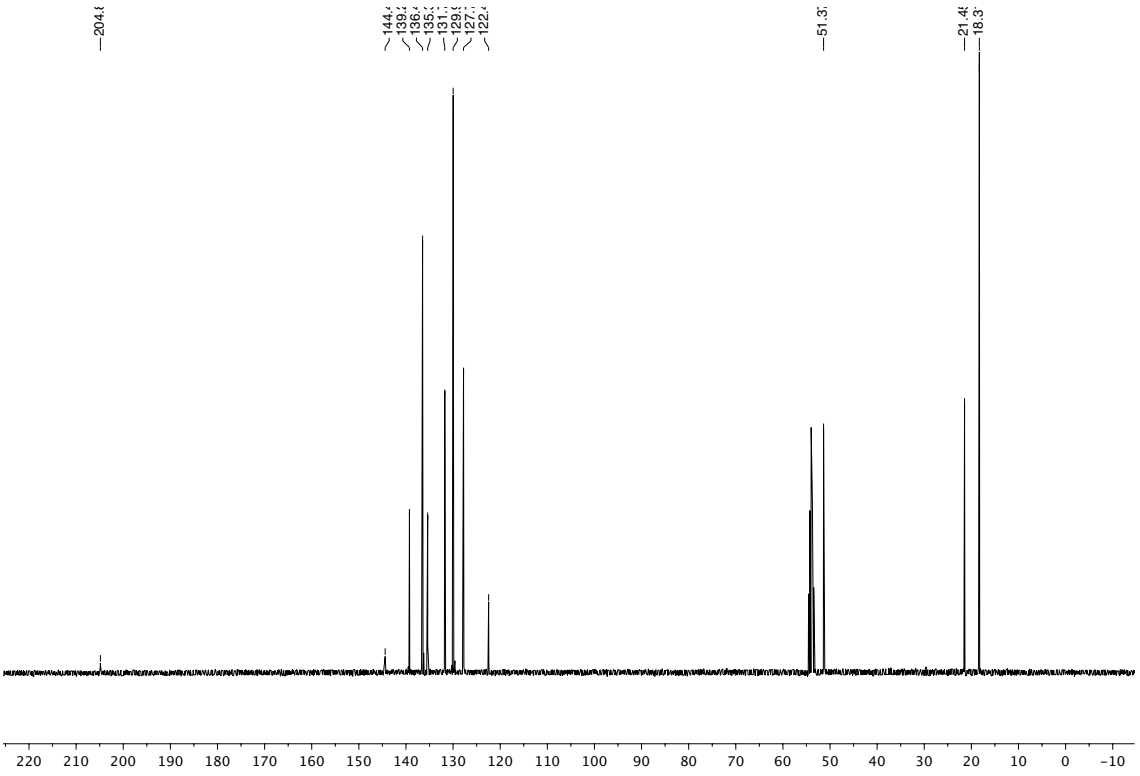

Figure 2.13. ^{13}C NMR spectrum of (SIMes)AuSPh in CD_2Cl_2.

2.4.4 X-Ray Diffraction Studies

Careful layering of hexanes onto a solution of **1b** in CH_2Cl_2 afforded crystals suitable for X-ray diffraction. A colourless prism-shaped crystal with dimensions 0.54 mm × 0.29 mm × 0.25 mm was mounted on a loop with Paratone oil. Data were collected using a Bruker APEX-II CCD diffractometer equipped with an Oxford Cryosystems low-temperature apparatus operating at T = 110(2) K.

Data were measured using ϕ and ω scans of 0.50° per frame for 20.00 s using MoK_α radiation (fine-focus sealed tube, 45 kV, 35 mA). The total number of runs and images was based on the strategy calculation from the program APEX2.[53] The achieved resolution was Θ = 29.131°.

Cell parameters were retrieved using the SAINT (Bruker, V8.34A, 2013) software[54] and refined using SAINT (Bruker, V8.34A, 2013) on 9900 reflections. Data reduction was

performed using the SAINT (Bruker, V8.34A, 2013) software which corrects for Lorentz polarization. The final completeness is 99.50 out to 29.131 in Θ. The absorption coefficient (μ) of this material is 5.948 mm^{-1} and the minimum and maximum transmissions are 0.4393 and 0.7460.

The structure was solved in the space group C2/c (# 15) by Direct Methods using the ShelXS-97[54] structure solution program and refined by Least Squares using version of ShelXL-97.[55-56] All non-hydrogen atoms were refined anisotropically. Hydrogen atom positions were calculated geometrically and refined using the riding model.

Crystal Data. $C_{68}H_{84}Au_3BCl_6F_4N_6O$, M_r = 1891.82, monoclinic, C2/c (No. 15), a = 26.3296 Å, b = 16.6923 Å, c = 35.211 Å, β = 94.1020(10)°, α = γ = 90°, V = 15435.6(17) $Å^3$, T = 110(2) K, Z = 8, Z' = 1, $\mu(MoK_\alpha)$ = 5.948 mm^{-1}, 85573 reflections measured, 20690 unique (R_{int} = 0.0500) which were used in all calculations. The final wR_2 was 0.1139 (all data) and R_1 was 0.0465 (I > 2(I)).

2.5 Acknowledgements

We thank the U.S. National Science Foundation (CHE- 1300659 to J.P.S.) and the Georgia Institute of Technology for generous support of this research. Professor Jake D. Soper kindly allowed us the use of his group's FTIR and UV−vis spectrometers.

2.6 References

1. Jensen, M. P.; Shriver, D. F. Carbon-carbon and carbonyl transformations in ketenylidene cluster compounds. *J. Mol. Catal.* **1992,** *74* (1-3), 73-84.

2. Hallgren, J. E.; Eschbach, C. S.; Seyferth, D. Carbatricobalt decacarbonyl cation. Novel acylating agent. *J. Am. Chem. Soc.* **1972,** *94* (7), 2547-2549.

3. Seyferth, D.; Hallgren, J. E.; Eschbach, C. S. Organocobalt cluster complexes. XV. New route to organofunctional organocobalt cluster complexes based on the tricobaltcarbon decacarbonyl cation. *J. Amer. Chem. Soc.* **1974,** *96* (6), 1730-7.

4. D'Agostino, M. F.; Mlekuz, M.; Kolis, J. W.; Sayer, B. G.; Rodger, C. A.; Halet, J. F.; Saillard, J. Y.; McGlinchey, M. J. Carbon-13 NMR and EHMO studies on Seyferth's $[Co_3(CO)_9CCO]^+$ cluster: to bend or not to bend. *Organometallics* **1986,** *5* (11), 2345-2350.

5. Sievert, A. C.; Strickland, D. S.; Shapley, J. R.; Steinmetz, G. R.; Geoffroy, G. L. Conversion of a bridging methylene ligand to a ketenylidene moiety. Synthesis and reactivity of carbomethoxymethylidynenonacarbonyldihydrotriosmium. *Organometallics* **1982,** *1* (1), 214-215.

6. Shapley, J. R.; Strickland, D. S.; St. George, G. M.; Churchill, M. R.; Bueno, C. Coupling of methylidyne and carbonyl ligands on the triosmium cluster framework. Crystal structure of $(\mu\text{-H})_2Os_3(CO)_9(\mu_3\text{-}\eta^1\text{-CCO})$. *Organometallics* **1983,** *2* (1), 185-187.

7. Holmgren, J. S.; Shapley, J. R. Synthesis, characterization, and reactivity of $HRu_3(CO)_{10}(CH)$ and $H_2Ru_3(CO)_9(CCO)$. *Organometallics* **1984,** *3* (8), 1322-1323.

8. Kolis, J. W.; Holt, E. M.; Drezdzon, M.; Whitmire, K. H.; Shriver, D. F. A reactive three-metal carbide cluster precursor, $[Fe_3(CO)_9(CCO)]^{2-}$. *J. Am. Chem. Soc.* **1982,** *104* (22), 6134-6135.

9. Kolis, J. W.; Holt, E. M.; Shriver, D. F. Synthesis, x-ray crystal structure, and chemistry of a metal cluster ketenylidene, $[Fe_3(CO)_9(CCO)]^{2-}$, with carbide-like reactivity. *J. Am. Chem. Soc.* **1983,** *105* (25), 7307-13.

10. Kolis, J. W.; Holt, E. M.; Hriljac, J. A.; Shriver, D. F. Mixed-metal cluster carbides and a mixed-metal ketenylidene with nucleophilic carbide sites. *Organometallics* **1984,** *3* (3), 496-498.

11. Sailor, M. J.; Shriver, D. F. Preparation, structure and reactivity of an anionic ruthenium ketenylidene: $[PPN]_2[Ru_3(CO)_6(\mu\text{-}CO)_3(\mu_3\text{-}CCO)]$. *Organometallics* **1985,** *4* (8), 1476-1478.

12. Sailor, M. J.; Brock, C. P.; Shriver, D. F. Alkylation reactions of the CCO ligand in triruthenium carbonyl clusters. Synthesis and x-ray crystal structure of $Ru_3(CO)_9(\mu_3\text{-}CO)[\mu_3\text{-}C{=}C(OCH_3)CH_3]$. *J. Am. Chem. Soc.* **1987,** *109* (20), 6015-6022.

13. Went, M. J.; Sailor, M. J.; Bogdan, P. L.; Brock, C. P.; Shriver, D. F. Synthesis and chemistry of $[Os_3(CO)_9(\mu_3\text{-}CCO)]^{2-}$. Metal ensemble effects on the reactions of the CCO ligand. *J. Am. Chem. Soc.* **1987,** *109* (20), 6023-6029.

14. Gunale, A. S.; Jensen, M. P.; Stern, C. L.; Shriver, D. F. Synthesis and crystal structure of a four-metal ketenylidene: $[PPN]_2[Fe_3CuI(CO)_9(CCO)]$. *J. Am. Chem. Soc.* **1991,** *113* (4), 1458-1460.

15. Hriljac, J. A.; Shriver, D. F. Cluster-assisted formation and cleavage of carbon-hydrogen and carbon-carbon bonds. $[Fe_3(CO)_9(CCO)]^{2-}$ and its acetylide and alkyne derivatives. *J. Am. Chem. Soc.* **1987,** *109* (20), 6010-6015.

16. Thöne, C.; Vahrenkamp, H. Aurated clusters derived from (μ3-ketenylidene)-Fe3 and -Fe2Co clusters. *Journal of Organometallic Chemistry* **1995,** *485* (1), 185-189.

17. Calderazzo, F.; Englert, U.; Guarini, A.; Marchetti, F.; Pampaloni, G.; Segre, A. $[Zr_3Cp_2\{O_2CN(CHMe_2)_2\}_6(\mu_3\text{-}O)(\mu_2\text{-}CCO)]$, the first structurally characterized Ketenylidene complex, a model for reductive CO cleavage on metal surface. *Angew. Chem.* **1994,** *106* (11), 1254-1256.

18. Calderazzo, F.; Englert, U.; Guarini, A.; Marchetti, F.; Pampaloni, G.; Segre, A.; Tripepi, G. Zirconium(II)- and hafnium(II)-assisted reductive coupling of coordinated carbonyl groups leading to ketenylidene complexes of zirconium(IV) and hafnium(IV). *Chem. - Eur. J.* **1996,** *2* (4), 412-419.

19. Neithamer, D. R.; LaPointe, R. E.; Wheeler, R. A.; Richeson, D. S.; Van Duyne, G. D.; Wolczanski, P. T. Carbon monoxide cleavage by $(silox)_3Ta$ (silox = *tert*-Bu_3SiO^-): physical, theoretical, and mechanistic investigations. *J. Am. Chem. Soc.* **1989,** *111* (25), 9056-9072.

20. List, A. K.; Hillhouse, G. L.; Rheingold, A. L. A carbon-carbon bond cleavage reaction of carbon suboxide at a metal center. Synthesis and structural characterization of $WCl_2(CO)(PMePh_2)_2\{C,C':\eta_2\text{-}C(O)CPMePh_2\}$. *J. Am. Chem. Soc.* **1988,** *110* (14), 4855-4856.

21. Blues, E. T.; Bryce-Smith, D.; Lawston, I. W.; Wall, G. D. Gold(I) ketenide. *Journal of the Chemical Society, Chemical Communications* **1974,** (13), 513-514.

22. Blues, E. T.; Bryce-Smith, D.; Hirsch, H.; Simons, M. J. Silver ketenide. *J. Chem. Soc. D* **1970,** (11), 699-701.

23. Blues, E. T.; Bryce-Smith, D.; Kettlewell, B.; Roy, M. Copper(I) ketenide. *J. Chem. Soc., Chem. Commun.* **1973,** (23), 921.

24. Blues, E. T.; Bryce-Smith, D.; Shaoul, R.; Hirsch, H.; Simons, M. J. Preparation, properties and structure of crystalline silver ketenide (μ-oxoethenylidene disilver) and its pyridine complex. *J. Chem. Soc., Perkin Trans. 2* **1993,** *9*, 1631-42.

25. Femi-Onadeko, B. Heterogeneous phase oxidation of propylene by molecular oxygen catalyzed by silver(I) and copper(I) ketenides. *Ann. Chim.* **1982,** *72* (9-10), 511-519.

26. Femi-Onadeko, B. Stoichiometric reaction of copper(I) ketenide-oxygen adduct with cyclohexene. *Pol. J. Chem.* **1986,** *60* (1-3), 297-299.

27. Femi-Onadeko, B. Heterogeneous phase oxidation of olefins by oxygen catalyzed by an organometallic compound (Cu_2C_2O). I. *Acta Chim. Hung.* **1986,** *122* (2), 175-180.

28. Bryce-Smith, D., Metal ketenides in the catalytic epoxidation of olefins. *Chem. Ind.* **1975,** (4), 154-157.

29. Girolami, G. S.; Jeffries, P. M.; Dubois, L. H. Mechanistic studies of copper thin-film growth from Cu^{I} and Cu^{II} β-diketonates. *J. Am. Chem. Soc.* **1993,** *115* (3), 1015-1024.

30. Alcarazo, M.; Lehmann, C. W.; Anoop, A.; Thiel, W.; Fürstner, A. Coordination chemistry at carbon. *Nat. Chem.* **2009,** *1* (4), 295-301, S295/1-S295/13.

31. Green, I. X.; Tang, W.; Neurock, M.; Yates, J. T., Jr. Localized partial oxidation of acetic acid at the dual perimeter sites of the Au/TiO_2 catalyst-formation of gold ketenylidene. *J Am Chem Soc* **2012,** *134* (33), 13569-13572.

32. Green, I. X.; Tang, W.; Neurock, M.; Yates, J. T., Jr. Mechanistic insights into the partial oxidation of acetic acid by O_2 at the dual perimeter sites of a Au/TiO_2 catalyst. *Faraday Discuss* **2013,** *162*, 247-265.

33. Green, I. X.; Tang, W.; Neurock, M.; Yates, J. T., Jr. Insights into Catalytic Oxidation at the Au/TiO_2 Dual Perimeter Sites. *Acc. Chem. Res.* **2014,** *47* (3), 805-815.
34. Kinastowski, S.; Nowacki, A., β-Lactone as intermediate in the Perkin reaction catalyzed by tertiary amines. *Tetrahedron Lett.* **1982,** *23* (36), 3723-3724.
35. Lazreg, F.; Cordes, D. B.; Slawin, A. M. Z.; Cazin, C. S. J. Synthesis of Homoleptic and Heteroleptic Bis-N-heterocylic Carbene Group 11 Complexes. *Organometallics* **2015,** *34* (2), 419-425.
36. Arduengo, A. J., III; Krafczyk, R.; Schmutzler, R.; Craig, H. A.; Goerlich, J. R.; Marshall, W. J.; Unverzagt, M. Imidazolylidenes, imidazolinylidenes and imidazolidines. *Tetrahedron* **1999,** *55* (51), 14523-14534.
37. Bondi, A. van der Waals volumes and radii. *J. Phys. Chem.* **1964,** *68* (3), 441-51.
38. Schmidbaur, H.; Schier, A. Aurophilic interactions as a subject of current research: an up-date. *Chem. Soc. Rev.* **2012,** *41* (1), 370-412.
39. Bertani, R.; Casarin, M.; Pandolfo, L. The organometallic chemistry of $Ph_3P{=}C{=}C{=}O$. A route to metal-substituted ketenes. *Coord. Chem. Rev.* **2003,** *236* (1-2), 15-33.
40. Raubenheimer, H. G.; Schmidbaur, H. Gold chemistry guided by the isolobality concept. *Organometallics* **2012,** *31* (7), 2507-2522.
41. Daly, J. J.; Wheatley, P. J. Structure of triphenylphosphoranylideneketene. *J. Chem. Soc., A* **1966,** (12), 1703-1706.
42. Davlieva, M. G.; Lindeman, S. V.; Neretin, I. S.; Kochi, J. K. Structural effects of carbon monoxide coordination to carbon centers. π and σ bindings in aliphatic acyl versus aromatic aroyl cations. *New J. Chem.* **2004,** *28* (12), 1568-1574.
43. Duncan, J. L.; Munro, B. The ground state average structure of ketene. *J. Mol. Struct.* **1987,** *161*, 311-319.
44. Palacios, F.; Alonso, C.; Aparicio, D.; Rubiales, G.; de los Santos, J. M. The aza-Wittig reaction. An efficient tool for the construction of carbon-nitrogen double bonds. *Tetrahedron* **2007,** *63* (3), 523-575.

45. Hartley, R. C.; McKiernan, G. J. Titanium reagents for the alkylidenation of carboxylic acid and carbonic acid derivatives. *J. Chem. Soc., Perkin Trans. 1* **2002,** (24), 2763-2793.

46. Hansmann, M. M.; Rominger, F.; Hashmi, A. S. K. Gold-allenylidenes - an experimental and theoretical study. *Chem. Sci.* **2013,** *4* (4), 1552-1559.

47. Xiao, X.-S.; Zou, C.; Guan, X.; Yang, C.; Lu, W.; Che, C.-M. Homoleptic gold(I) N-heterocyclic allenylidene complexes: excited-state properties and lyotropic chromonics. *Chem. Commun.* **2016,** *52* (28), 4983-4986.

48. Tsui, E. Y.; Müller, P.; Sadighi, J. P. Reactions of a stable monomeric gold(I) hydride complex. *Angew. Chem., Int. Ed.* **2008,** *47* (46), 8937-8940.

49. Kashyap, B.; Phukan, P. A new ferrocene-based bulky pyridine as an efficient reusable homogeneous catalyst. *RSC Adv.* **2013,** *3* (35), 15327-15336.

50. Bantreil, X.; Nolan, S. P. Synthesis of N-heterocyclic carbene ligands and derived ruthenium olefin metathesis catalysts. *Nat. Protocols* **2011,** *6* (1), 69-77.

51. Kuhn, K. M.; Grubbs, R. H. A Facile Preparation of Imidazolinium Chlorides. *Organic Letters* **2008,** *10* (10), 2075-2077.

52. Collado, A.; Gomez-Suarez, A.; Martin, A. R.; Slawin, A. M. Z.; Nolan, S. P. Straightforward synthesis of [Au(NHC)X] (NHC = N-heterocyclic carbene, X = Cl, Br, I) complexes. *Chemical Communications* **2013,** *49* (49), 5541-5543.

53. *APEX2 suite for crystallographic software*, Bruker AXS: 2014.

54. *SAINT-8.34A-2013 Software for the Integration of CCD Detector System Bruker Analytical X-ray Systems*, Bruker AXS: 2013.

55. Sheldrick, G. A short history of SHELX. *Acta Crystallographica Section A* **2008,** *64* (1), 112-122.

56. Sheldrick, G. SHELXT - Integrated space-group and crystal-structure determination. *Acta Crystallographica Section A* **2015,** *71* (1), 3-8.

CHAPTER 3

AN *N*-(TRIAUROMETHYL)PYRIDINIUM CATION AND RELATED SPECIES

3.1 Background

Surface-bound transition metal carbides are intermediates in Fischer-Tropsch synthesis.[1,2] Molecular transition metal carbide clusters have been studied as models of these intermediates.[3,4,5] Early reported molecular transition metal carbides were high nuclearity clusters composed of six or more metal atoms supported by carbonyl ligands. These compounds exhibited low reactivity at the carbide carbon due to shielding by the metal framework.[6] In an effort to increase reactivity at the bridging carbide carbon, lower nuclearity carbide clusters were sought. Terminal mononuclear carbides,[7,8] linear dinuclear carbides[9-13] and tetranuclear carbides have been well studied;[14-16] however, trigonal planar μ_3-carbide clusters are rare.[17] Known planar trinuclear carbide clusters include a $[Ru_2PtC]$ carbide, and a series of $[Ru_2MC]$ (M = Cu, Ag, Au) carbides prepared from a bent singlet-carbene-like diruthenium carbide precursor described by Matsuzaka.[5,18,19] In another example, Willis reports a cyclic tetramer containing four planar μ_3-carbides with the formula $[(Tp^*)(OC)_2WAuC]_4$. This species functions as an intermediate in carbide transfer from tin to palladium.[20] Popov described a μ_3-carbide with a $[Lu_2TiC]^{6+}$ core, which was stabilized by encapsulation in a fullerene cage.[21]

Adducts of μ_3-carbide clusters demonstrating both nucleophilic and electrophilic carbide-like behavior have been studied. The trinuclear carbonyl-supported iron ketenylidene dianion $[Fe_3(CO)_9(CCO)]^{2-}$ exhibits nucleophilic carbide-like reactivity, forming the corresponding μ_3-methylidyne and μ_3-ethylidyne clusters by reaction with acetic acid and methyl triflate respectively[2]. The trinuclear osmium cluster bridged by the

diazo(methylidyne) ligand exhibits electrophilic carbide-like reactivity with CO to form the corresponding μ_3-ketenylidene cluster.[23]

The search for a reactive planar trigold(I) carbido cation $\{[(L)Au]_3C\}^+$ bearing the C^{2-} bridging ligand has been elusive, whereas higher nuclearity gold(I) carbides bearing the C^{4-} bridging ligand were previously prepared quite serendipitously. These closed shell tetra-, penta-, and hexagold(I) carbides[24-27] exemplify the tendency of LAu^+ to aggregate about bridging main group elements to form hypercoordinate clusters due to aurophilic interactions.[28] Schmidbaur *et. al.* reported many examples of hypercoordinate gold(I) carbides, which resulted under reaction conditions that one could readily expect to give lower nuclearity species. For example, when two equivalents of $(Ph_3P)AuCl$ were combined with a single equivalent of trimethylsilylmethylene(triphenylphosphonium)ylide $H(Me_3Si)C{=}PPh_3$, followed by addition of excess CsF, the tri- rather than diaurated product resulted, $[(Me_3P)C[Au(PPh_3)]_3]Cl$.[29] In another example, when four equivalents of $(Ph_3P)AuCl$ were combined with a single equivalent of $C[B(OMe)_2]_4$ and excess CsF, the hexa- rather than tetraaurated species resulted, $[(C[Au(PPh_3)]_6]^{2+}$.[24] Similarly, when two equivalents of $(Ph_3P)AuCl$ were combined with a single equivalent of $H_2C[B(OMe)_2]_2$ and excess CsF, the penta- rather than diaurated species resulted, $C[Au(PPh_3)]_5]^+$.[27] In the latter case, the tendency LAu^+ to hypercoordinate carbon[31,32] due to aurophililic attractions[28,32-42] was counteracted by employing phosphines with increasingly large cone angles, resulting in decreased cluster nuclearity from six to five, and finally to four. This approach resulted in the neutral tris(*o*-tolyl)phosphine-supported tetragold(I) carbide $\{[(o\text{-tolyl})_3P]Au\}_4C$.[25] Intriguingly, the reaction of excess trimethylsilyl(diazomethane) with the triphenylphosphine-supported trigold(I) oxonium salt $[[(Ph_3P)Au]_3O]BF_4$ in the presence of triethylamine, seemingly poised to produce an open shell phosphine-supported trigold(I) carbido cation, instead formed the hexagold(I) carbido dication $[(C[Au(PPh_3)]_6]^{2+}$ in 64% yield.[26] Interestingly, the authors do not point out that the balanced reaction requires a

two-electron transfer to reduce the bridging carbide carbon originating from trimethylsilyl(diazomethane) to the formal 4- oxidation state. There was also no mention of the effects of more sterically demanding supporting ligands on the outcome of the reaction, nor of an attempt to access the trigold(I) carbido cation by a more stepwise substitution of trimethylsilyl(diazomethane) by LAu^+. Finally, there was no mention of an attempt to access the species in a manner analogous to the preparation of the (triauromethyl)phosphonium chloride salt $\{(Me_3P)C[Au(PPh_3)]_3\}Cl$.[29]

I envisaged that stepwise reaction of monoaurated (trimethylsilyl)diazomethane $(NHC)Au[C(N_2)SiMe_3]$[43] (Scheme 3.1) with suitable gold precursors would produce a cationic trigold(I) carbide with a $[Au_3C]^+$ core. In this work, such a species was stabilized as its pyridine adduct, the SIMes-supported *N*-(triauromethyl)pyridinium cation $\{[(SIMes)Au]_3C(Py)\}^+$ (**6**). This compound is isolobal with $\{[(o\text{-tol})_3PAu]_3B(PCy_3)\}$[44], $\{[(Me_2N)_3PAu]_3NP(NMe_2)_3\}^{2+}$,[45] and $[(Me_3P)C[Au(PPh_3)]_3]^+$.[29] Like $[(Me_3P)C[Au(PPh_3)]_3]^+$, **6** is a rare example of a trigold(I) cluster bridged by a central carbon. The *N*-(triauromethyl)pyridinium cation exhibits electrophilic carbide-like reactivity with CO to form trigold(I) ketenylidene cation (Figure 3.6),[46] while reaction with stronger nucleophiles results in deauration, including facile hydrolysis in air to give the *N*-(diauromethyl)pyridinium cation and bridged digold(I) hydroxide cation (Scheme 3.5). A series of trapping experiments are described that provide support for the generation of a transient trigold(I) carbido cation $\{[(SIMesAu)]_3C\}^+$. Other relevant species resulting from this work include an NHC-supported *N*-[diauro(trimethylsilyl)methyl]pyridinium cation, *N*-[diauro(trimethylsilyl)methyl]acetonitrilium cation, *N*-(diauromethyl)pyridinium cation, and gold(I) methoxymethyl complex.

3.2 Results and Discussion

Initial efforts to prepare the IDipp-supported trigold(I) carbido cation (IDipp = 1,3-bis(2,6-diisopropylphenyl)imidazol-2-ylidene) involved sequential installation of (IDipp)Au^+ at the diazo carbon of trimethylsilyl(diazomethane) via a series of three auration steps concomitant with deprotonation, dediazoniation, and desilylation. The first of these steps, deprotonation/auration, resulted in the IDipp-supported gold(I) trimethylsilyl(diazomethane) complex (IDipp)Au[$C(N_2)SiMe_3$] (**2**) (Figure 3.6). This was accomplished by combining six equivalents of trimethylsilyl(diazomethane) in hexanes solution with the gold(I) *tert*-pentyloxide (IDipp)Au(O*t*-Pent),[43] or with the gold(I) diisopropylamide (IDipp)AuN(*i*-Pr)$_2$[47] (Scheme 3.1) in THF solution. The gold(I) diisopropylamide was preferable for generation of the IDipp-supported complex due to reduced reaction times and improved reliability. The IR spectrum of **2** reveals a strong vibrational mode at 1985 cm^{-1} corresponding to the diazo group (Figure 3.6). The less sterically encumbered SIMes-supported (SIMes = 1,3-bis(2,4,6-trimethylphenyl)imidazolidin-2-ylidene) analogue (SIMes)Au[$C(N_2)SiMe_3$] (**3**) was prepared analogously from the SIMes-supported gold(I) *tert*-pentyloxide (SIMes)Au(O*t*-Pent) (Scheme 3.1). The IR spectrum of **3** revealed a strong vibrational mode at 1981 cm^{-1} corresponding to its diazo group (Figure 3.11). The SIMes-analogue was found to be more reactive with respect to light and moisture compared with the IDipp-analogue. In both cases, the pure yellow compounds were isolated quantitatively by removal of all volatiles *in vacuo*.

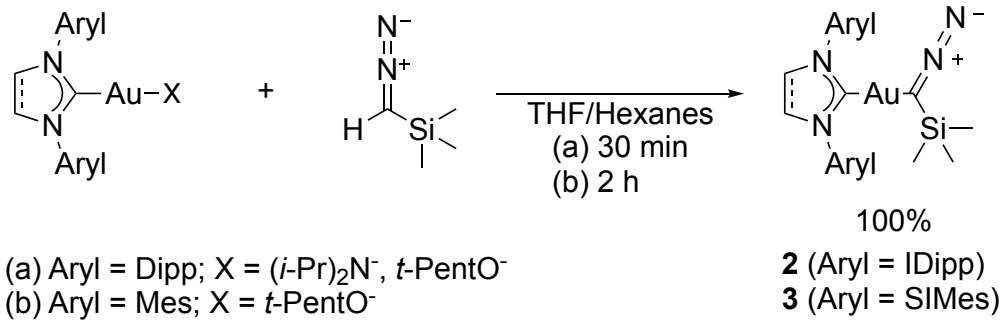

Scheme 3.1 Synthesis of gold(I) (trimethylsilyl)diazomethyl complexes **2**-**3**.

Synthesis of the IDipp-supported digold(I) trimethylsilylmethylidyne cation $\{[(IDipp)Au]_2C(SiMe_3)\}^+$ was attempted by installation of a second $(IDipp)Au^+$ fragment at the diazo carbon of **2** via electrophilic dediazoniation with IDipp-supported gold(I) trifluoromethanesulfonate (IDipp)Au(OTf) (OTf = trifluoromethanesulfonate)[43] (Scheme 3.2). When this reaction was carried out in CD_3CN solution at -41°C, the product mixture concentrated *in vacuo*, and the residue dissolved in CH_3CN, analysis of the product mixture by ESI-MS revealed several ions of interest (Figure 3.13). These ions included the CH_3CN adduct, not the CD_3CN adduct, of the digold(I) (trimethylsilyl)methylidyne cation $\{(IDipp)Au]_2C(SiMe_3)(MeCN)\}^+$ (m/z = 1296.6), indicating lability of the coordinated solvent molecule. A peak at m/z = 1255.6 was initially assigned to the free digold(I) (trimethylsilyl)methylidyne cation $\{(IDipp)Au]_2C(SiMe_3)\}^+$; however, this peak was subsequently reassigned as the protodesilylated 1,3-dipolar cycloaddition product of **2** and [(IDipp)Au(CD_3CN)]OTf, the IDipp-supported diauro(methyltriazolium)-d_3 cation (m/z = 1255.6) (Scheme 3.2). In support of this assignment, the corresponding silylated species, IDipp-supported diauro[trimethylsilyl(methyltriazolium)]-d_3 cation (m/z = 1327.7), was also detected. The 1,3-dipolar cycloaddition of **2** with [(IDipp)Au(CD_3CN)]OTf is analogous to reaction of electron-rich lithiated (trimethylsilyl)diazomethane $LiC(N_2)SiMe_3$ with various nitriles to give the corresponding lithiated triazoles.[48]

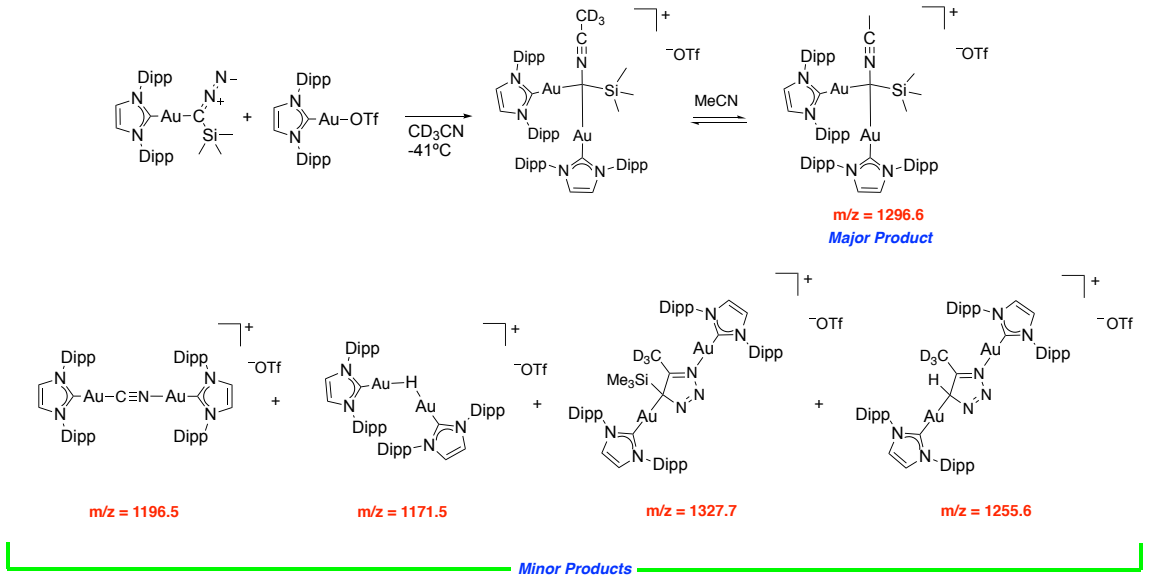

Scheme 3.2. Reaction of **2** with (IDipp)Au(OTf) in CD_3CN.

Other side products were detected including bridged digold(I) hydride cation $\{[(IDipp)Au]_2H\}^+$ (m/z = 1171.5),[43] and the linearly bridged digold(I) cyanide cation $\{[(IDipp)Au]_2(CN)\}^+$ (m/z = 1196.5) (Figure 3.13), but the major product of the reaction was determined to be $\{(IDipp)Au]_2C(SiMe_3)(MeCN)\}OTf$ (**4**) as judged by ^1H NMR (Figure 3.12). The trimethylsilyl resonance of this species appears at δ –0.66 ppm and the coordinated acetonitrile resonance appears at δ 1.96 ppm, distinct from that of free acetonitrile when both are present. Two sets of IDipp resonances corresponding to this compound integrate in a 1:1 ratio, apparently arising from symmetry-breaking between the IDippAu fragments due to restricted rotation about the Au-C bond. This species was unstable when dissolved in CD_2Cl_2 or THF-d_8, possibly resulting from dissociation of acetonitrile in non-coordinating or weakly coordinating solvents. The additional minor trimethylsilyl resonance detected at δ -0.13 ppm in the ^1H NMR spectrum may be assigned to the IDipp-supported diauro[trimethylsilyl(methyltriazolium)-d_3] cation. Optimization of reaction temperature and addition rate resulted in decreased formation of byproducts

during the reaction, however, they were not completely eliminated. Isolation of **4** from the remaining byproducts was unsuccessful; however, single crystals of the linearly bridged digold(I) cyanide byproduct were isolated as the trifluoromethanesulfonate salt [(IDipp)Au(CN)Au(IDipp)]OTf by fractional crystallization, and the compound was structurally characterized (Figure 3.1). The Au1-N1-C1 and Au2-C1-N1 angles measured 177(1)° and 178(1)°, respectively. The bridging cyanide C-N bond distance measured 1.15(1) Å, identical to the C-N bond distance reported for potassium cyanide of 1.15 Å.[49] The digold(I) cyanide species also resulted when experiments were performed excluding nitrile solvents, suggesting that the cyanide fragment originates from the trimethylsilyl(diazomethane) moiety rather than from acetonitrile.

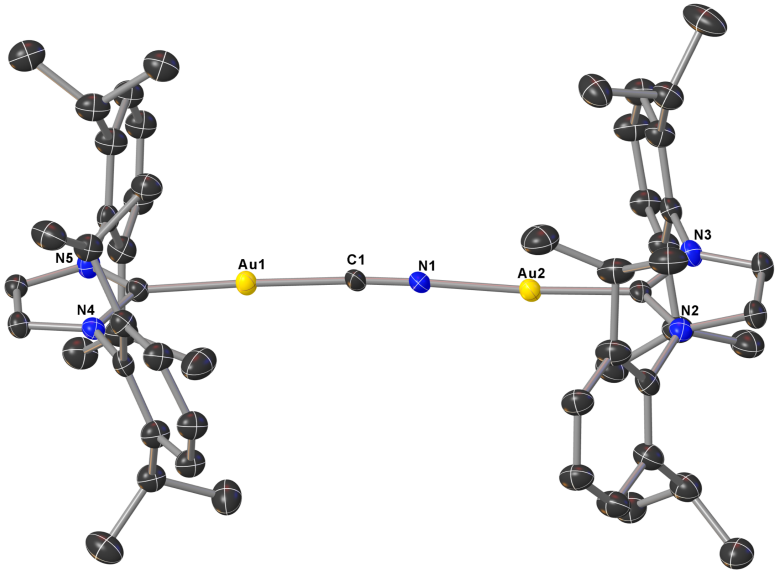

Figure 3.1. Solid state structure of [(SIMes)Au(CN)Au(SIMes)]OTf (50% probability ellipsoids). H atoms, trifluoromethanesulfonate anion, and cocrystallized benzene omitted for clarity. Selected interatomic distances (Å) and angles (deg): Au1-C29, 1.962(8); Au1-C1, 1.965(8); C1-N1A, 1.15(1); Au2-N1A, 1.990(8); Au2-C2, 1.984(8); C2-Au2-N1A, 176.2(5); Au2-N1A-C1A, 178(1); N1A-C1A-Au1, 177(1); C1A-Au1-C29 177.9(5).

Installation of a third (IDipp)Au^+ fragment at the bridging carbon of **4** through nucleophilic desilylation by (IDipp)Au(X) (X = F^-, CH_3COO^-, $(CH_3)_3SiO^-$) in acetonitrile

solution was envisaged to produce the trigold(I) carbido cation, its acetonitrile adduct, or an equilibrium mixture of the two species. These reactions did not proceed as desired. For example, while reaction of **4** with (IDipp)AuF did result in the formation of Me_3SiF as evidenced by ^1H NMR, the reaction was slow and produced multiple (IDipp)Au-containing products. Sluggish reactivity was attributed in part to the steric bulk of the IDipp supporting ligands, which may prevent the pyramidal arrangement of three IDippAu fragments about a centrally bridging carbon. As a result all subsequent experiments were performed using gold precursors supported by SIMes.

The above results prompted exploration of another route to the trigold(I) carbido cation. According to a previous report by Blues *et. al.,* the reaction of simple silver salts (ie., silver acetate) with diazomethane afforded an explosive disilver(I) diazomethane coordination polymer with the formula $[Ag_2CN_2]_n$.[50] Silver cyanide species were detected as byproducts of reactions conducted in standard aprotic solvents. For reactions conducted in pyridine, however, cyanide formation was suppressed. I reasoned that pyridine might also suppress the formation of gold cyanide species during the formation of SIMes-supported digold(I) diazomethane $[(SIMesAu)_2CN_2]$, analogous to the main group dimetallodiazomethanes of Ge, Sn, Pb, Sb, and Hg.[51-56] When pyridine solutions of **3** and (SIMes)AuF (**5**)[57,58] were cooled to -35°C and combined, an immediate color change to deep magenta resulted. The reaction was allowed to proceed for 2.5 hours at low temperature. Volatiles were then removed *in vacuo* followed by recrystallization of the residue from THF/hexanes to give an air-sensitive magenta powder. Interestingly, bifluoride anion was detected by ^1H NMR spectroscopy, from the triplet resonance at δ 16.3 ppm in CD_3CN, and by IR spectroscopy with vibrational modes at 1924 cm^{-1} and 2002 cm^{-1}. The presence of bifluoride indicated the formation of a salt and suggested 2:1 reactivity between (SIMes)AuF and **3**. The ^1H NMR also revealed resonances attributed to a bound pyridine, including a doublet at δ 7.44 ppm, and two triplets at δ 6.48 ppm and

δ 5.99 ppm integrating to 2H, 1H, and 2H by comparison to three SIMes ligands. Crystals of the magenta compound suitable for X-ray diffraction were grown by carefully layering a DCM solution of the magenta solid with hexanes at -35°C. X-Ray diffraction measurements revealed the formation of the SIMes-supported *N*-(triauromethyl)-pyridinium cation as the bifluoride salt $[(SIMesAu)_3C(Py)]HF_2$ (**6a**) (Scheme 3.3). Significant quantities of byproducts always accompanied the formation of **6a**, possibly as a result of the reactive bifluoride anion, the formation of which was attributed to reaction of generated fluoride anions with protons at the surface of the glass reaction vessel. The IDipp analogue was not successfully generated under these conditions, which was attributed to the greater steric bulk of IDipp compared with SIMes.

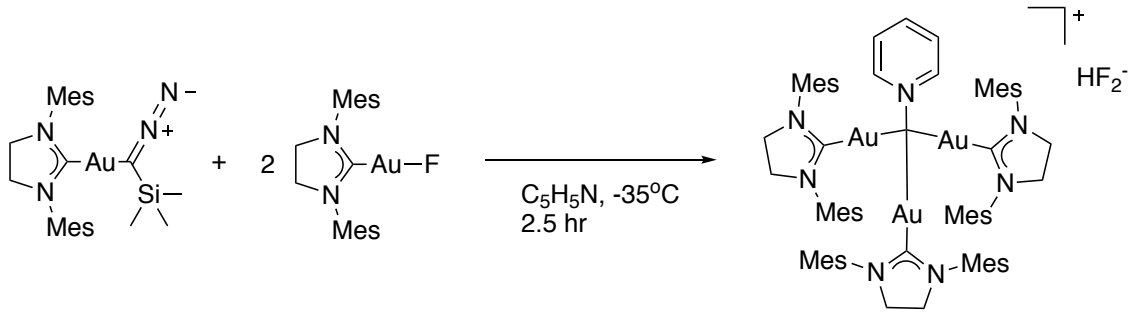

3 **5** **6a**

Scheme 3.3 Synthesis of $[(SIMesAu)_3C(Py)]HF_2$.

The solid state structure of **6a** (Figure 3.2) reveals a pseudo-tetrahedral carbon center with significant distortion from local ideal symmetry. The plane of the NHC heterocycles bound to Au1, Au2, and Au3 make a torsion angle of 51.3(9)°, 1.0(9)°, 37.4(9)° with respect to the C-N vector created by the bond between the bound pyridine and the triply bridging carbon, resulting in a propeller-shaped arrangement. The Au-C1-N5 angles are 111.3(5)°, 117.2(6)°, and 113.1(5)° for Au1, Au2, and Au3. These angles contrast with the contracted Au-C1-Au angles of 98.0(4)° and 98.6(4)° for Au1-C1-Au3

and Au2-C1-Au3; however, the Au1-C1-Au2 angle of 116.2(4)° compares similarly with the Au-C-N angles of the pseudo-tetrahedron. The contracted Au2-Au3 and Au3-Au1 distances are 3.1129(6) Å and 3.1048(6) Å, much shorter than the Au2-Au1 distance of 3.4836(5) Å, placing the shorter two of the three distances within two van der Waals radii of each other. The Au-C1 distances range narrowly from 2.049(8) Å to 2.058(9) Å. The Au-C_{NHC} distances are likewise quite similar, ranging from 2.012(9) Å to 2.03(1) Å. Interestingly, the C-N distance between the triply bridging carbon and the pyridine nitrogen of 1.45(1) Å compares similarly with the C-N distance in *N*-methylpyridinium tetraphenylborate of 1.473(3) Å.[59]

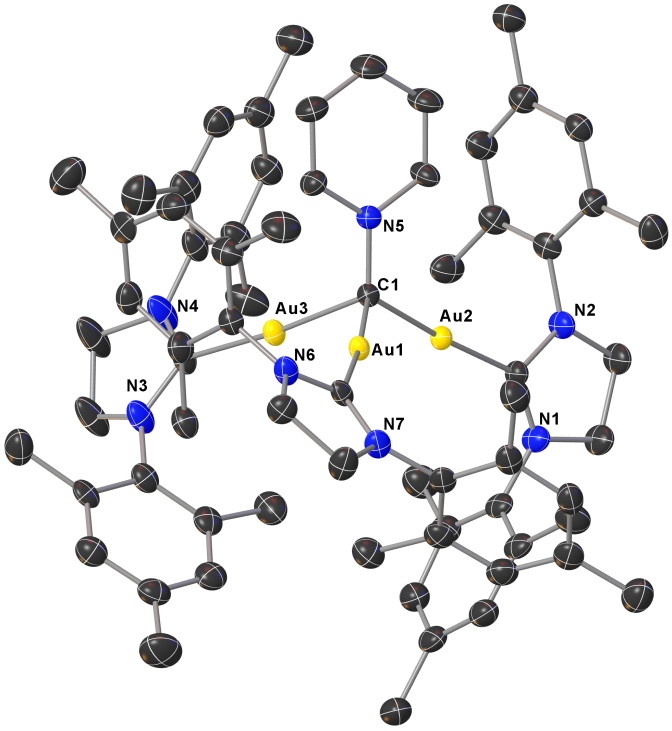

Figure 3.2. Solid state structure of **6a** (50% probability ellipsoids). H atoms, HF_2^- anion are omitted for clarity. Selected interatomic distances (Å) and angles (deg): Au2-Au3, 3.1129(6); Au3-Au1, 3.1048(6); Au2-Au1, 3.4836(5); Au1-C1, 2.055(8); Au3-C1, 2.058(9); Au2-C1, 2.049(8); Au1-C49, 2.012(9); Au2-C2, 2.018(8); Au3-C23, 2.03(1); C1-N5, 1.45(1); Au1-C1-N5, 111.3(5); Au2-C1-N5, 117.2(6); Au3-C1-N5, 113.1(5); Au1-C1-Au3, 98.0(4); Au2-C1-Au3, 98.6(4); Au1-C1-Au2, 116.2(4).

To prepare the *N*-(triauromethyl)pyridinium cation as the salt of the more inert trifluoromethanesulfonate anion, a pyridine solution of **3** was combined with a pyridine solution of **5** and [(SIMes)Au(Py)]OTf[60] (**7**) at -35°C, conditions analogous to those employed in the preparation of the bilfuoride salt. The resulting reaction mixture was worked up as before to give the analytically pure compound {[(SIMes)Au]$_3$C(Py)}OTf (**6b**) (Scheme 3.4). The ^{1}H NMR reveals that all three SIMes ligands are equivalent on the NMR time scale (Figure 3.18).

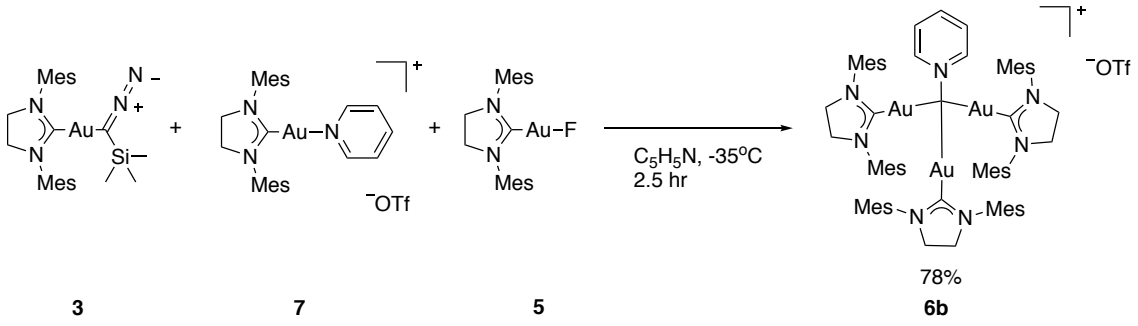

3 **7** **5** **6b**

Scheme 3.4 Synthesis of {[(SIMes)Au]$_3$C(Py)}OTf (**6b**).

Like the bifluoride salt, **6b** is air sensitive in both solution and solid state, changing from magenta to yellow upon exposure to air. ESI-MS of the resulting yellow product mixture indicated hydrolysis of the *N*-(triauromethyl)pyridinium cation to give bridged digold(I) hydroxide cation {[(SIMes)Au]$_2$OH}$^+$ (m/z = 1024.5) and the *N*-(diauromethyl)pyridinium cation {[(SIMes)Au]$_2$CH(Py)}$^+$ (m/z = 1099.5) (Scheme 3.5). The *N*-(diauromethyl)pyridinium cation {[(SIMes)Au]$_2$CH(Py)}$^+$ was independently prepared as the acetate salt by addition of a pyridine solution of (SIMes)Au(OAc) dropwise to one equivalent of **3** in THF at -41°C over the course of 30 minutes (Scheme 3.6). Solvent was removed from the reaction mixture *in vacuo*, and the residue was recrystallized from THF by addition of cold hexanes to give {[(SIMes)Au]$_2$CH(Py)}OAc. The ^{1}H NMR spectrum of

{[(SIMes)Au]$_2$CH(Py)}OAc reveals two sets of SIMes-derived resonances apparently arising from restricted rotation of the ligands about the Au-C_{NHC} vector. A resonance corresponding to the proton of the bridging carbon appears at δ 5.02 ppm (Figure 3.26).

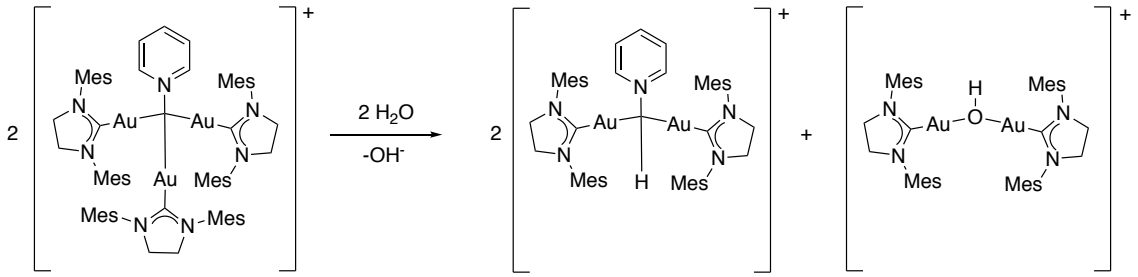

Scheme 3.5 Hydrolysis of {[(SIMes)Au]$_3$C(Py)}$^+$.

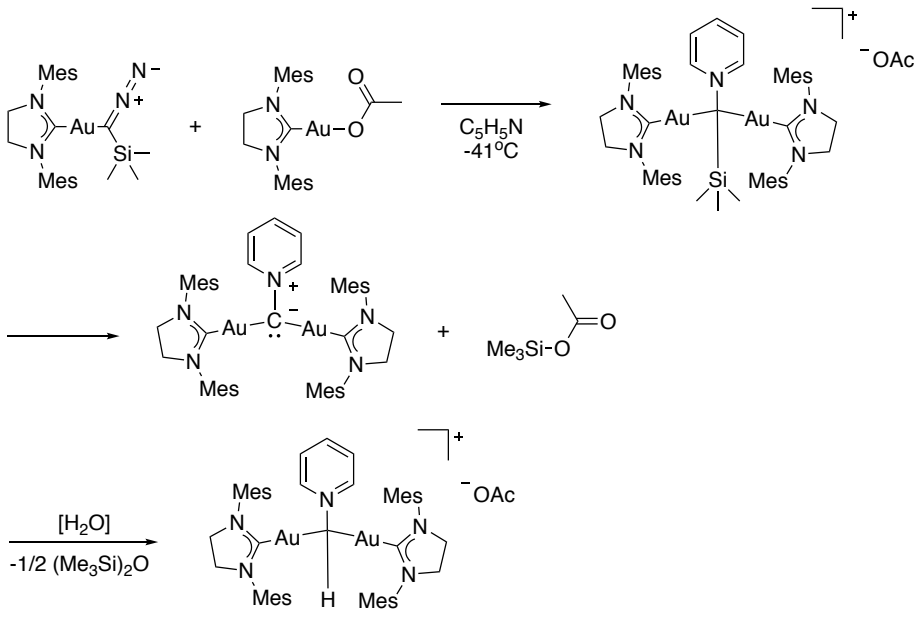

Scheme 3.6. Proposed sequence of {[(SIMes)Au]$_2$CH(Py)}OTf formation.

When a DCM-d_2 solution of **6b** containing 4,4'-dimethylbiphenyl as an internal standard was placed under 2 atmospheres of carbon monoxide, exchange with pyridine gave rise to the previously reported SIMes-supported trigold(I) ketenylidene cation[46] (*see*

Chapter 2) as the trifluoromethanesulfonate salt {[(SIMes)Au]$_3$(μ_3-CCO)]OTf in 85% NMR yield (Figure 3.20) after five hours (Scheme 3.7).

Addition of trimethylphosphite to **6b** in DCM-d_2 solution did not result in substitution, but instead formed the bis-phosphite complex [((MeO)$_3$P)$_2$Au]OTf and the bis-NHC complex [(SIMes)$_2$Au]OTf as judged by ^{1}H NMR, ^{31}P NMR, and ESI-MS. Addition of tetrabutylammonium chloride to a DCM-d_2 solution of **6b** also resulted in deauration to give SIMesAuCl as judged by ^{1}H NMR, indicating lability of the Au-C bonds. Similarly, the compound slowly decomposed to the bis-NHC complex [(SIMes)$_2$Au]OTf when subjected to 2 atmospheres of hydrogen for two weeks.

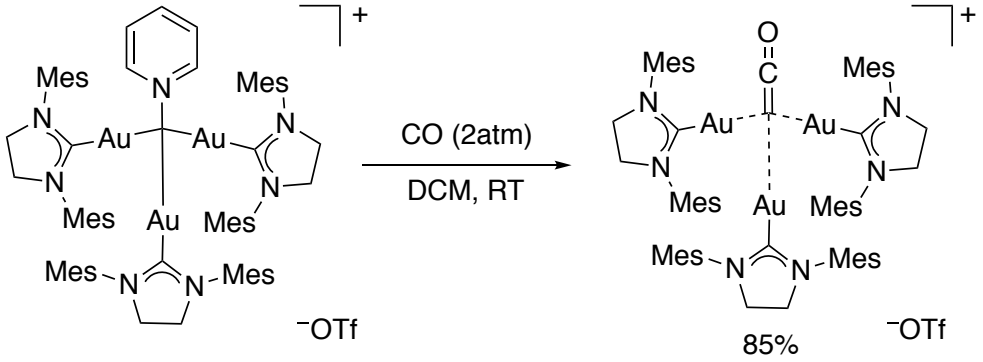

Scheme 3.7. Reaction of **6b** with carbon monoxide to give the trigold(I) ketenylidene cation.

Trapping experiments were carried out in an effort to generate the SIMes-supported trigold(I) carbido cation in non-coordinating solvent, observe it spectroscopically, and trap it as the stable pyridine adduct. Initial experiments involved addition of a DCM solution of **3** to a DCM solution of (SIMes)AuF (2 eq) at -35°C. Addition of pyridine to the product mixture generated a magenta solution of **6a**, which also contained unreacted (SIMes)AuF and several unidentified species as judged by ^{1}H NMR (Figure 3.21). Two plausible reaction pathways passing through a trigold(I) carbido cation

intermediate (a) or a (triauromethyl)diazonium intermediate (b) are shown below (Scheme 3.8). Suspecting that side reactions could be occurring between a transient species and bifluoride, subsequent experiments were carried out with $[(SIMes)Au]_2X^+$ reagents in place of terminal (SIMes)AuF. Digold(I) μ-fluoride cations were previously shown to undergo halide exchange with DCM,[58] therefore bridged acetate salts were initially chosen for these experiments. Addition of **3** to SIMes-supported digold(I) μ-acetate tetrafluoroborate $\{[(SIMes)Au]_2(OAc)\}BF_4$ at -41°C resulted in a nearly colorless solution. Addition of excess pyridine to this reaction mixture resulted in a color change to magenta, suggesting formation of the *N*-(triauromethyl)pyridinium cation. On warming, however, the trimethylsilyl acetate generated during the reaction appears to react with the BF_4^- to give BF_3 and Me_3SiF as judged by ^1H NMR. In order to avoid this side reaction, subsequent experiments were carried out using the trifluoromethanesulfonate salt of the digold(I) μ-acetate $\{[(SIMes)Au]_2(OAc)\}OTf$. As before, when a DCM solution of **3** was added to a DCM solution of $\{[(SIMes)Au]_2(OAc)\}OTf$ at -41°C, a nearly colorless solution resulted. Addition of excess pyridine to this reaction mixture once again resulted in a color change to magenta, suggesting formation of **6b**. On warming, however, the magenta color gave way to orange. The major products in the resulting orange mixture were $\{[(SIMes)Au]_2CH(Py)\}^+$ and (SIMes)Au(OAc) as judged by ^1H NMR, which seemed to suggest that **6b** could be reacting with Me_3SiOAc at room temperature to give the digold(I) species $\{[(SIMes)Au]_2C(SiMe_3)(Py)\}^+$, which could then undergo protonolysis with an adventitious proton source to give $\{[(SIMes)Au]_2CH(Py)\}^+$. Analogous experiments were carried out using the bridged digold(I) μ-*tert*-butoxide $\{[(SIMes)Au]_2(O\textit{t}Bu)\}OTf$, but the low nucleophilicity of *tert*-butoxide resulted in long reaction times. Finally, attempts were made to generate the thermally unstable SIMes-supported gold(I) triflate (SIMes)AuOTf in the absence of pyridine at -78°C. It was envisaged that addition of **3** to the reaction mixture,

followed by addition of (SIMes)AuF would generate the trigold(I) carbide. When this was carried out, addition of pyridine to the reaction mixture resulted in a deep magenta color, which again gave way to an orange color on warming, suggesting unwanted side reactions with byproducts at room temperature. The ^{1}H NMR spectrum of the product mixture was complicated, but showed trace amounts of **6b**.

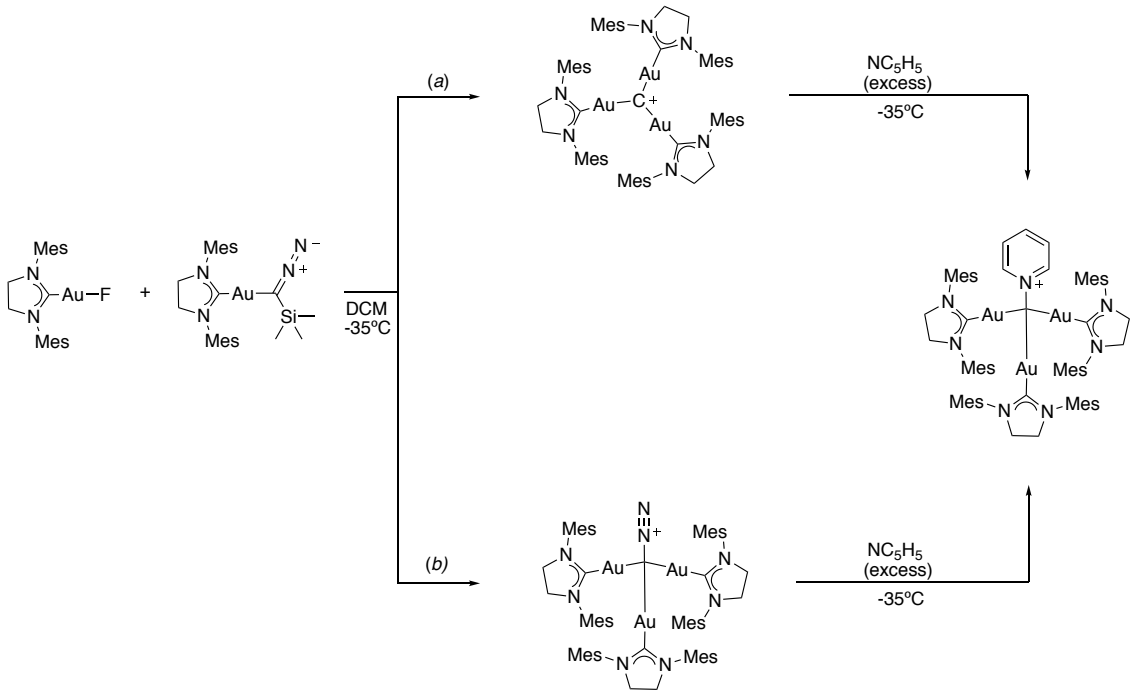

Scheme 3.8. Plausible pathways leading to the Formation of **6** via the formation of a transient species in non-coordinating solvent.

Given the successful suppression of digold(I) cyanide and digold(I) hydride species by pyridine during the formation of the *N*-(triauromethyl)pyridinium cation, and given the promising formation of **4** by reaction of **2** with (IDipp)AuOTf, it seemed probable that the SIMes-supported N-[diauro(trimethylsilyl)methyl]pyridinium cation could also be formed. Electrophilic dediazoniation/auration of **3** by [(SIMes)Au(Py)]OTf in pyridine at -35°C gave

the desired yellow compound {[(SIMes)Au]$_2$C(SiMe$_3$)(Py)]OTf (**8**) in 88% NMR yield based on total integration (Scheme 3.9).

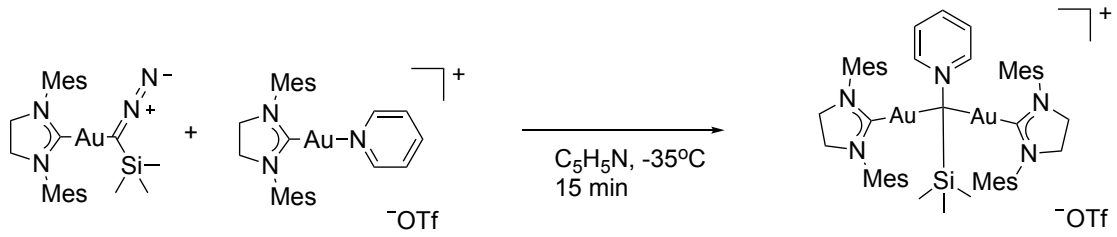

3 **7** **8**

Scheme 3.9. Synthesis of {[(SIMes)Au]$_2$C(SiMe$_3$)(Py)}OTf (**8**).

Unfortunately, it was always accompanied by a significant quantity of the bis-NHC complex [(SIMes)$_2$Au]OTf (*ca.* 10%) and trace quantities of the protonolyzed product {[(SIMes)Au]$_2$CH(Py)}OTf. Attempts to intentionally protonolyze the compound with phenol and methanol resulted in no reaction over the course of several hours, even with gentle heating. Similar to **4**, the ^{1}H NMR of **8** reveals that the *ortho*-aryl alkyl protons and the *meta*-CH protons of the two SIMes ligands are rendered chemically inequivalent, giving rise to two sets of SIMes-derived signals (Figure 3.22). Single crystals of **8** suitable for X-ray diffraction were grown by carefully layering a DCM solution of the compound with hexanes at -35°C. The solid state structure (Figure 3.3) reveals a pseudo-tetrahedral arrangement with a constricted Au-C1A-Au angle of 94.0(2)°, and an expanded Si-C1A-N angle of 119.9(3)°. The Au1-C1A-Si and Au2-C1A-N angles are close to ideal at 108.1(2)° and 108.2(3)° respectively. Similarly, the Au2-C1A-Si and Au1-C1A-N angles are only slightly expanded at 111.2(2)° and 112.5(3)° respectively. The contracted Au1-Au2 distance is within two van der Waals radii at 3.0391(6) Å, indicating a weak aurophilic interaction. The Au1-C1A and Au2-C1A distances are 2.076(3) Å and 2.080(4) Å

respectively, slightly longer than the corresponding distances in **6a** (Δd = *ca*. 0.02-0.03 Å). The Au-C_{NHC} distances are 2.012(3) Å and 2.015(4) Å. The C1-N3 distance of 1.481(5) Å compares closely with the corresponding distance in **6a** (1.45(1) Å), and in *N*-methylpyridinium tetraphenylborate (1.473(3) Å).[59] A small portion of the protonolyzed product {[(SIMes)Au]$_2$CH(Py)}OTf cocrystallized with **8**, accounting for *ca*. 10% of the total diffraction. The structure of {[(SIMes)Au]$_2$CH(Py)}OTf (Figure 3.4) was resolved from **8**, and the chemically distinct portions of the molecules were refined separately, however, the remaining coordinates were crystallographically indistinguishable.

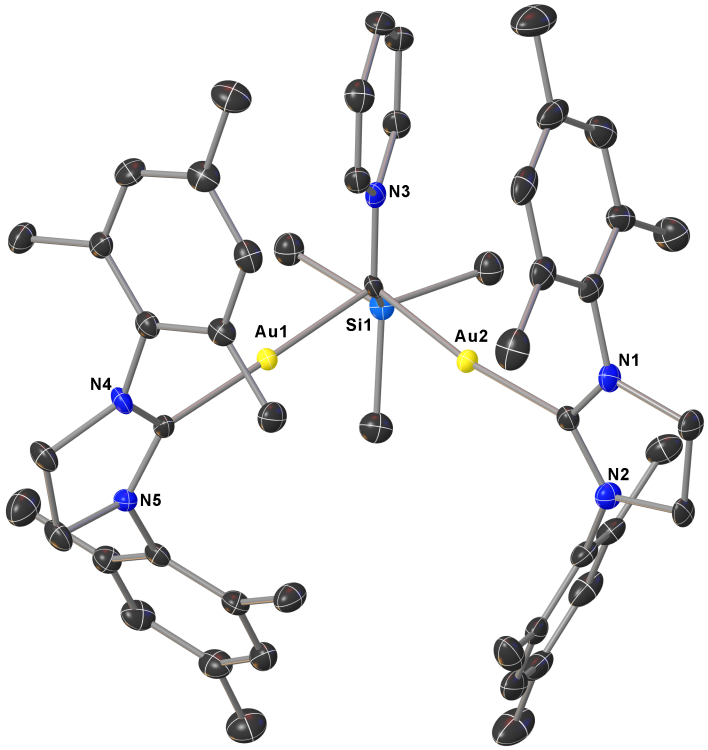

Figure 3.3. Solid state structure of **8** (50% probability ellipsoids). H atoms, $F_3CSO_3^-$ anion, and cocrystallized solvent molecules are omitted for clarity. Selected interatomic distances (Å) and angles (deg): Au1-Au2, 3.0391(6); Au1-C1A, 2.076(3); Au2-C1A, 2.076(3); Si-C1A, 1.879(5); C1A-N3, 1.481(5); C31-Au1, 2.012(3); Au2-C2, 2.015(4); C2-Au2-C1A, 172.2(2); C1A-Au1-C31, 177.5(2); Au2-C1A-Au1, 94.0(2); Au2-C1A-Si, 111.2(2); Au1-C1A-Si, 108.1(2); Au1-C1A-N3, 112.5(3); Au2-C1A-N3, 108.2(3).

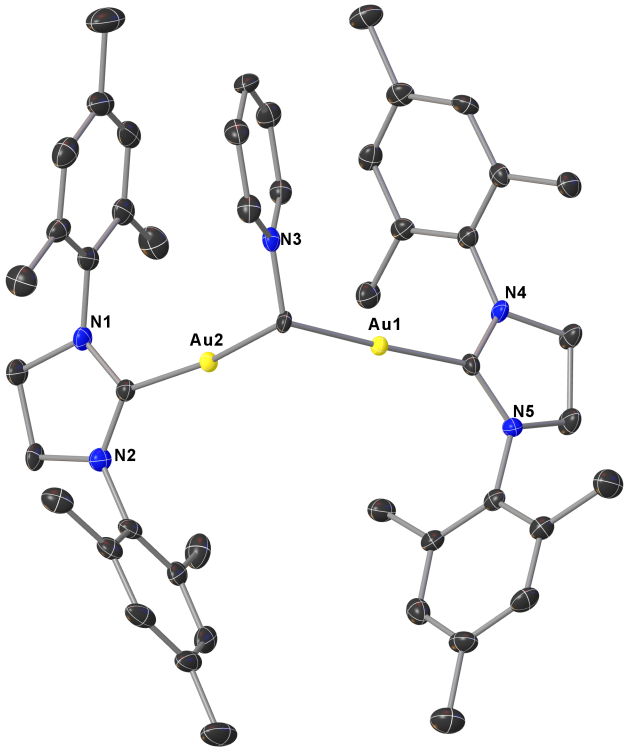

Figure 3.4. Solid state structure of {[(SIMes)Au]$_2$CH(Py)}OTf (50% probability ellipsoids). H atoms, $F_3CSO_3^-$ anion, and cocrystallized solvent molecules are omitted for clarity. Selected interatomic distances (Å) and angles (deg): Au1-Au2, 3.0391(6); Au1-C1B, 2.076(3); Au2-C1A, 2.076(3); Si-C1B, 1.879(5); C1B-N3, 1.481(5); C31-Au1, 2.012(3); Au2-C2, 2.015(4); C2-Au2-C1B, 172.2(2); C1B-Au1-C31, 177.5(2); Au2-C1B-Au1, 94.0(2); Au2-C1B-Si, 111.2(2); Au1-C1B-Si, 108.1(2); Au1-C1B-N3, 112.5(3); Au2-C1B-N3, 108.2(3).

In an effort to protodesilylate (IDipp)AuC(N_2)$SiMe_3$ to give (IDipp)AuC(N_2)H, a methanol solution of (IDipp)AuC(N_2)$SiMe_3$ was sonicated with excess potassium bifluoride. However, protodesilylation was accompanied by insertion into a methanol O-H bond, resulting in the gold(I) methoxymethyl complex (IDipp)AuCH_2OCH_3 (Scheme 3.10). The ^{1}H NMR spectrum reveals resonances at δ 3.90 ppm and δ 2.83 ppm corresponding to the -CH_2- and -CH_3 of the methoxymethyl moiety (Figure 3.24). This compound is reminiscent of LAuCH_2Cl complexes, which are known to cyclopropanate alkenes.[47,61]

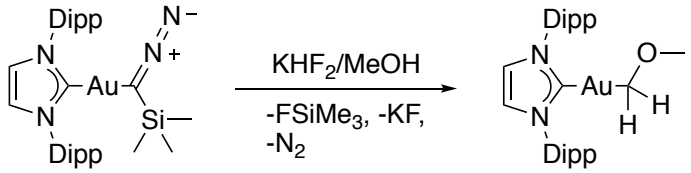

Scheme 3.10. Synthesis of (IDipp)Au(CH_2OCH_3).

3.3 Conclusion

Solvent adducts of an NHC-supported diglold(I) trimethylsilyl(methylidyne) cation, digold(I) methylidyne cation, and trigold(I) carbide cation were generated from the corresponding gold(I) trimethylsilyl(diazomethane) complexes. A gold(I) methoxymethyl carbenoid-species was also generated. The SIMes-supported *N*-(triauromethyl)pyridinium cation, which may be thought of as the pyridine adduct of the trigold(I) carbido cation, reacts with CO to form a trigold(I) ketenylidene cation. Reaction with stronger Lewis bases including Cl^- and $(MeO)_3P$ resulted in cleavage of the Au-C bonds. Trapping experiments intended to provide evidence of a transient non-coordinated trigold(I) carbido cation were not definitive, but suggest the possible intermediacy of this species.

3.4 Experimental

3.4.1 General Considerations

Unless otherwise indicated, manipulations were performed in an MBraun glovebox under nitrogen atmosphere, or using standard Schlenk techniques under argon atmosphere. Glassware was dried in a ventilated oven at 160 °C or flame-dried and allowed to cool under vacuum. Molecular sieves (Alfa Aesar) and Celite (EMD 545) were dried under vacuum for at least twelve hours at 160°C. Dichloromethane (EMD Millipore Omnisolv), hexanes (EMD Millipore Omnisolv), toluene (EMD Millipore Omnisolv), and tetrahydrofuran (EMD Millipore Omnisolv) were sparged with ultra-high purity argon for 30

minutes and dried using an MBraun solvent purification system. DCM was then transferred onto calcium hydride and further dried for at least 12 hours. It was then degassed and vacuum-transferred to a resealable flask, and stored over 3Å molecular sieves in the glovebox. THF, hexanes, and toluene were then transferred onto sodium benzophenone ketyl and further dried until a purple color was achieved. They were then degassed and vacuum-transferred to a resealable flask, and stored over molecular sieves in the glovebox. Pyridine (Sigma-Aldrich) and acetonitrile (EMD HPLC) were stirred over calcium hydride (Alfa Aesar) in sealed flasks for at least twelve hours. They were then degassed and vacuum-transferred to resealable flasks, and stored over 3Å molecular sieves in the glove box. Benzene (Alfa Aesar ACS) was dried over sodium benzophenone ketyl in a sealed flask until a purple color was achieved. It was then degassed, vacuum-transferred to a resealable flask, and stored over 3Å molecular sieves in the glovebox. Methanol (BDH), acetone (BDH), and hexanes used in benchtop work (BDH) were used as received.

THF-d_8 (Cambridge Isotope Laboratories) was dried over sodium benzophenone ketyl, degassed by several freeze-pump-thaw cycles, and vacuum-transferred into a resealable flask. Dichloromethane-d_2 and acetonitrile-d_3 (Cambridge Isotope Laboratories) were dried over calcium hydride for at least twelve hours, degassed by several freeze-pump-thaw cycles, and vacuum-transferred into resealable flasks. Methanol-d_4 (Cambridge Isotope Laboratories) was used as received.

Tetrachloroauric acid (Strem), dimethyl sulfide (Alfa Aesar), potassium carbonate (Alfa Aesar), potassium bifluoride (Alfa Aesar), calcium hydride (Alfa Aesar), silver acetate (Sigma-Aldrich), 2,4,6-trimethylaniline (Alfa Aesar), sodium metal (Alfa Aesar), benzophenone (Alfa Aesar), 1,2-dichloroethane (EMD Millipore Omnisolv), 4,4'-dimethylbiphenyl (Alfa Aesar), nitrogen (NexAir), argon (both industrial and ultra-high purity grades, NexAir), and carbon monoxide (Sigma-Aldrich) were used as received.

N,*N*'-bis(2,4,6-trimethylphenyl)imidazolinium chloride,[52] (SIMes)AuCl[53], (IDipp)AuN(*i*-Pr)$_2$,[47] (IDipp)Au(O*t*-Pent),[43] (IDipp)Au(OTf),[43] (IDipp)AuF,[58] and (SIMes)Au(OAc)[46] were prepared according to literature protocol and were characterized by ^{1}H NMR spectroscopy.

3.4.2 Analytical Measurements

^{1}H and ^{13}C spectra were obtained using a Varian Vx 400 MHz spectrometer, Bruker Avance IIIHD 500 spectrometer, or Bruker Avance IIIHD 700 spectrometer. ^{1}H and ^{13}C NMR chemical shifts are referenced with respect to solvent signals and reported relative to tetramethylsilane. Infrared spectra were collected from neat solid samples using a Bruker Alpha-P infrared spectrometer equipped with an attenuated total reflection (ATR) attachment inside of a glovebox. Elemental analyses were performed by Atlantic Microlab, Inc. in Norcross, Georgia.

3.4.3 Synthetic Procedures

3.4.3.1 (IDipp)AuC(N$_2$)SiMe$_3$ (**2**)

A solution of trimethylsilyl(diazomethane) (0.1 mL, 2.0M) in hexanes was added to a solution of (IDipp)Au(N(*i*-Pr)$_2$) in THF (23 mg, 0.033 mmol) in a 25-mL Schlenk flask. The flask was covered in foil to exclude light, and left to stand for 2 hours. All volatiles were then removed *in vacuo* to give the pure yellow solid (23 mg, 100% yield). ^{1}H NMR (400 MHz, CD_3CN): δ (ppm) 7.52 (t, J = 7.8 Hz, 2H, *para*-C*H*), 7.43 (s, 2H, NC*H*), 7.36 (d, J = 7.8 Hz, 4H, *meta*-C*H*), 2.59 (sep, J = 6.9 Hz, 4H, $(CH_3)_2CH$), 1.30 (d, J = 6.9 Hz, 12H, $(CH_3)_2CH$), 1.21 (d, J = 6.9 Hz, 12H, $(CH_3)_2CH$), -0.31 (s, 9H, $Si(CH_3)_3$). IR: ν (cm^{-1}) 2961,

1985, 1471, 1457, 1413, 1383, 1364, 1351, 1327, 1242, 1212, 1180, 1059, 947, 937, 876, 832, 804, 759, 747, 703, 645, 627, 532.

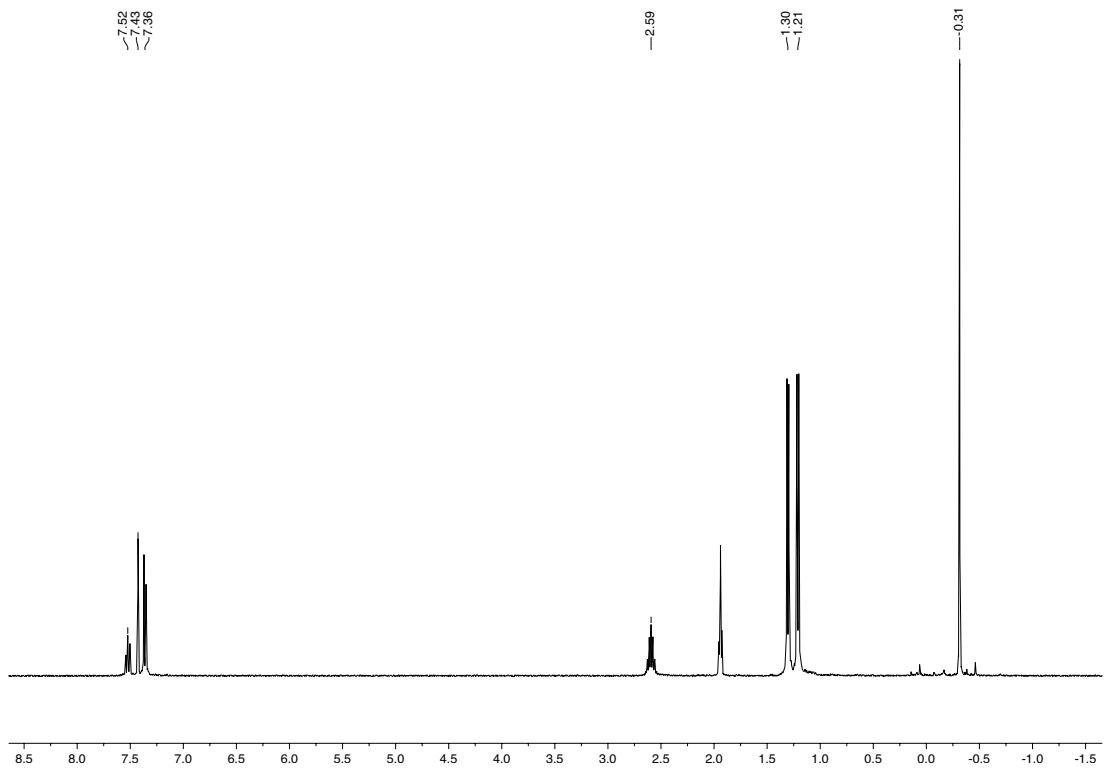

Figure 3.5. ^{1}H NMR (400 MHz, CD_3CN) spectrum of (IDipp)AuC(N_2)SiMe_3 (**2**).

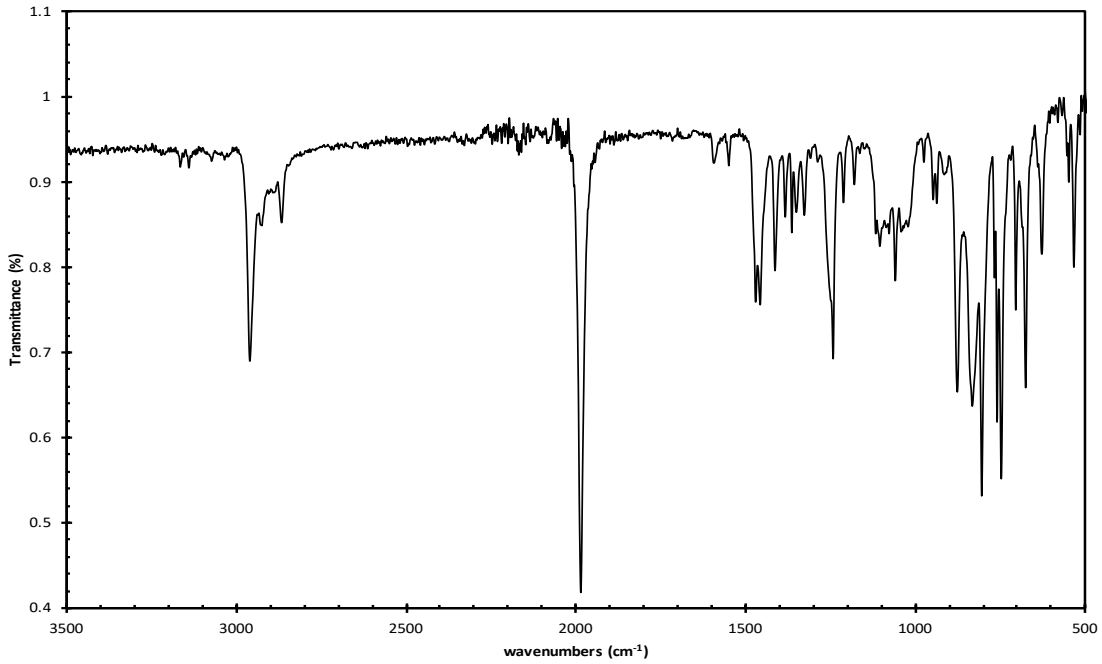

Figure 3.6. ATR-FTIR spectrum of (IDipp)AuC(N_2)$SiMe_3$ (**2**).

3.4.3.2 **(**SIMes)Au(O*t*-Pent)

SIMesAuCl (54 mg, 0.10 mmol) and 1.13 equivalents of sodium *tert*-pentyloxide (12 mg, 0.100 mmol, 87% purity) were combined in a 20-mL scintillation vial equipped with a stir bar. Toluene (6 mL) was added, the reaction mixture was stirred for 4 hours, and then filtered through a plug of Celite into a 25-mL Schlenk flask. After the Celite was washed with three additional portions of toluene, the solvent was removed *in vacuo* at 40°C overnight to afford the pure white compound (53 mg, 90%). ^{1}H NMR (700 MHz, CD_2Cl_2): δ (ppm) 6.97 (s, 4H, *meta*-C*H*), 3.94 (s, 4H, NCH_2), 2.31 (s, 12H, *ortho*-CH_3), 2.30 (s, 6H, *ortho*-CH_3), 0.94 (q, 2H, O(CH$_3$)$_2$*CCH$_2$CH$_3$)*, 0.67 (s, 6H, O(CH_3)$_2$CCH$_2$CH$_3$), 0.59 (t, 3H, O(CH$_3$)$_2$CCH$_2$CH_3). ^{13}C{^{1}H} NMR (176 MHz, CD_2Cl_2): δ (ppm) 193.88 (N*C*Au), 139.1 (C_{Ar}), 136.5 (C_{Ar}), 135.9 (C_{Ar}), 129.8 (C_{Ar}), 72.52 (O(CH$_3$)$_2$*C*CH$_2$CH$_3$), 50.97 (NCH$_2$), 40.82 (O(CH$_3$)$_2$C*C*H$_2$CH$_3$), 33.20 (O(*C*H$_3$)$_2$CCH$_2$CH$_3$), 21.31 (CH$_3$), 18.27 (CH$_3$), 9.41

($O(CH_3)_2CCH_2CH_3$). IR: ν (cm^{-1}) 1673, 1599, 1493, 1445, 1377, 1267, 1170, 1115, 1092, 1072, 1038, 970, 899, 855, 755, 701, 668, 625, 544, 457. Anal. Calcd for $C_{26}H_{37}AuN_2O$: C, 52.88; H, 6.32; N, 4.74. Found C, 52.67; H, 6.51; N, 4.78.

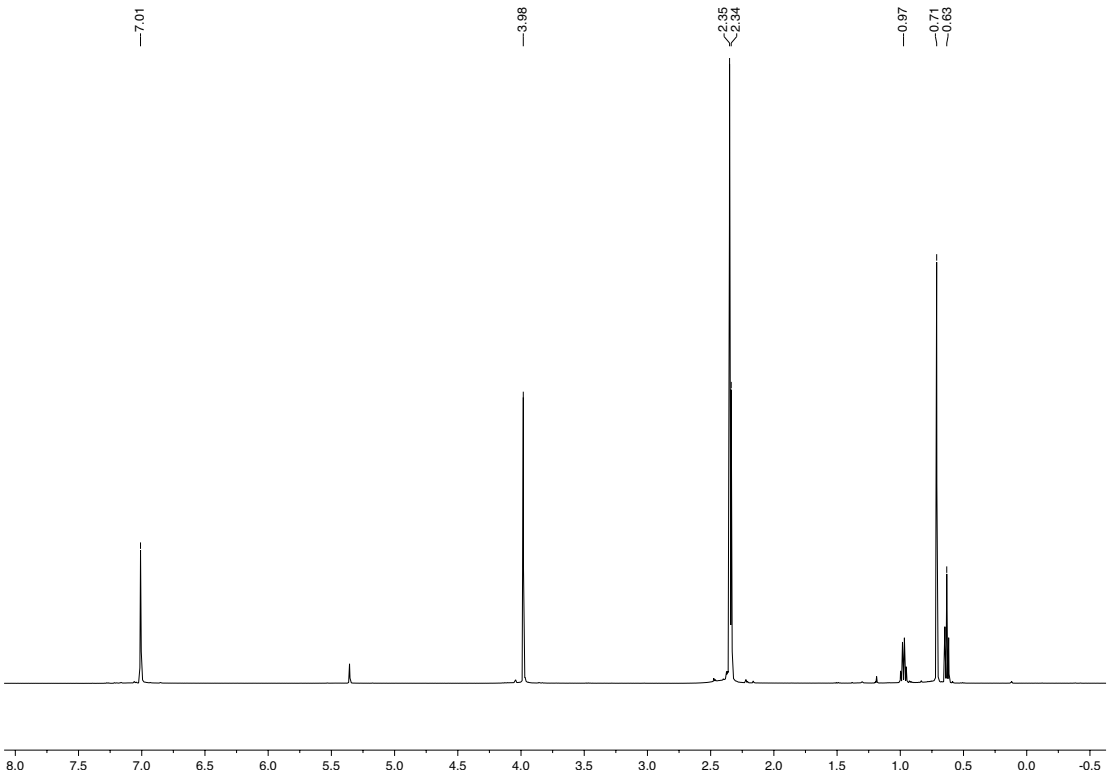

Figure 3.7. ^1H NMR (700 MHz, CD_2Cl_2) spectrum of (SIMes)Au(O*t*-Pent).

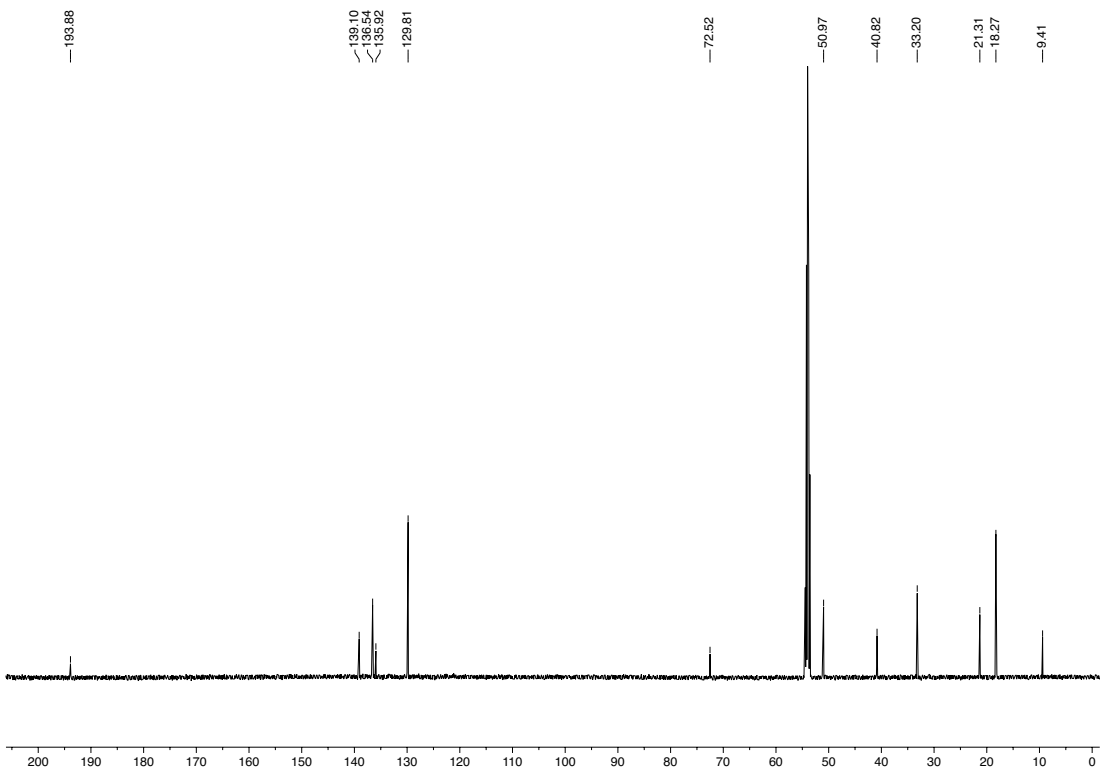

Figure 3.8. ^{13}C NMR (176 MHz, CD_2Cl_2) spectrum of (IDipp)Au(O*t*-Pent).

3.4.3.3 (SIMes)AuC(N_2)SiMe_3 (**3**)

In a 50-mL Schlenk flask, SIMesAu(O*t*-Pent) (329 mg, 0.557 mmol) was dissolved in THF (10 mL), and trimethylsilyl(diazomethane) (1.7 mL, 2.0 M in hexanes) was added. The reaction vessel was covered in foil to exclude light, and the reaction was allowed to proceed for 30 minutes. Volatiles were removed *in vacuo* overnight affording the pure compound as a yellow crystalline solid (343 mg, 100%). ^1H NMR (400 MHz, CD_2Cl_2): δ (ppm) 6.98 (s, 4H, *meta*-C*H*), 3.94 (s, 4H, NCH_2), 2.33 (s, 12H, *ortho*-CH_3), 2.30 (s, 6H, *para*-CH_3), -0.29 (s, 9H, Si(CH_3)$_3$) $^{13}C\{^1H\}$ NMR (176 MHz, CD_2Cl_2): δ (ppm) 208.67 (N*C*Au), 138.6 (C_{Ar}), 135.8 (C_{Ar}), 135.1 (C_{Ar}), 129.4 (C_{Ar}), 50.82 (NCH_2), 33.58 (CN_2), 20.77 (CH_3), 17.73 (CH_3), -0.29 (Si(CH_3)$_3$). IR: ν (cm^{-1}) 2848, 1981, 1490, 1454, 1269, 1241, 1011, 868, 828, 744, 685, 627, 572, 530. Anal. Calcd for $C_{25}H_{35}AuN_4Si$: C, 48.70; H, 5.72; N, 9.09. Found C, 49.06; H, 5.78; N, 8.69.

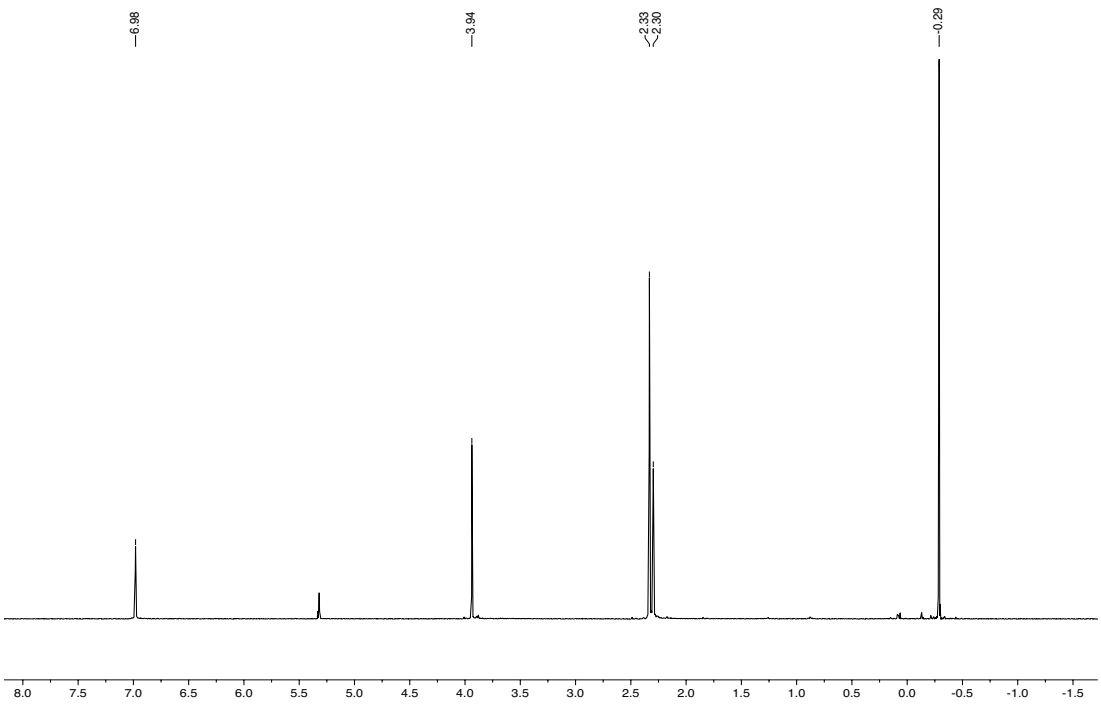

Figure 3.9. ^{1}H NMR (400 MHz, CD_2Cl_2) spectrum of (SIMes)AuC(N_2)$SiMe_3$ (**3**).

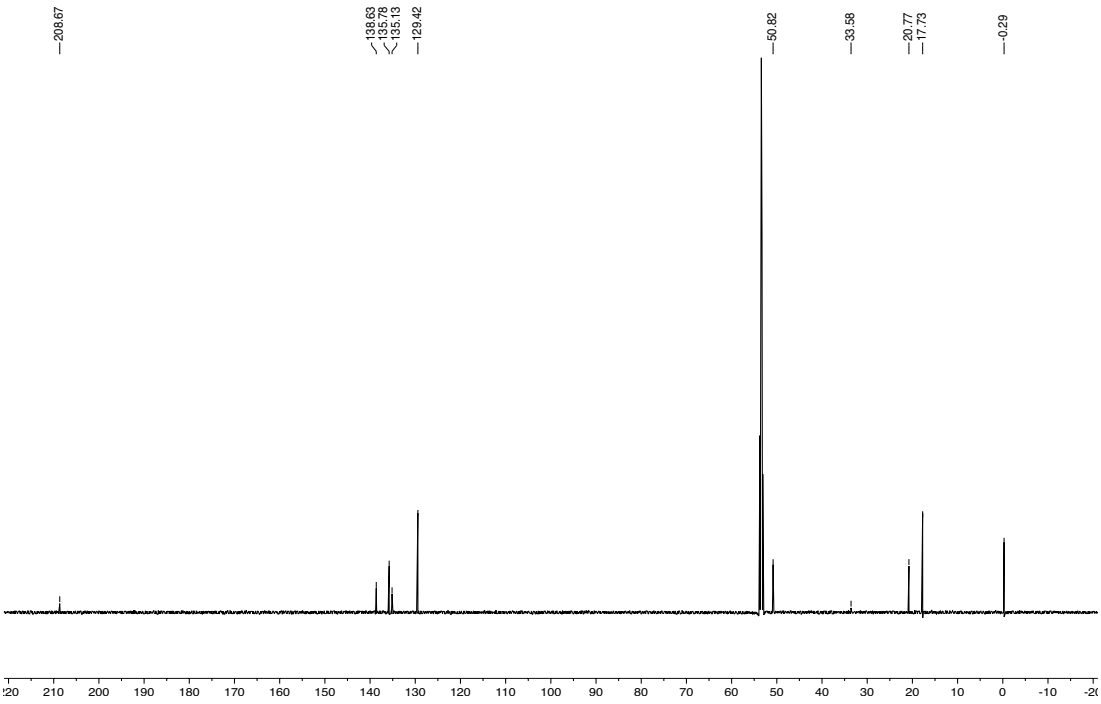

Figure 3.10. ^{13}C NMR (176 MHz, CD_2Cl_2) spectrum of (SIMes)AuC(N_2)$SiMe_3$ (**3**).

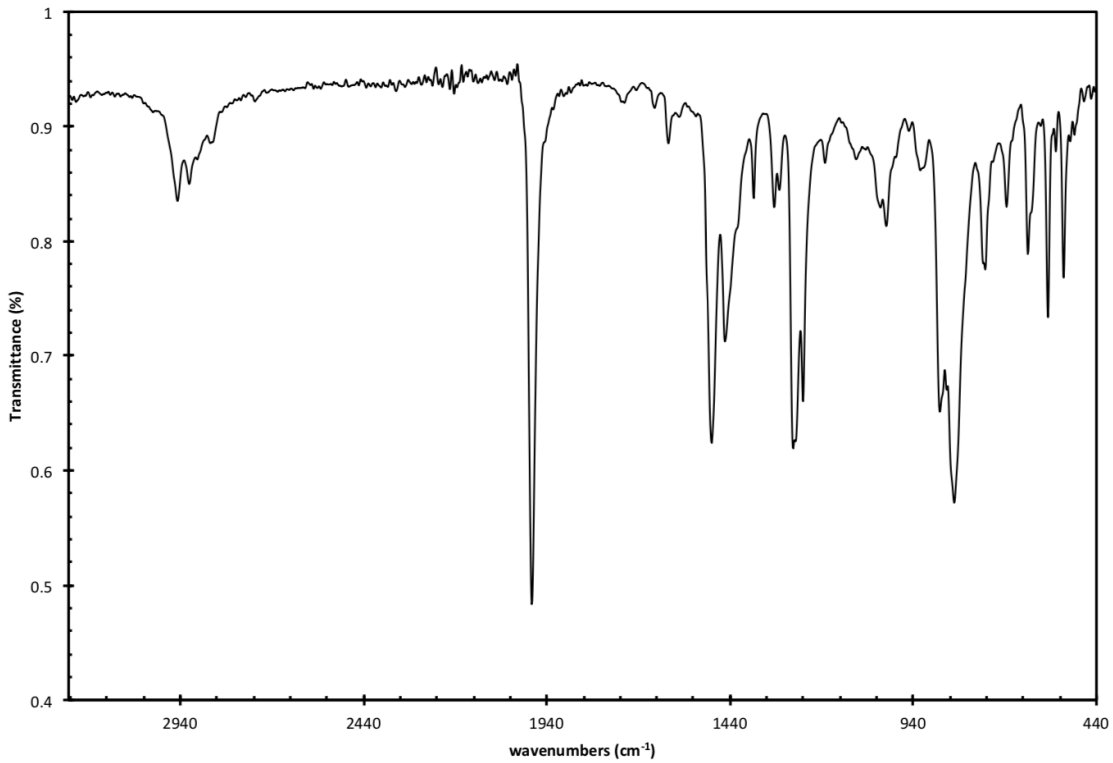

Figure 3.11. ATR-FTIR spectrum of (SIMes)AuC(N_2)$SiMe_3$ (**3**).

3.4.3.4 Reaction of (IDipp)AuC(N_2)$SiMe_3$ (**2**) with (IDipp)Au(OTf) in acetonitrile to give a product mixture containing {[(IDipp)Au]$_2$C($SiMe_3$)(MeCN)}OTf (**4**)

In a typical iteration of this experiment, a solution of (IDipp)AuC(N_2)$SiMe_3$ (61 mg, 0.087 mmol) in acetonitrile (3 mL) was cooled to -41°C and a solution of (IDipp)AuOTf (64 mg, 0.087 mmol) in acetonitrile was added dropwise with stirring. The reaction mixture was stirred at cold temperature for an additional 20 minutes, after which time it was allowed to warm to room temperature. Solvent was removed *in vacuo* to give a colorless oil consisting of {(IDipp)Au]$_2$C($SiMe_3$)(MeCN)}OTf as the major product (127 mg, 101%). ^{1}H NMR (400 MHz, CD_3CN): δ (ppm) 7.48 (t, *J* = 7.8 Hz, 4H, *para*-C*H*), 7.33 (s, 4H, NC*H*), 7.28 (d, *J* = 8.04 Hz, 8H, *meta*-C*H*), 2.57 (sep, *J* = 6.9 Hz, 4H, $(CH_3)_2CH$), 2.51 (sep, *J* = 6.9 Hz, 4H, $(CH_3)_2CH$), 1.96 (s, 3H, NCCH_3), 1.16 (d, *J* = 6.9 Hz, 12H, $(CH_3)_2CH$), 1.13 (d,

J = 6.9 Hz, 12H, (C*H*$_3$)$_2$CH), 1.11 (d, *J* = 6.9 Hz, 12H, (C*H*$_3$)$_2$CH), 1.09 (d, *J* = 6.9 Hz, 12H, (C*H*$_3$)$_2$CH), -0.66 (s, 9H, Si(CH$_3$)$_3$).

In another typical iteration of the experiment, a solution of (IDipp)AuC(N$_2$)SiMe$_3$ 32 mg, 0.046 mmol) in CD$_3$CN (1 mL) was cooled to -41°C and a solution of (IDipp)AuOTf (34 mg, 0.046 mmol) in CD$_3$CN (1 mL) was slowly added to it. The product was warmed to room temperature and the CD$_3$CN solution was evaporated to dryness. The solid obtained was then dissolved in CH$_3$CN prior to collecting ESI-MS data. ESI-MS: (m/z) {[(IDipp)Au]$_2$(C$_2$N$_3$)(H)(CD$_3$)}$^+$ (1327.7), {[(IDipp)Au]$_2$(C$_2$N$_3$)(SIMe$_3$)(CD$_3$)}$^+$ (1255.6), {(IDipp)Au]$_2$C(SiMe$_3$)(MeCN)}$^+$ (1296.6), {[(IDipp)Au]$_2$H}$^+$ (1171.5), {[(IDipp)Au]$_2$(CN)}$^+$ (1196.5).

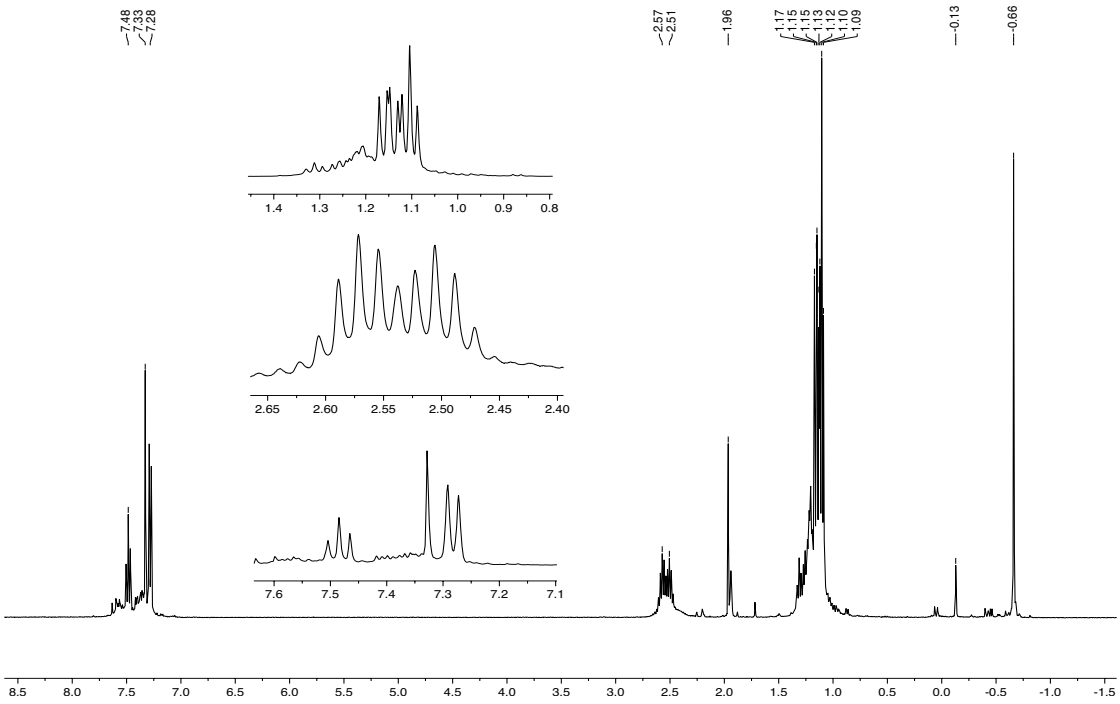

Figure 3.12. ^{1}H NMR (400 MHz, CD$_3$CN) spectrum of the reaction products of (IDipp)AuC(N$_2$)SiMe$_3$ (**2**) and (IDipp)Au(OTf) in acetonitrile to produce {[(IDipp)Au]$_2$C(SiMe$_3$)(MeCN)}OTf (**4**). Impurities: unlabeled overlapping peaks are attributed to several impurities including {[(IDipp)Au]$_2$CN}OTf and {[(IDipp)Au]$_2$H}OTf. The labelled resonance at δ -0.13 ppm may be attributable to Si(C*H*$_3$)$_3$ in {[(IDipp)Au]$_2$(C$_2$N$_3$)(SIMe$_3$)(CD$_3$)}OTf. All other labelled resonances are assigned to **4**.

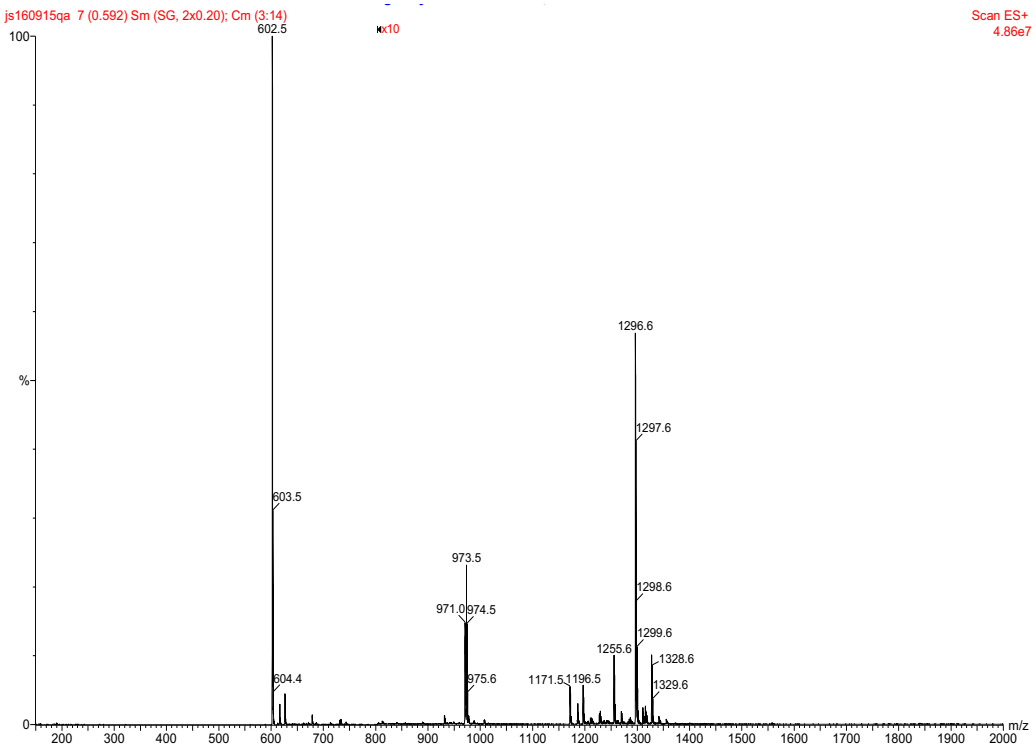

Figure 3.13. ESI-MS(+) spectrum of the products from the reaction of (IDipp)AuC(N_2)SiMe_3 (**2**) and (IDipp)Au(OTf) in CD_3CN.

3.4.3.5 (SIMes)AuF (**5**)

In a 20-mL scintillation vial equipped with a stir bar, benzoyl fluoride (103 mg, 0.830 mmol) was added to a solution of SIMesAu(O*t*-Pent) (164 mg, 0.278 mmol) in benzene (10 mL). The reaction was stirred for three hours affording the product as a white precipitate. The suspension was filtered, and solid was washed with hexanes (3 x 1 mL) to give the pure compound (115 mg, 79%). ^{1}H NMR (400 MHz, CD_2Cl_2): δ (ppm) 7.02 (s, 4H, *meta*-C*H*), 4.01 (s, 4H, NCH_2), 2.33 (s, 6H, *para*-CH_3), 2.30 (s, 12H, *ortho*-CH_3). ^{13}C{^{1}H} NMR (176 MHz, CD_2Cl_2): δ (ppm) 184.4 (d, N*C*Au), 139.1 (C_{Ar}), 135.8 (C_{Ar}), 134.8 (C_{Ar}), 129.6 (C_{Ar}), 50.53 (NCH_2), 20.82 (CH_3), 17.73 (CH_3). ^{19}F NMR (376 MHz, CD_2Cl_2): δ (ppm) -246.1 (AuF). IR: ν (cm^{-1}) 2908, 1606, 1490, 1454, 1372, 1327, 1259, 1164, 1015, 854, 739, 572, 497. Anal. Calcd for $C_{21}H_{26}AuFN_2$: C, 48.28; H, 5.02; N, 5.36. Found C, 48.54; H, 5.16; N, 5.35.

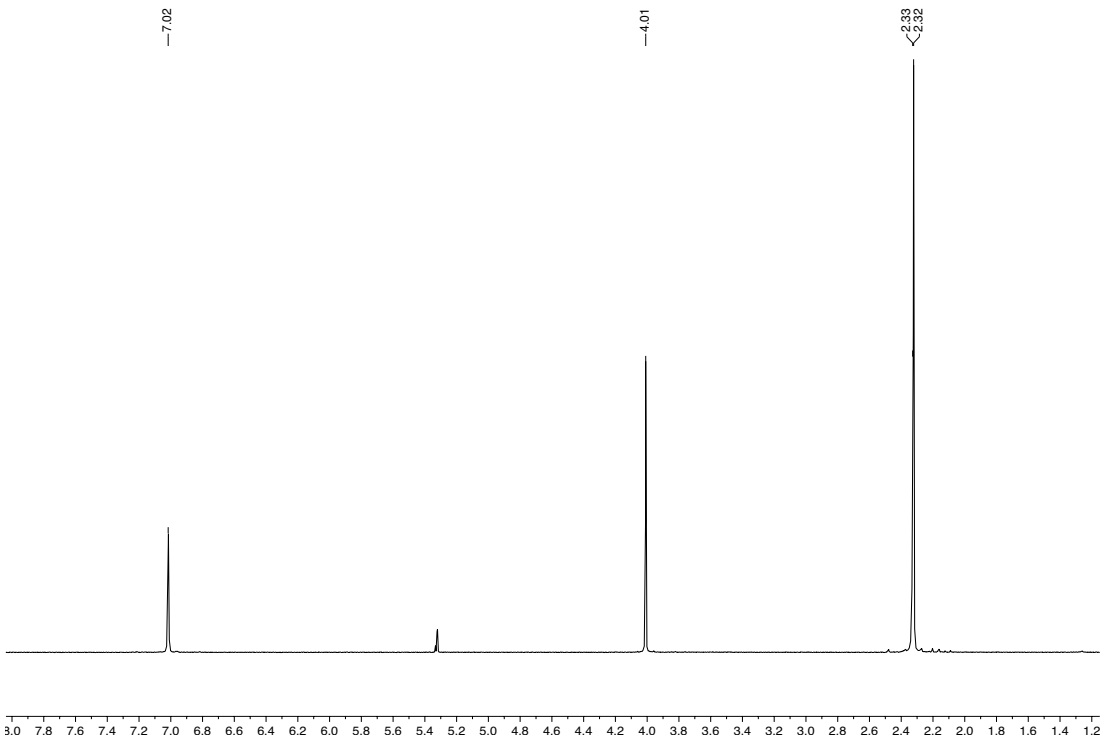

Figure 3.14. ^{1}H NMR (400 MHz, CD_2Cl_2) spectrum of (SIMes)AuF (**5**).

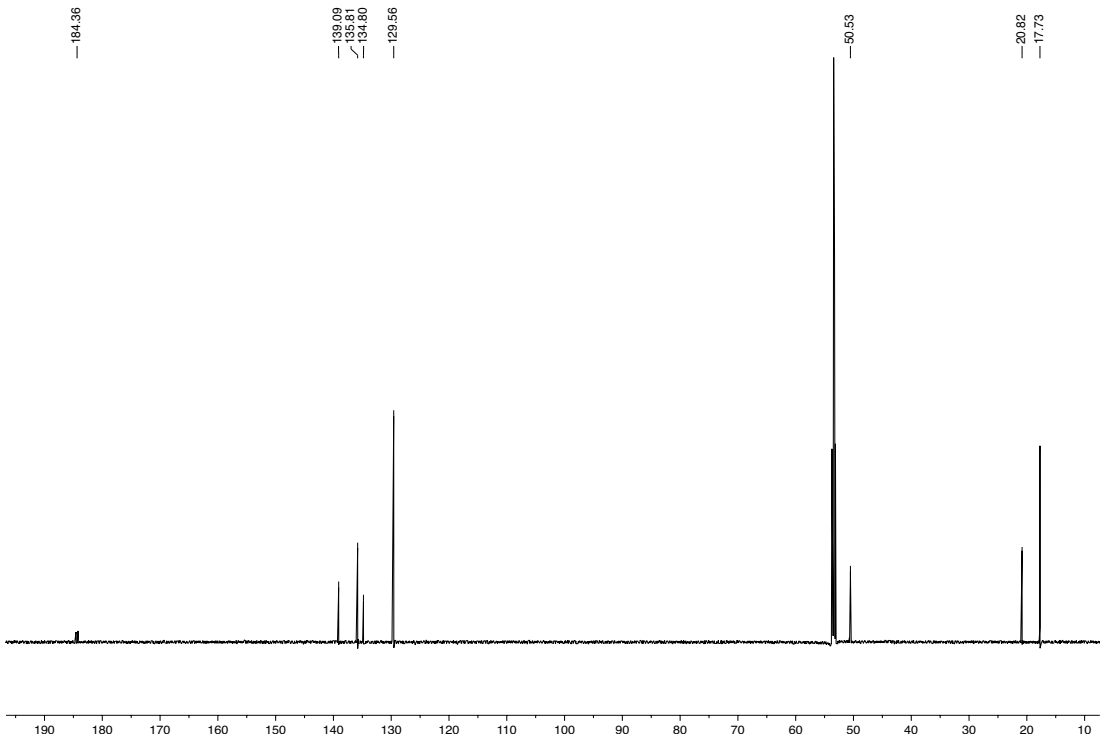

Figure 3.15. ^{13}C NMR (176 MHz, CD_2Cl_2) spectrum of (SIMes)AuF (**5**).

3.4.3.6 [(SIMes)Au(Py)]OTf (**7**)

SIMesAuCl (105 mg, 0.195 mmol), silver trifluoromethanesulfonate (50 mg, 0.19 mmol), and pyridine (47 μL, 0.58 mmol) were combined in a 20-mL scintillation vial equipped with a stir bar. DCM (10 mL) was added, and the reaction mixture was stirred in the dark for 20 minutes. The suspension was then filtered through a plug of Celite. The solvent and excess pyridine were removed *in vacuo* to give a colorless oily residue. The residue was dissolved in THF (2 mL) and crystallized by addition of cold hexanes (20 mL). The solid was collected by vacuum filtration and washed with three additional portions of hexanes (3 x 1 mL) to give the pure white solid (124 mg, 87%). ^{1}H NMR (400 MHz, CD_2Cl_2): δ (ppm) 7.99 (t, 1H, *para*-NC_5H_5), 7.93 (d, 2H, *ortho*-NC_5H_5), 7.53 (t, 2H, *meta*-NC_5H_5), 7.04 (s, 4H, *meta*-C*H*), 4.18 (s, 4H, NC*H*$_2$), 2.38 (s, 12H, *ortho*-C*H*$_3$), 2.32 (s, 6H, *ortho*-C*H*$_3$). ^{13}C{^{1}H} NMR (176 MHz, CD_2Cl_2): δ (ppm) 189.9 (N*C*Au), 151.42 (NC_5H_5 139.1 (C_{Ar}), 135.8 (C_{Ar}), 134.8 (C_{Ar}), 129.6 (C_{Ar}), 50.53 (N*C*H$_2$), 20.82 (CH_3), 17.73 (CH_3). IR: ν (cm^{-1}) 2918, 1611, 1514, 1450, 1380, 1328, 1275, 1259, 1218, 1137, 1072, 1028, 853, 753, 693, 636, 571, 517. Anal. Calcd for $C_{27}H_{31}AuF_3N_3O_3S$: C, 44.33; H, 4.27; N, 5.36. Found C, 44.47; H, 4.40; N, 5.77.

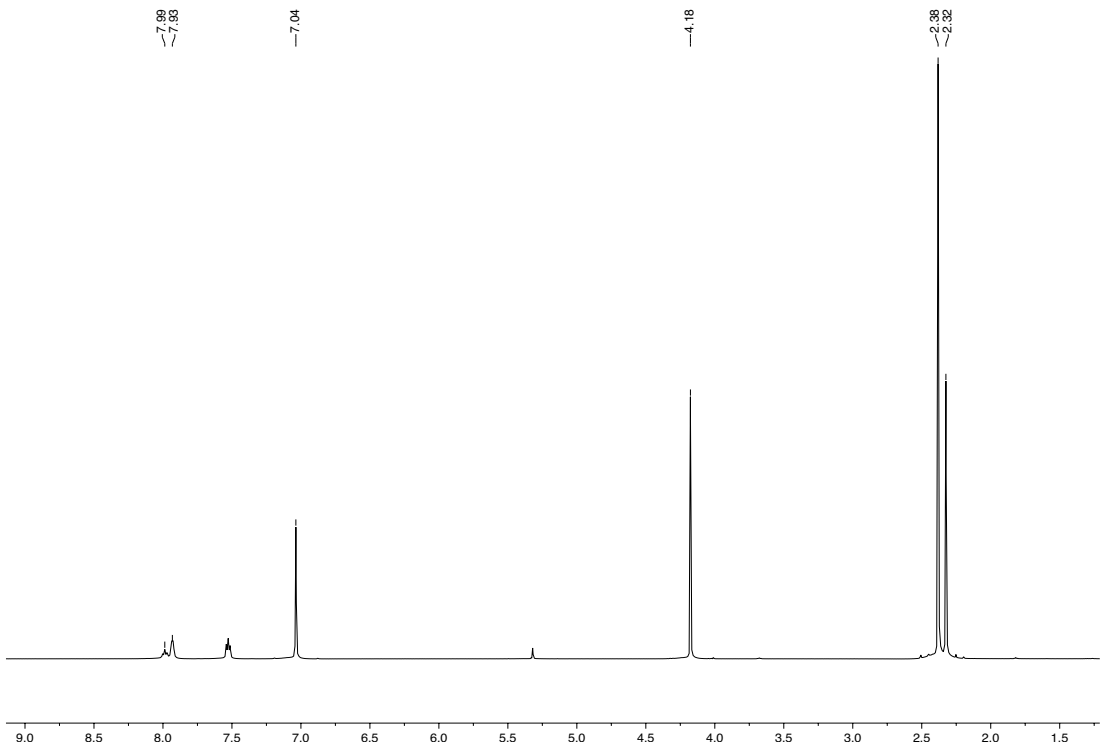

Figure 3.16. ^{1}H NMR (400 MHz, CD_2Cl_2) spectrum of [(SIMes)Au(Py)]OTf (**7**).

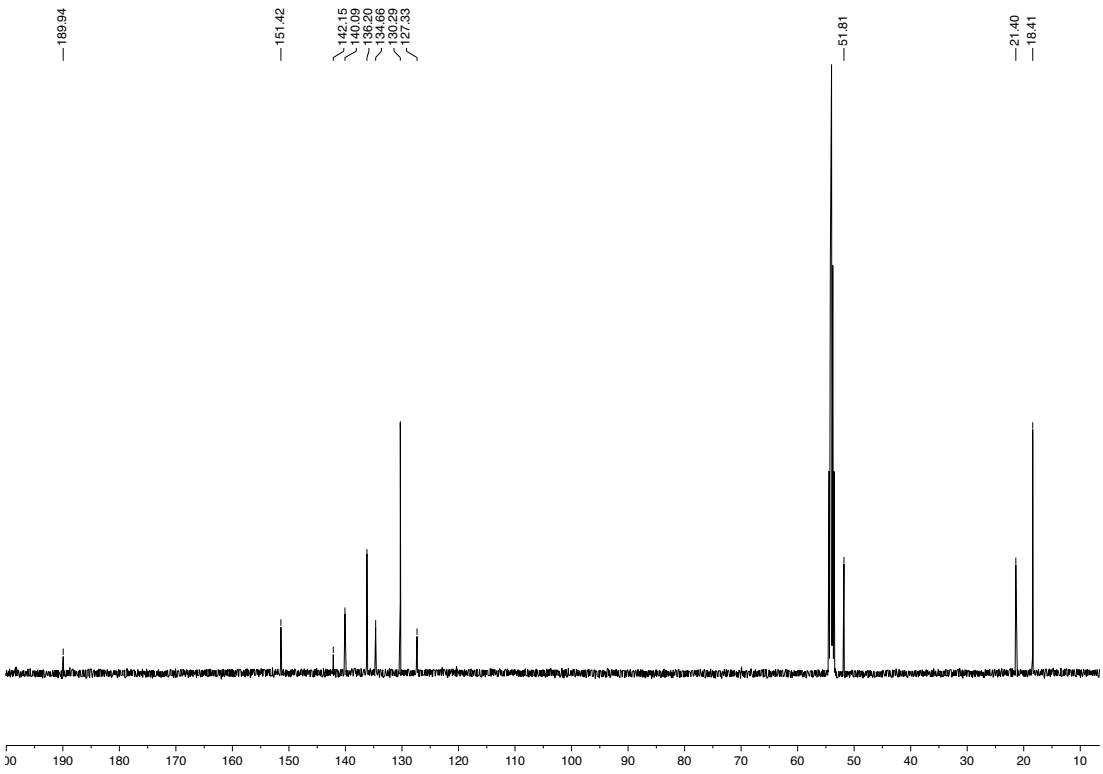

Figure 3.17. ^{13}C NMR (176 MHz, CD_2Cl_2) spectrum of [(SIMes)Au(Py)]OTf (**7**).

3.4.3.7 {[(SIMes)Au]$_3$C(Py)]OTf (**6b**)

Solutions of (SIMes)AuC(N_2)SiMe_3 (37 mg, 0.060 mmol) in pyridine (3 mL), and of SIMesAuF (37 mg, 0.060 mmol) and [SIMesAu(Py)]OTf (47 mg, 0.060 mmol) in pyridine (3 mL) were prepared in 20 mL scintillation vials and cooled to -35^{o}C in a glovebox freezer. With a precooled pipette, the solution of (SIMes)AuC(N_2)SiMe_3 was added quickly to the solution of SIMesAuF and [SIMesAu(Py)]OTf resulting in an immediate color change to magenta. The reaction mixture was transferred between vials several times to ensure adequate mixing and placed back into the glovebox freezer for 2.5 hours. Volatiles were then removed *in vacuo* at room temperature. The resulting residue was dissolved in THF (3 mL) and crystallized by addition of cold hexanes (15 mL). The precipitate was collected by vacuum filtration, and washed with hexanes (3 x 1 mL) to give the pure magenta solid (82 mg, 78%). ^{1}H NMR (700 MHz, CD_3CN): δ (ppm) 7.62 (d, 2H, *ortho*-NC5H5), 6.88 (s, 12H, CH_{Ar}), 6.74 (t, 2H, *para*-NC5H5), 6.21 (t, 2H, *meta*-NC5H5), 3.76 (s, 12H, NCH_2), 2.30 (s, 18, *para*-CH_3), 2.17 (s, 36H, *ortho*-CH_3). ^{13}C{^{1}H} NMR (176 MHz,CD_3CN): δ (ppm) 211.61 (N*C*Au), 145.63 (Au_3C), 144.50 (*ortho*-NC5H5), 138.55 (C_{Ar}), 136.84 (C_{Ar}), 136.71 (C_{Ar}), 133.02 (*para*-NC5H5), 130.13 (C_{Ar}), 122.12 (*meta*-NC5H5), 51.38 (NCH_2), 21.33 (CH_3),18.22 (CH_3). IR: ν(cm^{-1}) 2917, 1598, 1487, 1454, 1376, 1265, 1245, 1146, 1031, 990, 850, 776, 638, 574. Anal. Calcd for $C_{70}H_{83}N_7O_3Au_3$: C, 48.03; H, 4.78; N, 5.60. Found C, 48.14; H, 4.91; N, 5.60.

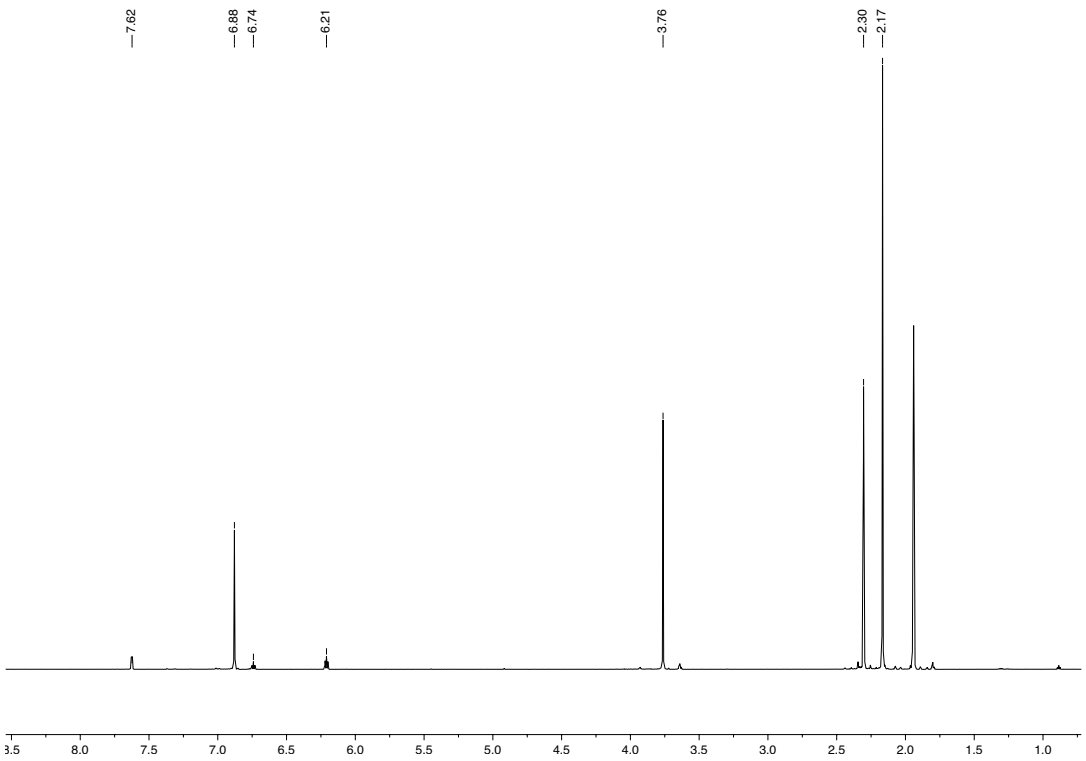

Figure 3.18. ^{1}H NMR (700 MHz, CD_3CN) spectrum of {[(SIMes)Au]$_3$C(Py)]OTf (**6b**).

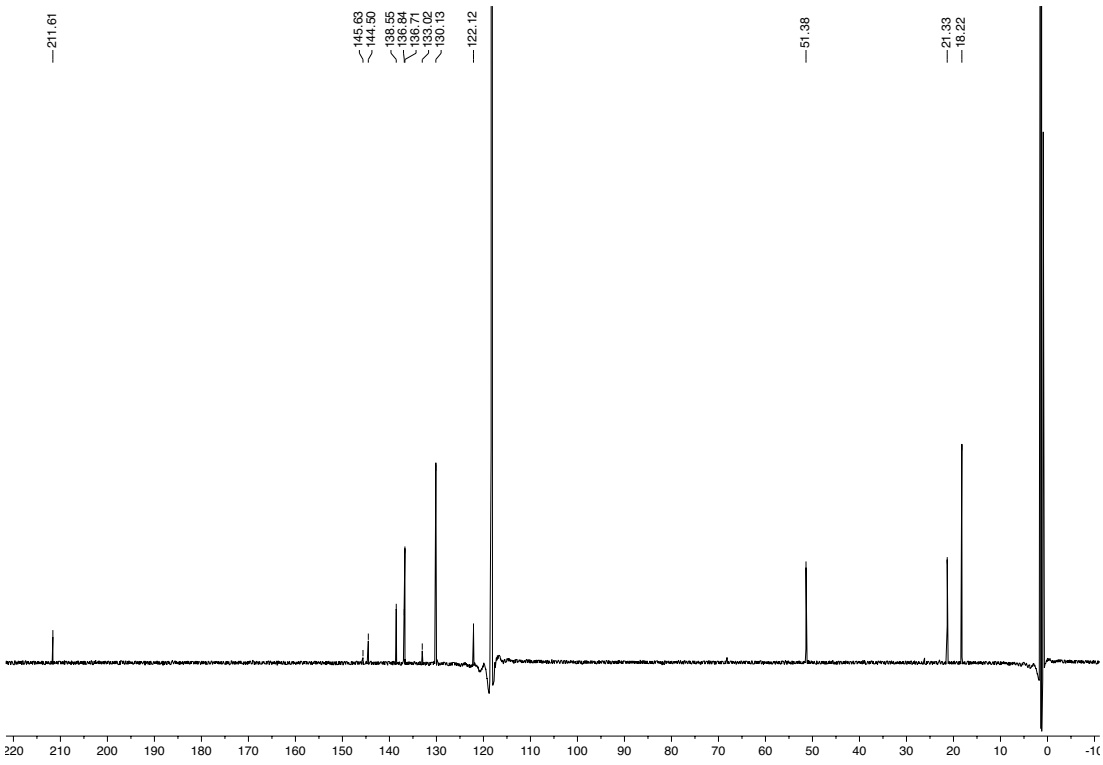

Figure 3.19. ^{13}C NMR (176 MHz, CD_3CN) spectrum of {[(SIMes)Au]$_3$C(Py)]OTf (**6b**).

3.4.3.8 Reaction of $[(SIMesAu)_3C(Py)]OTf$ with Carbon Monoxide

A $[(SIMesAu)_3C(Py)]OTf$ (15 mg, 0.0086 mmol) and 4,4'-dimethylbiphenyl (10 mg, 0.054 mmol), as an internal standard, were combined and dissolved in CD_2Cl_2 (1.5 mL) in a J. Young NMR tube. The solution was degassed and the headspace was charged with carbon monoxide (2 atm). Substitution of pyridine with CO gave the trigold ketenylidene cation as the triflate salt in 85% NMR yield after five hours. ^1H NMR (400 MHz, CD_2Cl_2): δ (ppm) 6.89 (s, 4H, *meta*-C*H*), 3.84 (s, 4H, NCH_2), 2.32 (s, 6H, *ortho*-CH_3), 2.12 (s, 12H, *ortho*-CH_3). IR: ν (cm^{-1}) 2004 (CO).

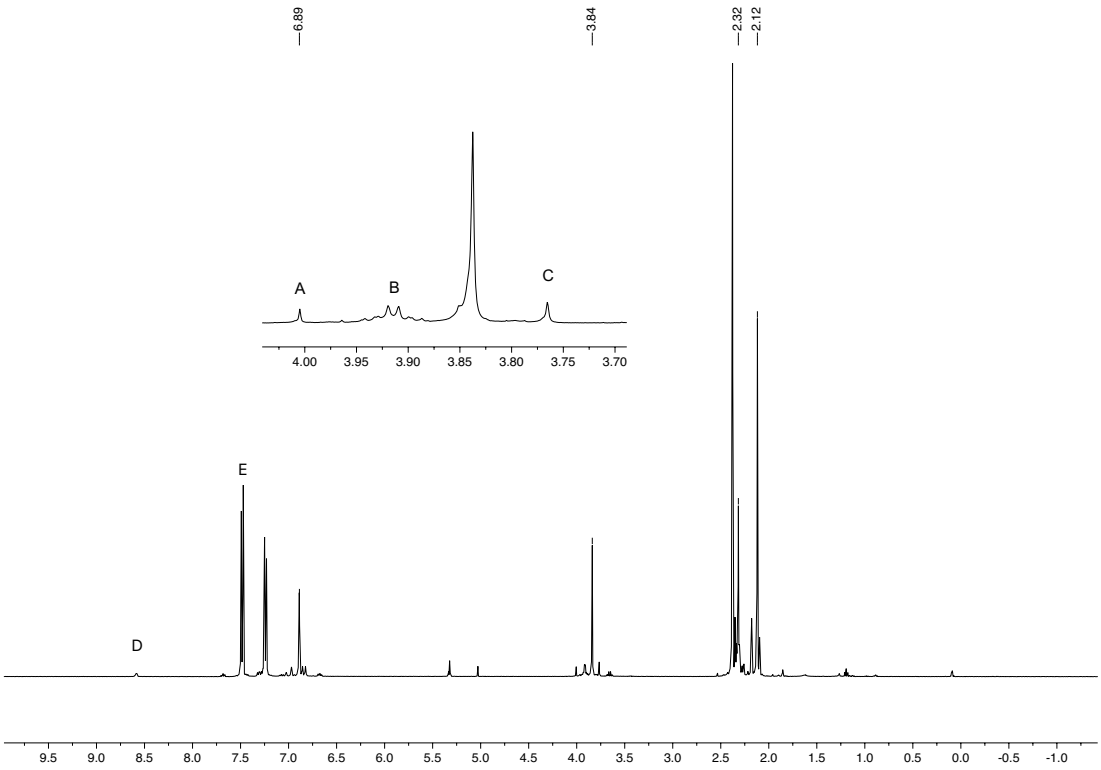

Figure 3.20. ^1H NMR (400 MHz, CD_2Cl_2) spectrum of the reaction between **6b** and CO showing 85% conversion of **6b** to $\{[(SIMes)Au]_3CCO\}OTf$. (A) unidentified byproduct; (B) $\{[(SIMes)Au]_2CH(Py)\}OTf$; (C) unreacted **6b** (NCH_2); (D) free pyridine (*ortho*-NC_5H_5); (E) 4,4'-dimethylbiphenyl (2,2'-C*H*). Traces of adventitious hexane (δ 0.89, δ 1.27) and ethanol (δ 3.66, δ 1.19) are present.

3.4.3.9 Reaction of (SIMes)AuF (**5**) with (SIMes)AuC(N_2)$SiMe_3$ (**3**) in CD_2Cl_2 Followed by Addition of Pyridine.

A solution of (SIMes)AuC(N_2)$SiMe_3$ (10 mg, 0.016 mmol) in CD_2Cl_2 (1mL) was added dropwise to a scintillation vial containing (SIMes)AuF (17 mg, 0.032 mmol) in CD_2Cl_2 (1 mL) at -35°C to give a yellow-green solution. Excess pyridine was immediately added to the reaction mixture, resulting in a color change to deep magenta. The ^{1}H NMR spectrum of the reaction mixture reveals that *ca*. 50% of the [(SIMes)Au] was converted to **6a** based on total integration.

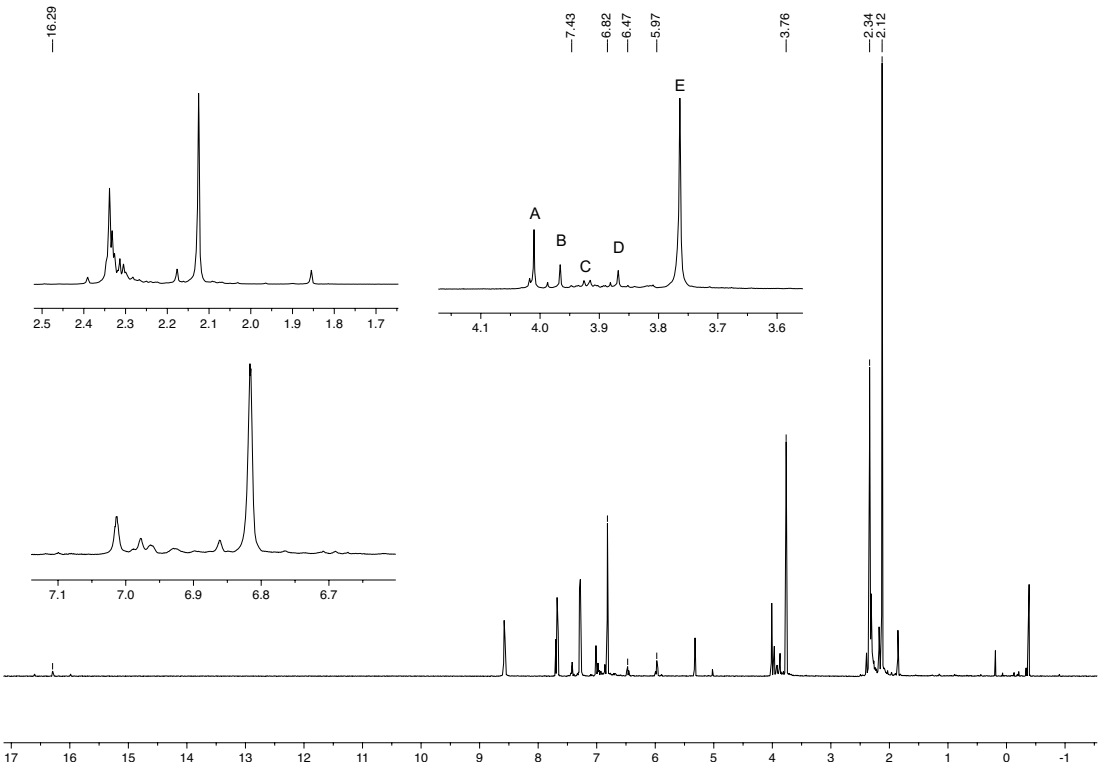

Figure 3.21. ^{1}H NMR (400 MHz) of the reaction products of (SIMes)AuF with (SIMes)AuC(N_2)$SiMe_3$ in CD_2Cl_2 followed by addition of Pyridine. The (NCH_2) resonance corresponding to the target product and byproducts of the reaction are labeled. (A) (SIMes)AuF, (B) unidentified product, (C) {[(SIMes)Au]$_2$CH(NC_5H_5)}OTf, (D) [(SIMes)$_2$Au]OTf, (E) **6a**.

3.4.3.10 {[(SIMes)Au]$_2$C(SiMe$_3$)(Py)}OTf (**8**)

In separate 20-mL scintillation vials, [(SIMes)Au(Py)]OTf (31 mg, 0.042 mmol) and (SIMes)AuC(N_2)SiMe$_3$ (26 mg, 0.042 mmol) were dissolved in pyridine (2 mL) and cooled to -35°C in the glove box freezer. With a precooled pipette, the solution of (SIMes)AuC(N_2)SiMe$_3$ was quickly added to the solution of [(SIMes)Au(Py)]OTf, accompanied by a slight change in color, and the reaction mixture was placed back in the glovebox freezer for 15 minutes. The solution was then evaporated to give an oily residue, which was dissolved in THF (3 mL) and crystallized by addition of cold hexanes (15 mL). The yellow precipitate was collected by vacuum filtration and washed with hexanes (3 x 2 mL) (45 mg, 88 mol%). ^{1}H NMR indicated the presence of impurities including [(SIMes)$_2$Au]OTf (10 mol%) and [[(SIMes)Au]$_2$CH(Py)]OTf (1.6 mol%). ^{1}H NMR (500 MHz, CD_2Cl_2): δ (ppm) 8.00 (d, *J* = 6.0 Hz, 2H, *ortho*-NC$_5$*H*$_5$), 7.40 (t, *J* = 7.6 Hz, 1H, *para*-NC$_5$*H*$_5$), 6.89 (s, 4H, *meta*-C*H*), 6.86 (s, 4H, *meta*-CH), 6.83 (t, *J* = 7.3 Hz, 2H, *meta*-NC$_5$*H*$_5$), 3.93 (s, 4H, NC*H*$_2$), 2.30 (s, 12H, *para*-C*H*$_3$), 2.26 (s, 12H, *ortho*-C*H*$_3$), 2.22 (s, 12H, *ortho*-C*H*$_3$), -0.68 (s, 9H, Si(C*H*$_3$)$_3$). ^{13}C{^{1}H} NMR (176 MHz, CD_2Cl_2): δ (ppm) 211.3 (NCAu), 146.2 (*ortho*-NC$_5$H$_4$), 138.7 (C_{Ar}),136.4 (C_{Ar}), 136.3 (C_{Ar}), 135.9 (C_{Ar}) 129.8 (*meta*-CH), 129.7 (*meta*-CH$_3$), 124.1 (*meta*-NC$_5$H$_5$), 106.2 (Au_2C), 51.32 (NCH_2), 21.40 (*para*-CH$_3$), 18.36 (*ortho*-CH$_3$) 18.33 (*ortho*-CH$_3$) 1.45 (Si(CH$_3$)$_3$).

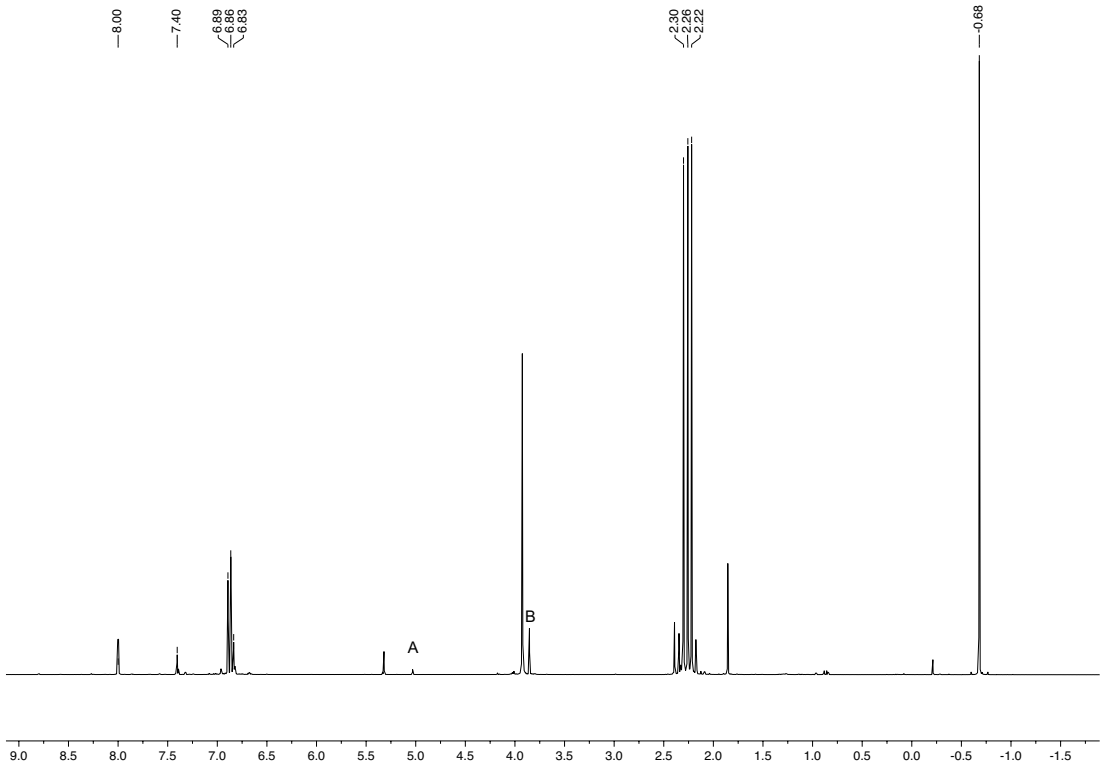

Figure 3.22. ^{1}H NMR (500 MHz, CD_2Cl_2) spectrum of {[(SIMes)Au]$_2$C(SiMe$_3$)(Py)}OTf (**8**). Impurities: (A) of [[(SIMes)Au]$_2$CH(Py)]OTf (1.6 mol%); (B) [(SIMes)$_2$Au]OTf (10 mol%).

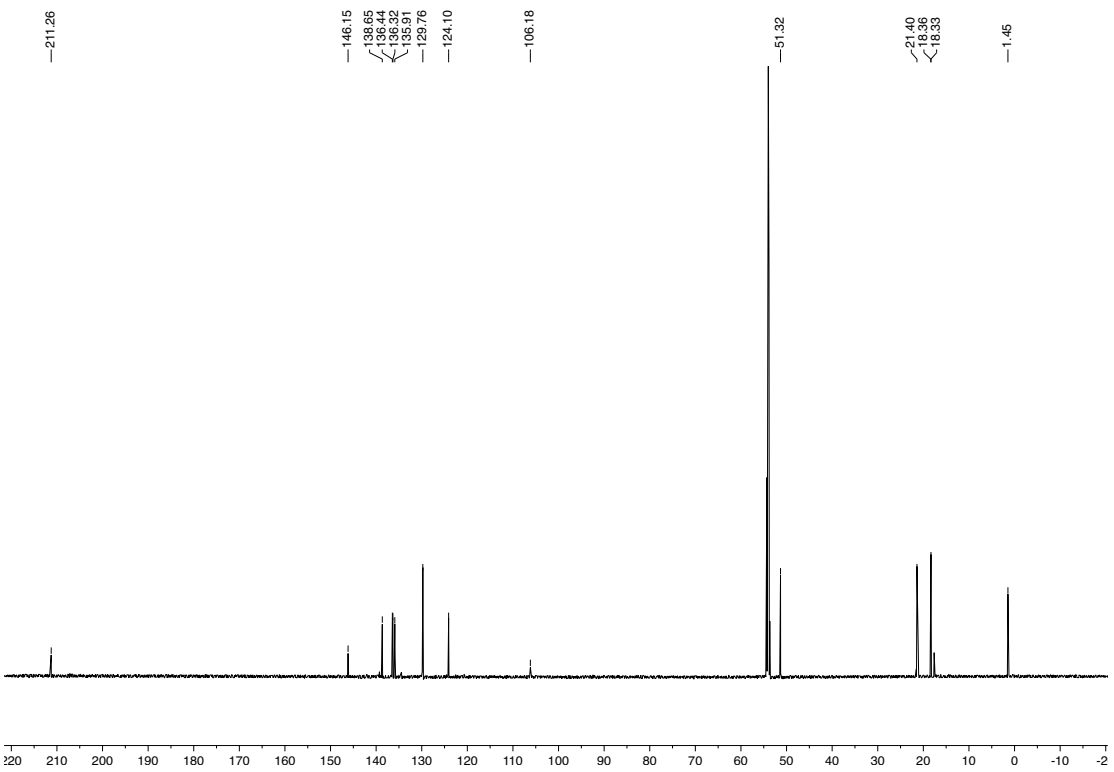

Figure 3.23. ^{13}C NMR (176 MHz, CD_2Cl_2) spectrum of {[(SIMes)Au]$_2$C(SiMe$_3$)(Py)}OTf (**8**).

3.4.3.11 (IDipp)Au(CH_2OCH_3)

In a 20-mL scintillation vial, (IDipp)AuC(N_2)SiMe$_3$ (28 mg, 0.040 mmol) and KHF_2 (10.8 mg, 0.138 mmol) were combined outside of the glove box. Wet methanol (10 mL) was added, and the reaction mixture was sonicated for 15 minutes. The reaction mixture was rotary evaporated to dryness, triturated with acetonitrile (ca. 10mL), and filtered through silica gel to give a colorless solution, which was rotary evaporated to dryness to give the pure white solid (21 mg, 81%). ^1H NMR (500 MHz, CD_3OD): δ (ppm) 7.49 (t, *J* = 7.9 Hz, 2H, *para*-C*H*), 7.48 (s, 2H, NC*H*), 7.34 (d, *J* = 7.9 Hz, 4H, *meta*-C*H*), 4.03 (s, 2H, AuCH_2), 2.85 (s, 3H, OCH_3), 2.67z (sep, *J* = 6.9 Hz, 4H, $(CH_3)_2CH$), 1.35 (d, *J* = 6.9 Hz, 12H, $(CH_3)_2CH$), 1.23 (d, *J* = 6.9 Hz, 12H, $(CH_3)_2CH$). ^{13}C NMR (126 MHz, CD_3OD): δ (PPM) 199.9 (NCAu), 147.1 (*ortho*-C), 136.2 (*ipso*-C), 131.2 (*para*-C), 124.9 (*meta*-C), 124.8 (*ipso*-C), 82.94 ($AuCH_2$), 61.66 (OCH_3), 29.94 ($CH(CH_3)_2$), 24.73 ($CH(CH_3)_2$), 24.30

($CH(CH_3)_2$). IR ν (cm^{-1}): 2960, 2923, 2866, 2788, 2759, 1593, 1546, 1471, 1469, 1413, 1384, 1364, 1348, 1328, 1255, 1233, 1215, 1173, 1170, 1106, 1073, 1058, 947, 936, 875, 804, 760, 746, 690, 548, 449. Anal. Calcd for $C_{29}H_{41}AuN_2O$: C, 55.23; H, 6.55; N, 4.44. Found C, 54.64; H, 6.45; N, 4.75.

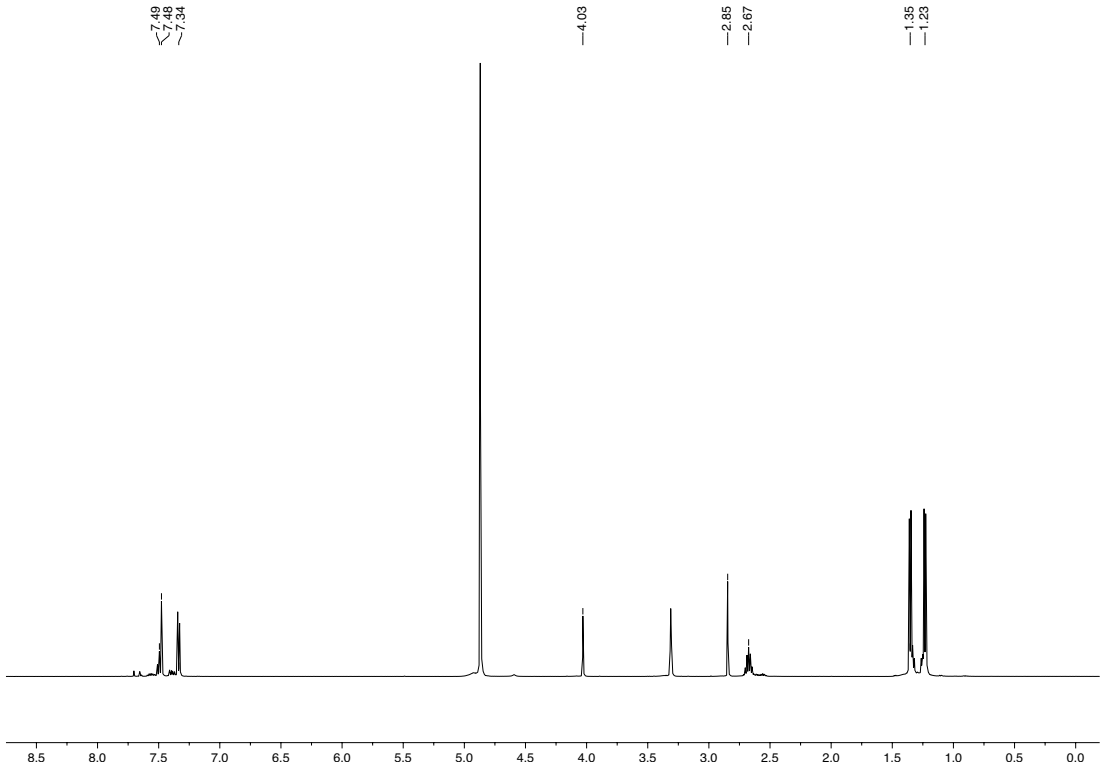

Figure 3.24. ^1H NMR (500 MHz, CD_3OD) spectrum of (SIMes)Au(CH_2OCH_3).

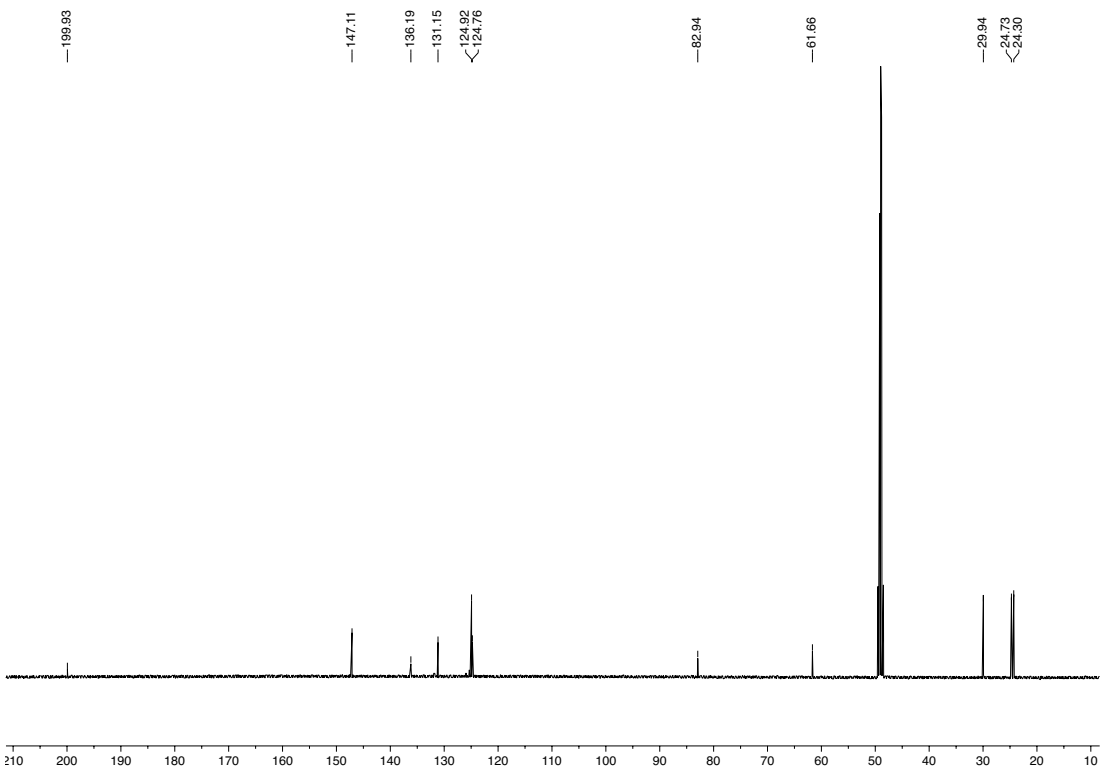

Figure 3.25. ^{13}C NMR (126 MHz, CD_3OD) spectrum of (SIMes)Au(CH_2OCH_3).

3.4.3.12 {[(SIMes)Au]$_2$CH(Py)}OAc

A solution of (SIMes)Au(OAc) (13 mg, 0.023 mmol) in pyridine (3 mL) was added to a solution of (SIMes)AuC(N_2)SiMe_3 (14 mg, 0.023 mmol) in THF (5 mL) at -41°C over the course of 30 minutes with stirring. The reaction was allowed to proceed at low temperature for 1.75 h over which time a yellow color developed. The reaction mixture was then allowed to warm to room temperature, and volatiles were removed *in vacuo*. The residue was dissolved in THF (*ca.* 1 mL) and recrystallized by addition of cold hexanes (*ca.* 20 mL). ^1H NMR (300 MHz, CD_2Cl_2): δ (ppm) 7.32 (d, J = 6.0 Hz, 2H, *ortho*-NC_5H_5), 7.09 (t, J = 7.7 Hz, 1H, *para*-NC_5H_5), 6.96 (s, 4H, *meta*-C*H*), 6.82 (s, 4H, *meta*-CH), 6.68 (t, J = 7.3 Hz, 2H, *meta*-NC_5H_5), 5.02 (s, 1H, Au_2CH), 3.92 (m, 4H, NCH_2), 2.35 (s, 12H, *para*-CH_3), 2.30 (s, 12H, *ortho*-CH_3), 2.17 (s, 12H, *ortho*-CH_3), 1.76 (s, 9H, CH_3COO^-). IR

ν (cm^{-1}): 2913, 1584, 1489, 1364, 1317, 1269, 1183, 1109, 1012, 850, 776, 679, 630, 574, 459.

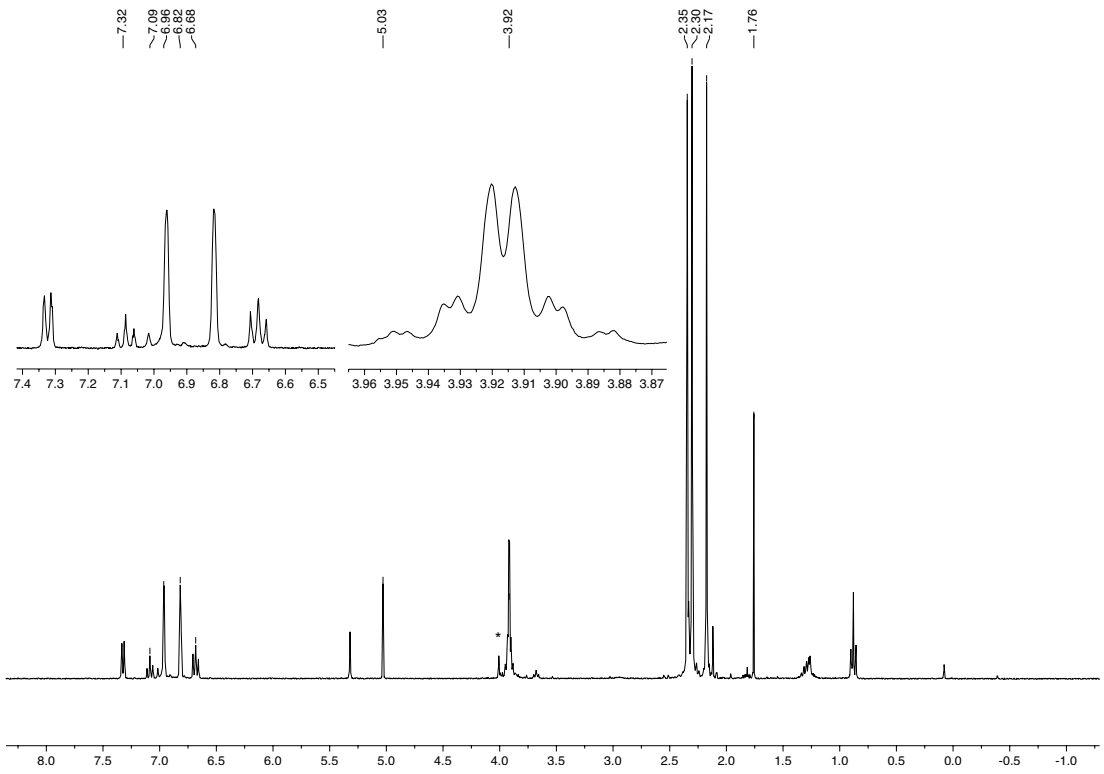

Figure 3.26. ^{1}H NMR (300 Mhz, CD_2Cl_2) spectrum of {[(SIMes)Au]$_2$CH(Py)}OAc. Impurity: (*) unidentified NC*H*$_2$ resonance corresponding to a (SIMes)Au containing product (*ca.* 5 mol%), hexanes (δ 0.89, δ 1.27).

3.4.3.13 {[(SIMes)Au]$_2$(OAc)}BF_4

(SIMes)Au(OAc) (104 mg, 0.184 mmol) and triphenylcarbenium tetrafluoroborate (30 mg, 0.18 mmol) were combined in a 20-mL scintillation vial equipped with a stir bar, and THF (20 mL) was added. The solution was stirred for three hours. Cold hexanes (20-mL) was added to precipitate the product, which was collected by vacuum filtration and washed with hexanes (1 mL) to afford the white solid (99 mg, 93%). ^{1}H NMR (300 MHz,

CD_2Cl_2): δ (ppm) 6.93 (s, 4H, *meta*-C*H*), 4.09 (s, 4H, NCH_2), 2.29 (s, 6H, *para*-CH_3), 2.26 (s, 12H, *ortho*-CH_3), 1.31 (OAc).

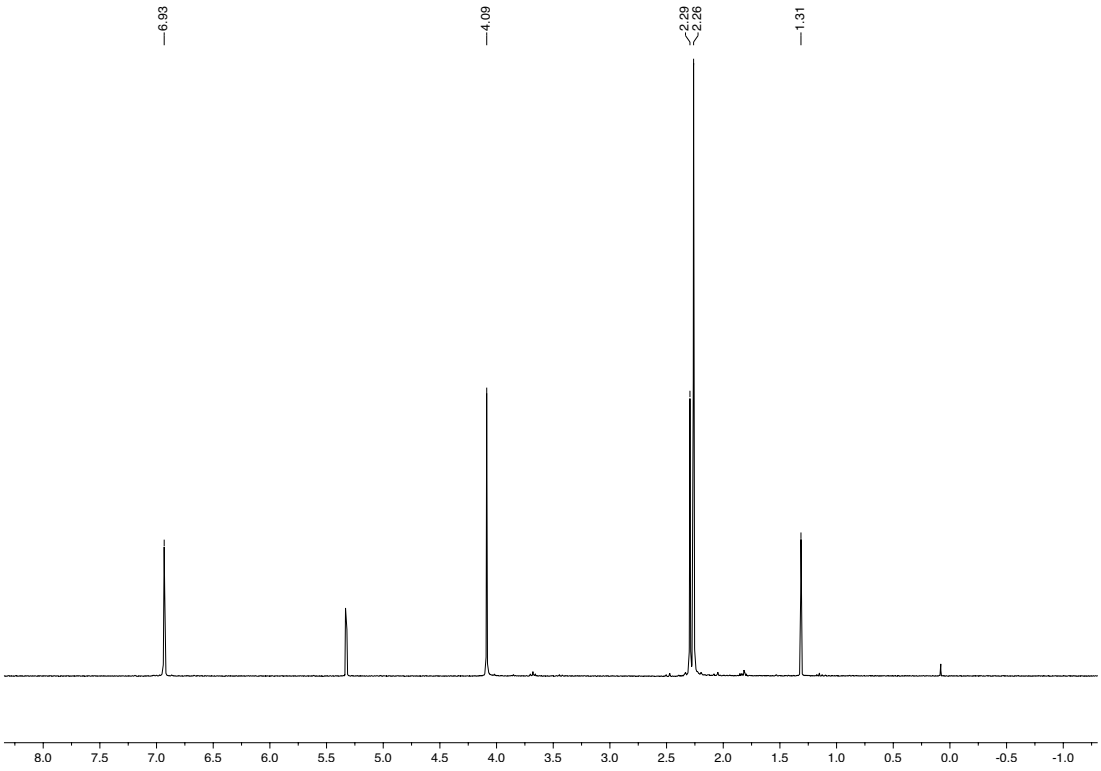

Figure 3.27. ^{1}H NMR (300 MHz, CD_2Cl_2) spectrum of {[(SIMes)Au]$_2$(OAc)}BF_4.

3.4.3.14 {[(SIMes)Au]$_2$(OAc)}OTf

(SIMes)AuCl (65 mg, 0.12 mmol) and silver acetate (10mg, 0.060 mmol) and silver trifluoromethanesulfonate (15 mg, 0.060 mmol) were combined in a 20-mL scintillation vial equipped with a stir bar. DCM (15 mL) was added, and the reaction was stirred in the dark for three hours. The suspension was then filtered through Celite and dried *in vacuo* to afford the white powder. ^{1}H NMR (300 MHz, CD_2Cl_2): δ (ppm) 6.93 (s, 4H, *meta*-C*H*), 4.09 (s, 4H, NCH_2), 2.29 (s, 6H, *para*-CH_3), 2.26 (s, 12H, *ortho*-CH_3), 1.31 (OAc).

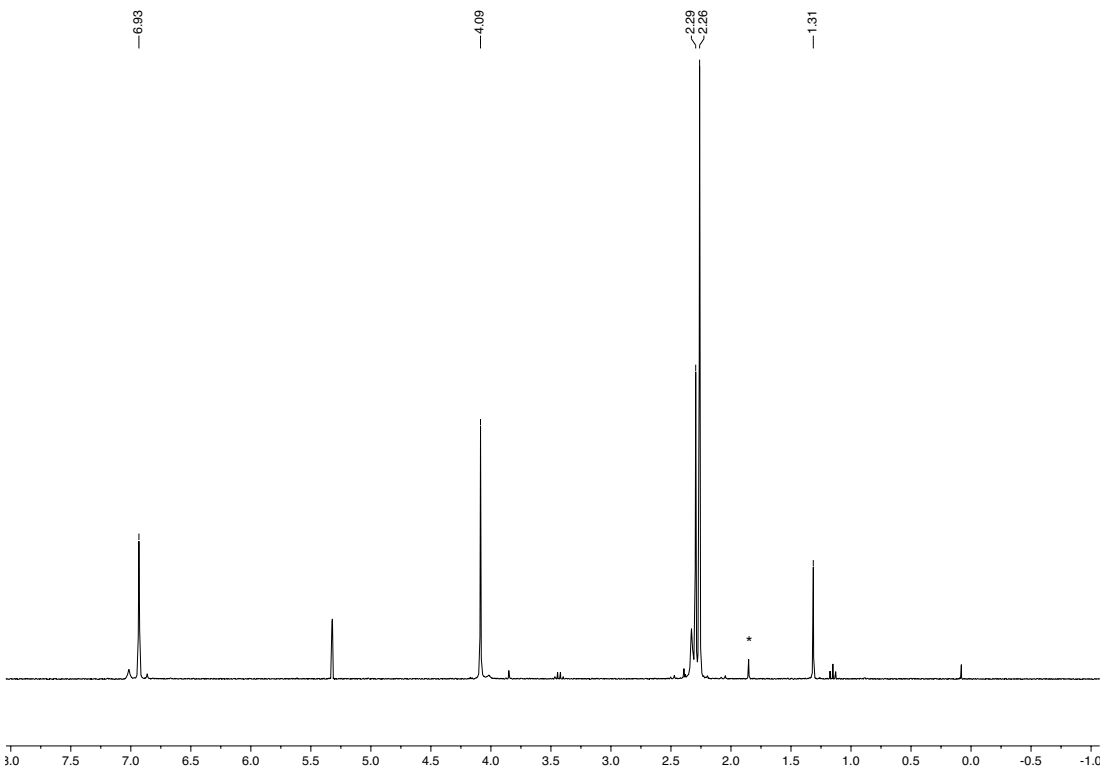

Figure 3.28. ^{1}H NMR (300 MHz, CD_2Cl_2) spectrum of {[(SIMes)Au]$_2$(OAc)}OTf. Impurities: (*) [(SIMes)$_2$Au]OTf (*ortho*-CH, δ 1.86), adventitious diethyl ether (δ 3.44, 1.14 ppm).

3.4.3.15 (SIMes)Au(O*t*-Bu)

Following the same procedure as for the preparation of (SIMes)Au(O*t*-Pent), (SIMes)AuCl (72 mg, 0.13 mmol) and sodium *tert*-butoxide (13 mg, 0.14 mmol) were combined in a 20-mL scintillation vial equipped with a stir bar. Toluene (15 mL) was added, and the solution was stirred for two hours. The suspension was then filtered through Celite and dried *in vacuo* to afford the white powder. ^{1}H NMR (400 MHz, CD_2Cl_2): δ (ppm) 6.97 (s, 4H, *meta*-C*H*), 3.94 (s, 4H, NCH_2), 2.31 (s, 6H, *para*-CH_3), 2.29 (s, 12H, *ortho*-CH_3), 0.74 (OC(CH_3)$_3$).

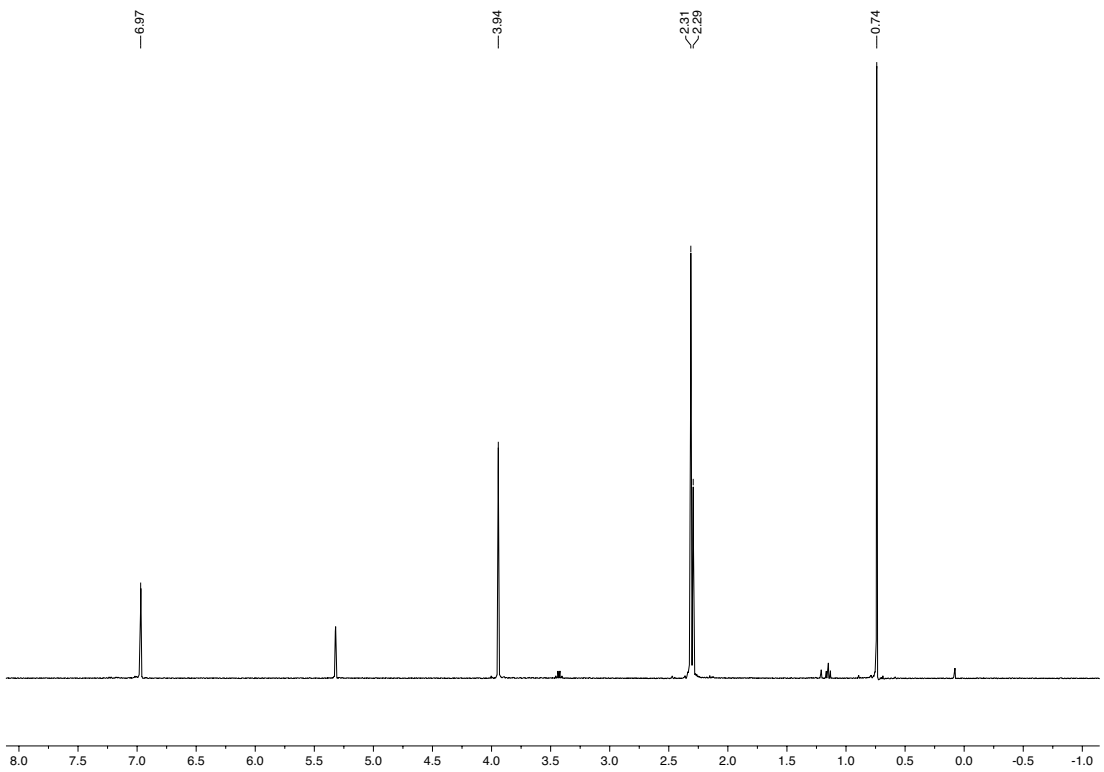

Figure 3.29. ^{1}H NMR (400 MHz, CD_2Cl_2) spectrum of (SIMes)Au(O*t*-Bu). Impurities: adventitious diethyl ether (δ 3.43, δ 1.15).

3.4.3.16 {[(SIMes)Au]$_2$(O*t*-Bu)}OTf

(SIMes)Au(O*t*-Bu) (41 mg, 0.071 mmol), (SIMes)AuCl (38 mg, 0.071 mmol), and silver triflate (18 mg, 0.070 mmol) were combined in a 20-mL scintillation vial equipped with a stir bar. DCM (15 mL) was added, and the reaction was stirred for 20 minutes, then filtered through Celite, and dried *in vacuo* to afford the white solid (65 mg, 75%). ^{1}H NMR (400 MHz, CD_2Cl_2): δ (ppm) 6.95 (s, 4H, *meta*-C*H*), 4.03 (s, 4H, NCH_2), 2.33 (s, 6H, *para*-CH_3), 2.23 (s, 12H, *ortho*-CH_3), 0.52 (OC(CH_3)$_3$).

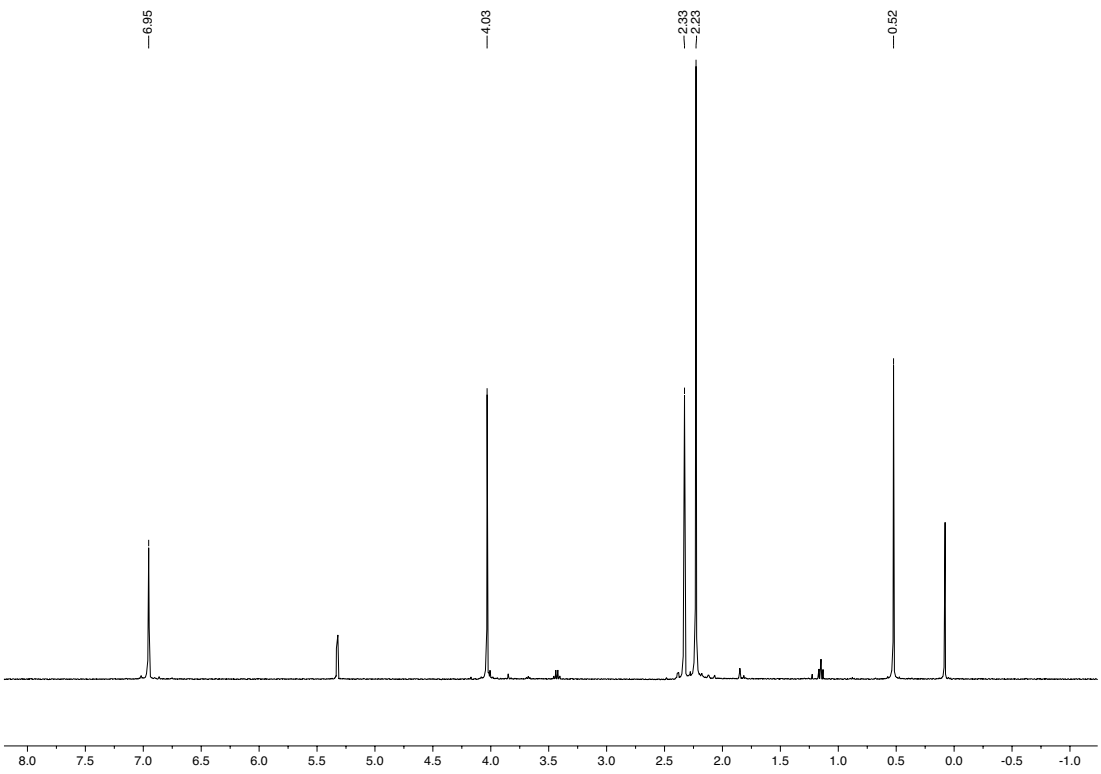

Figure 3.30. ^{1}H NMR (400 MHz, CD_2Cl_2) spectrum of {[(SIMes)Au]$_2$(O*t*-Bu)}OTf. Impurities: silicone grease (δ 0.08 ppm), adventitious diethyl ether (δ 3.43, δ 1.15).

3.4.4 X-Ray Diffraction Studies

3.4.4.1 {[(SIMes)Au]$_2$CN}OTf

Single crystals of {[(SIMes)Au]$_2$CN}OTf were grown by carefully layering an acetonitrile solution with benzene. A suitable crystal was selected with the dimensions 0.7 mm × 0.3 mm × 0.1 mm and was mounted on a loop with paratone oil. Data were collected using a Bruker APEX-II CCD diffractometer equipped with an Oxford Cryosystems low-temperature apparatus operating at T = 100(2) K. Using Olex2,[62] the structure was solved with the ShelXT[63] structure solution program using Intrinsic Phasing and refined with the ShelXL[64] refinement package using Least Squares minimization.

Crystal Data for $C_{62}H_{78}Au_2F_3N_5O_3S$ (M =1424.30 g/mol): monoclinic, space group

$P2_1$ (no. 4), a = 11.9363(6) Å, b = 14.5150(6) Å, c = 18.6846(9) Å, β = 107.440(5)°, V = 3088.4(3) Å^3, Z = 2, T = 100(2) K, μ(MoKα) = 4.834 mm^{-1}, *Dcalc* = 1.532 g/cm^3, 77053 reflections measured (3.576° ≤ 2Θ ≤ 54.968°), 14103 unique (R_{int} = 0.0658, R_{sigma} = 0.0439) which were used in all calculations. The final R_1 was 0.0435 (I > 2σ(I)) and wR_2 was 0.1096 (all data).

3.4.4.2 {[(SIMes)Au]$_3$C(Py)]}OTf (**6a**)

Single, red, prism-shaped crystals of {[(SIMes)Au]$_3$C(Py)]}OTf (**6a**) were grown by layering a DCM solution with hexanes at -35°C. A suitable crystal with the dimensions 0.42 mm × 0.41 mm × 0.33 mm was selected and mounted on a loop with paratone oil on an Bruker D8 VENTURE diffractometer. The crystal was kept at a steady T = 100(2) K during data collection. The structure was solved with the ShelXT[63] structure solution program using the Intrinsic Phasing solution method and by using Olex2[62] as the graphical interface. The model was refined with version 2017/1 of ShelXL[65] using Least Squares minimization.

Crystal Data. $C_{69}H_{84}Au_3F_2N_7$, M_r = 1640.33, monoclinic, $P2_1/n$ (No. 14), a = 13.7035(10) Å, b = 21.3842(14) Å, c = 22.0544(15) Å, β = 96.435(3)°, $\alpha = \gamma$ = 90°, V = 6422.1(8) Å^3, T = 100(2) K, Z = 4, Z' = 1, μ(MoK$_\alpha$) = 6.888 mm^{-1}, 48171 reflections measured, 13102 unique (R_{int} = 0.0606) which were used in all calculations. The final wR_2 was 0.1282 (all data) and R_1 was 0.0516 (I > 2σ(I)).

3.4.4.3 {[(SIMes)Au]$_2$C(SiMe$_3$)(Py)]}OTf (**8**) and {[(SIMes)Au]$_2$CH(Py)}OTf

Single crystals of {[(SIMes)Au]$_2$C(SiMe$_3$)(Py)]}OTf (**8**) cocrystallized with *ca*. 10 mol% {[(SIMes)Au]$_2$CH(Py)}OTf were grown by carefully layering a DCM solution with hexanes at -35°C. A suitable crystal was selected with the dimensions 0.158 mm × 0.141

mm × 0.03 mm and was mounted on a loop with paratone oil. Data were collected on a 'Bruker APEX-II CCD' diffractometer equipped with an Oxford Cryosystems low-temperature apparatus operating at T = 100(2) K. Using Olex2,[62] the structure was solved with the ShelXT[63] structure solution program using Intrinsic Phasing and refined with the ShelXL[65] refinement package using Least Squares minimization.

Crystal Data for $C_{52.805}H_{67.41}Au_2Cl_{2.195}F_3N_5O_3SSi_{0.9}$ (M =1406.27 g/mol): triclinic, space group P-1 (no. 2), a = 10.5936(14) Å, b = 16.2304(16) Å, c = 17.0114(18) Å, α = 103.553(5)°, β = 92.797(7)°, γ = 98.433(5)°, V = 2802.2(6) Å^3, Z = 2, T = 100(2) K, μ(MoKα) = 5.446 mm^{-1}, *Dcalc* = 1.667 g/cm^3, 40117 reflections measured (4.434° ≤ 2Θ ≤ 62.176°), 17821 unique (R_{int} = 0.0491, R_{sigma} = 0.0781) which were used in all calculations. The final R_1 was 0.0421 (I > 2σ(I)) and wR_2 was 0.0757 (all data).

3.5 Acknowledgements

We thank the U.S. National Science Foundation (CHE- 1300659 to J.P.S.) and the Georgia Institute of Technology for generous support of this research. Professor Jake D. Soper and Henry S. La Pierre kindly allowed us the use of their groups' FTIR and spectrometers.

3.6 References

1. Deng, C. M.; Huo, C. F.; Liu X. W.; Zhao, X. H.; Li, Y. W.; Wang, J.; Jiao, H. Density Functional Theory Study on Surface C_xH_y Formation form CO Activation $Fe_3C(100)$. *J. Phys. Chem. C*, **2010**, *114*, 21585-21592.

2. Maitlis, P.M.; Zanotti, V. The role of electrophilic species in the Fischer-Tropsch reaction. *Chem. Commun.*, **2009**, 1619-1634.

3. Bradley, J. S.; Ansell, G. B.; Hill, E. W. Homogenous carbon monoxide hydrogenation on multiple sites: a dissociative pathway to oxygenates. *J. Am. Chem. Soc.* **1979**, *101*, 7417-7419.

4. Drezdon, M. A.; Whitmire, K. H.; Bhattacharyya, A. A.; Hsu, W. L.; Nagel, C. C.; Shore, S. G.; Shriver, D. F. Proton-Induced Reduction of CO to CH_4 in Homonuclear and Heteronuclear Metal Carbonyls: A Survey of the Influence of the Metal and Nuclearity. J. Am. Chem. Soc. **1982**, *104*, 5633-5640.

5. Takemoto, S.; Morita, H.; Karitani, K; Fujiwara, H.; Matsuzaka, H.; A Bimetallic Ru_2Pt Complex Containing a Trigonal-Planar μ_3-Carbido Ligand: Formation, Structure, and Reactivity Relevant to the Fischer-Tropsch Process. *J. Am. Chem. Soc.*, **2009**, *131*, 18026-18027.

6. Tachikawa, M.; Muetterties, E. L. Metal Carbide Clusters. *Prog. Inorg. Chem.* **1981**, 203-238.

7. Hejl, A.; Trnka, T. M.; Day, M. W.; Grubbs, R. H. Terminal ruthenium carbido complexes as σ-donor ligands. *Chem. Comm.* **2002**, 2524-2525

8. Takemoto, S.; Matsuzaka, H. Recent advances in the chemistry of ruthenium carbido complexes. *Coord. Chem. Rev.* **2012**, *256*, 574-588.

9. Miller, R. L.; Wolczanski, P. T. Carbide Formation via Carbon Monoxide Dissociation Across a W≡W Bond. *J. Am. Chem. Soc.* **1993**, *115*, 10422-10423.

10. Mansuy, D.; Cytochrome P-450 and model systems: great diversity of catalyzed reactions. *Pure & Appl. Chem.* **1994**, *66*, 737.

11. Beck, W.; Knauer, W.; Robl, C. Synthesis and Structure of the Novel μ_2-Carbido Complexes [(TPP)Fe=CRe(CO)$_4$Re(CO)$_5$. *Angew. Chem. Int. Ed. Engl.* **1990**, 3.

12. Solari, A. Antonijevic, S.; Gauthier, S.; Scopelliti, R.; Severin, K. Formation of a Ruthenium μ-Carbide Complex with Acetylene as the Carbon Source. *Eur. J. Inorg. Chem.* ***2007***, 367-371.

13. Latesky, S.; Selegue, J. P. Preparation and Structure of [(Me$_3$CO)$_3$W≡C-Ru(CO)$_2$(Cp)], a Heteronuclear, μ_2-Carbide Complex. *J. Am. Chem. Soc.* **1987**, *109*, 4731.

14. Takahashi, Y.; Akita, M.; Moro-Oka Yoshihiko. Synthesis and structural characterization of a tetrahedral sp^3 carbide cluster compound. *Chem. Commun.* **1997**, 1557-1558.

15. Tachikawa, M.; Muetterties, E. L. Metal clusters. 25. A uniquely bonded C-H group and reactivity of a low-coordinate carbidic carbon atom. *J. Am. Chem. Soc.* **1980**, *102*, 4541-4542.

16. Davis, J. H.; Beno, M. A.; Williams, J. M.; Zimmie, J.; Tachikawa, M.; Muetterties, E. L. Structure and chemistry of a metal cluster with a four-coordinate carbide carbon atom. *Proc. Natl. Acad. Sci. USA.* **1981**, *78*, 668-671.

17. Caselli, A.; Solari, E.; Scopelliti, R.; Floriani, C. The Stepwise Four- and Six-Electron Reduction of Carbon Monoxide to Oxyalkylidyne, to Carbide and Oxide, Then to Carbide over an Nb-Oxo Surface Modeled by Calix[4]arene. *J. Am. Chem. Soc.*, **2000**, *122*, 538-539.

18. Takemoto, S.; Ohata, J.; Umetani, K.; Yamaguchi, M.; Matsuzaka, H. A Diruthenium μ-Carbido Complex That Shows Singlet-Carbene Reactivity. *J. Am. Chem. Soc.* **2014**, *136*, 15889-15892.

19. Takemoto, S.; Tsujita, M.; Matsuzaka, H. Diruthenium Carbido Complexes as *N*-Heterocyclic Carbene Like C-Donor Ligands to Group 11 Metals. *Organometallics*, **2017**, *36*, 3686-3691.

20. Borren, E. S.; Hill, A. F.; Shang, R.; Sharma, M.; Willis, A. C. A Golden Ring: Molecular Gold Carbido Complexes. *J. Am. Chem. Soc.*, **2013**, *135*, 4942.

21. Svitova, A. L.; Ghiassi, K. B.; Schlesier, C.; Junghans, K.; Zhang, Y.; Olmstead, M. M.; Balch, A. L.; Dunsch, L.; Popov, A. A. Endohedral fullerene with μ_3-carbido ligand and

titanium-carbon double bond stabilized inside a carbon cage. *Nat. Commun.* **2014**, *5*, 1-8.

22. Kolis, J. W.; Holt, E. M.; Drezdon, M.; Whitmire, K. H.; Shriver, D. F. A Reactive Three-Metal Carbide Cluster Mimic $[Fe_3(CO)_9(CCO)]^{2-}$. *J. Am. Chem. Soc.* **1982**, *104*, 6134-6135.

23. Abedin, S. M. T.; Hardcastle, K. I.; Kabir, S. E.; Malik, K. M. A.; Mottalib, A.; Roseberg, E.; Abedin, M. J. Carboxylation of a μ_3-Diazo Methylidyne Triosmium Cluster. *Organometallics*. **2000**, *19*, 5623-5627.

24. Scherbaum, F.; Grohmann, A.; Huber, B.; Krüger, C.; Schmidbaur, H. "Aurophilicity" as a Consequence of Relativistic Effects: The Hexakis(triphenylphosphaneaurio)-methane Dication $[Ph_3PAu)_6C]^{2+}$. *Angew. Chem. Int. Ed. Engl.* **1988**, *27*, 1544.

25. Schmidbaur, H.; Steigelmann, O. The First Complexes of Tetragoldmethane CAu_4. **1992**, *47b*, 1721.

26. Gabbaï, F.; Schier, A.; Riede, J.; Schmidbaur, H. Synthesis of the Hexakis[(triphenyl-phosphane)gold(I)]methanium(2+) Cation from Trimethylsilyldiazomethane; Crystal Structure Determination of the Tetrafluoroborate Salt. *Chem. Ber./Recueil*. **1997**, *130*, 111.

27. Scherbaum, F.; Grohmann, A.; Müller, G.; Schmidbaur, H. Synthesis, Structure, and Bonding of the Cation $[\{C_6H_5)_4PAu\}_5C]^+$. *Angew. Chem. Int. Ed. Engl.* **1989**, 463.

28. Schmidbaur, H.; Schier, A. Aurophilic interactions as a subject of current research: an up-date. *Chem. Soc. Rev.,* **2012**, *41*, 370.

29. Schmidbaur, H.; Scherbaum, F.; Huber, B.; Müller, G. Polyauriomethane Compounds. *Angew. Chem. Int. Ed. Engl.* **1988**, *27*, 419.

30. Steigelmann, O.; Bissinger, P.; Schmidbaur, H. 1,1,1,1-Tetrakis[triorganylphosphine-aurio(I)]ethanium(+) Tetrafluoroborates – Hypercoordinated Species Containing $[H_3C\text{-}C(AuL)_4]^+$ Cations. *Z. Naturforsch*. **1993**, *48b*, 72.

31. Defour, N.; Schier, A.; Schmidbaur, H. Hypercoordinate Carbon in Bis(trimethylsilyl)-tris[(triphenylphosphine)aurio(I)]methanium Tetrafluoroborate. *Organometallics* **1993**, *12*, 2408.

32. Schmidbaur, H.; Schier, A. A Briefing on aurophilicity. *Chem. Soc. Rev.* **2008**, *37*, 1931.

33. Schmidbaur, H. The Aurophilicity Phenomenon: A Decade of Experimental Findings, Theoretical Concepts and Emerging Applications. *Gold Bull*. **2000**, *33*, 3.

34. Bardaji, M.; Laguna, A. Heteronuclear Metal-Metal Contacts between Gold(I) and Group-11, 12, and 13 Centers. *Eur. J. Inorg. Chem.* **2003**, 3069.

35. Pyykö, P.; Runeberg, N.; Medizabal, F. Theory of the d^{10}-d^{10} Closed-Shell Attraction: 1. Dimers Near Equilibrium. *Chem. Eur. J.* **1997**, *3*, 1451.

36. Pyykö, P.; Medizabal, F. Theory of the d^{10}-d^{10} Closed-Shell Attraction: 2. Long-Distance Behaviour and Nonadditive Effects in Dimers and trimers of Type $[(X\text{-}Au\text{-}L)_n]$ (n=2, 3; X=Cl, I, H; L=PH_3, PMe_3, -N≡CH). *Chem. Eur. J.* **1997**, *3*, 1458.

37. Pyykö, P.; Medizabal, F. Theory of the d^{10}-d^{10} Closed-Shell Attraction: III. Rings. *Inorg. Chem.* **1998**, *37*, 3018.

38. Pyykö, P.; Tamm, T. Theory of the d^{10}-d^{10} Closed-Shell Attraction: 4. $X(AuL)_n^{m+}$ Centered Systems. *Organometallics*. **1998**, *17*, 4842.

39. Pyykö, P. Strong Closed-Shell Interactions in Inorganic Chemistry. *Chem. Rev.* **1997**, *97*, 597.

40. Raubenheimer, H. G.; Schmidbaur, H. The Late Start and Amazing Upswing in Gold Chemistry. *J. Chem. Ed.* **2014**, *91*, 2024.

41. Bardahi, M.; Laguna, A. Gold chemistry: The Aurophilic Attraction. *J. Chem. Ed.* **1999**, *76*, 201.

42. McKelvey, D. R. Relativistic Effects on Chemical Properties. *J. Chem. Ed.* **1983**, *60*, 112.

43. Tsui, E. Y.; Müller, P.; Saidighi, J. P. Reactions of a Stable Monomeric Gold(I) Hydride Complex. *Angew Chem. Int. Ed.* **2008,** *47*, 8937-8940.

44. Schmidbaur, H.; Blumenthal, M. A.; Kraus, F. Synthesis of a Tri(gold)boride Complex $(Cy_3P)B[AuP(o\text{-}Tol)_3]_3$. *Z. Naturforsch.* **2013**, *68b*, 1321.

45. Bauer, A.; Mitzel, N. W.; Schier, A.; Rankin, D. W. H.; Schmidbaur, H. Tris(dimethylamino)phosphane as a New Ligand in Gold(I) Chemistry: Synthesis and Crystal Structures of $[(Me_2N)_3P]AuCl$, $\{[Me_2N)_3PAu_3O\}^+BF_4^-$, $\{[(Me_2N)_3PAu]_3NP(N\text{-}Me_2)_3\}^{2+}$ $\{BF_4^-\}_2$ and the Precursor Molecule $(Me_2N)_3PNSiMe_3$. *Chem. Ber. Recueil*. **1997**, *130*, 323-328.

46. Daugherty, T. N.; Bacsa, J.; Sadighi, J. P. A Trigold(I) Ketenylidene Cation. *Organometallics*, **2017**, *36*, 3171-3174.

47. Johnson, M. W.; Toste, F. D.; Bergman, R. G. Preparation and reactivity of terminal gold(I) amides and phosphides. *Chem. Sci.* **2013**, *4*, 1023-1027.

48. Aoyama, T.; Sudo, K.; Shioiri, T. New Methods and Reagents in Organic Synthesis. 32. Lithium Trimethylsilyldiazomethane: A New Synthon for the Preparation of 1,2,3-Triazoles. *Chem. Pharm. Bull.* **1982**, *30*, 3849-3851.

49. Bozorth, R, M. Crystal Structure of Potassium Cyanide. *J. Am. Chem. Soc.* **1922**, *44*, 317-323.

50. Blues, E. T.; Bryce-Smith, D.; Irwin, J. G.; Lawston, I. W. Disilverdiazomethane. *J.C.S. Chem. Comm.*, **1974**, 466.

51. Lorbeth, J. Metallorganische Diazoalkane III*. Diazoalkane Mit Germanium, Blei Und Den IIB-Elementen Zink, Cadmium Und Quecksilber Als Substituenten. *J. Organometallic Chem*., **1971**, *27*, 303-325.

52. Grüning, R.; Krommes, P.; Lorbeth, J. Organometallic Diazoalkanes. *J. Organometallic Chem.*, **1977**, *127*, 167-172.

53. Fadini, A.; Glozbach, E.; Krommes, P.; Lorberth, J. Metallorganische Diazoalkane XV*. Bindugsverhältnisse Und Elektronenstrukturen In Metallorganischen Diazoalkanen: Das Beispiel Bis(Trimethylstannyl)diazomethane $(Me_3Sn)_2CN_2$. *J. Organometallic Chem.* **1978**, *149*, 297-307.

54. Wright, A. N.; Kramer, K. A. W.; Steel, G. Mercuration of Diazomethane. *Nature*, **1963**.

55. Lappert, M. F.; Lorberth, J.; Poland, J. S. Organometallic Diazoalkanes. Part I. Synthesis and Characterization of Simple Group IVB Organometallic Diazomethanes,

and the Tin-Carbon Cleavage Reactions of Bis(trimethylstannyl)diazomethane. *J. Chem. Soc. (A)*. **1970**, 2954-2959.

56. Valenty, S. J.; Skell, P. S. α-Diazomercurials. Synthesis and Photochemistry. *J. Org. Chem.* **1973**, *28*, 3937-3941.

57. Laitar, D. S.; Müller, P.; Gray, T. G.; Sadighi, J. P. A Carbene-Stabilized Gold(I) Fluoride: Synthesis and Theory. *Organometallics*, **2005**, *24*, 4503-4505.

58. Wyss, C. M.; Tate, B. K.; Bacsa, J.; Wieliczko, M.; Sadighi, J. P. Dinuclear μ-fluoro cations of copper, silver, and gold. *Polyhedron*, **2014**, *84*, 87-95.

59. Kiviniemi, S.; Nissinen, M.; Alaviuhkola, T.; Rissanen, K.; Pursiainen, J. The complexation of tetraphenylborate with organic *N*-heteroaromatic cations. *Journal of the Chemical Society Perkin Transactions 2*, **2001**, 2364.

60. Frémont, P.; Marion, N.; Nolan, S. P. Cationic NHC-gold(I) complexes: Synthesis, isolation, and catalytic activity. Cationic NHC-gold(I) complexes: Synthesis, isolation, and catalytic activity. *J. Organometallic Chem.*, **2009**, *694*, 551-560.

61. Nesmeyanov, A. N.; Perevalova, É. G.; Smyslova, E. I.; Dyadchenko; Grandberg, K. I. Reaction of Gold Compounds and Diazomethane. *Russ. Chem. Bull*. **1977**, *26*, 2417.

62. Dolomanov, O. V.; Bourhis, L. J.; Gildea, R. J; Howard, J. A. K.; Puschmann, H. OLEX2: a complete structure solution, refinement and analysis program. *J. Appl. Cryst.* **2009**, *42*, 339-341.

63. Sheldrick, G.M. SHELXT – Integrated space-group and crystal-structure determination. Acta Cryst. **2015**, *A71*, 3-8.

64. Sheldrick, G. SHELXT - Integrated space-group and crystal-structure determination. *Acta Cryst.* **2015,** C*71*, 3-8.

65. Sheldrick, G.M. Crystal structure refinement with ShelXL, *Acta Cryst.*. **2015**, *C27*, 3-8.

CHAPTER 4

SYNTHESIS OF *N*-AURATED TETRAZOLATES

4.1 Background

The Huisgen 1,3-dipolar cycloaddition of alkynes with azides[1] is considered to be the prototypical example of a click reaction. Such reactions are powerful synthetic tools for the assembly of small molecular building blocks to create complex molecular structures via carbon-heteroatom bonds.[2] Finn *et. al.* have applied copper(I) catalyzed azide-alkyne cycloaddition to the bioconjugation of functionalized viruses with dyes.[3] The mechanism of the copper(I)-catalyzed 1,3-dipolar cycloaddition of azides and alkynes has been studied by DFT, and was proposed early on to pass through a three-coordinate intermediate involving LCu^+, an organic acetylide, and an organic azide.[4] However, more recent work by Fokin *et. al.* suggests the participation of a second LCu^+ in the formation of a dicopper intermediate.[5] Gray *et. al.* have demonstrated that [3 + 2] cycloaddition of gold(I) acetylides with (trimethylsilyl)azide gives isolable, hydrolytically stable C-bound gold(I) triazolates in good yield.[6] Similarly, [3 + 2] cycloaddition of gold(I) azides with terminal alkynes also results in the C-bound gold(I) triazolates in good yield.[6,7,8]

Tetrazoles are accessible by 1,3-dipolar cycloaddition as well.[9] Sharpless *et. al.* have demonstrated the effectiveness of Zn(II) in catalyzing the conversion of nitriles to tetrazoles by reaction with sodium azide.[10] Sedelmeier, *et. al.* demonstrated that the reaction of dialkylaluminum azides, generated from the corresponding dialkylaluminum chlorides and sodium azide, with nitriles results in 5-substituted tetrazoles under mild conditions and relatively short reaction times.[11] Yamamoto *et. al.* describe the copper(I) catalyzed [3 + 2] addition of nitriles with azide to give 5-substituted tetrazoles. In this case,

CuN_3 is generated from Cu_2O in a methanolic solution of (trimethylsilyl)azide. The reaction is proposed to proceed through a two-coordinate (RCN)Cu(N_3) intermediate, which undergoes intramolecular cycloaddition to give the N-bound copper tetrazolate. Subsequent protonolysis of the organometallic species results in the organic tetrazole.[12]

A review by Voitekhovich, Gaponik, and Koldobskii describes two approaches toward preparing 5-metallated tetrazoles. These are metalation of organic tetrazoles, and cycloaddition of coordinated azides with isonitriles.[13] Beck and Fehlhammer were the first to employ the latter approach in preparing C-bound gold(III) tetrazolates.[14] This work was later extended to generate a C-bound tetrakis(tetrazolyl)Au(III) species.[15] Raubenheimer *et. al.* have explored both metalation and cycloaddition approaches in their preparation of C-bound gold(I) tetrazolates, which they subsequently methylate in the 4-position to give the corresponding gold(I) tetrazolylidenes.[16] Kukushkin *et. al.* describe a similar approach toward preparation of C-bound Au(III) tetrazolylidenes by cycloaddition of Au(III) isonitriles with azide.[17] Neutral N-Bound gold(I) tetrazolates have also been described.[18,19]

Veige *et. al.* were the first to document the cycloaddition of a metal-bound azide with a metal-bound acetylide.[20] They describe this approach as the inorganic version of a 1,3-dipolar Huisgen cycloaddition. In this case, reaction of triphenylphosphine gold(I) azide with triphenylphosphine gold(I) phenylacetylide in chloroform results in the neutral 1,5-diaurated triazole, 1,5-bis-triphenylphosphinegold(I) 1,2,3-triazolate in 88% yield over the course of 2.5 hours. The 1,4-diaurated species was formed as a minor product (<3%). Variable temperature ^{1}H NMR did not conclusively reveal whether or not the two species were in equilibrium.

In this chapter, synthesis of a 1-auro(5-methyltetrazole)-d_3 is described. The *N*-auration of 1*H*-tetrazole to give an isomeric mixture of neutral 1- and 2-aurated tetrazole is also described. Diauration and attempted triauration of this equilibrium mixture are discussed.

4.2 Results and Discussion

Initially, a metalation approach was taken toward synthesis of the IDipp-supported (IDipp = N,N′-bis(2,6-diisopropylphenyl)imidazol-2-ylidene) *N,C,N′*-triauro(tetrazolylidene) cation $\{[(IDipp)Au]_3(CN_4)\}^+$. Generation of the *N*-monoauro(tetrazolate) was accomplished straightforwardly by stirring an acetone solution of (IDipp)AuCl and 1*H*-tetrazole over potassium carbonate (Scheme 4.1). Filtration of the reaction mixture and removal of solvent by rotary evaporation afforded the product as a white solid in 96% yield. The ^{1}H NMR spectrum reveals the expected IDipp-derived resonances corresponding to the 1-auro(tetrazolate) with a major tetrazolate-derived CH resonance at δ 7.98 ppm, and a second set of IDipp-derived resonances corresponding to the 2-auro(tetrazolate) with a minor tetrazolate-derived CH resonance at δ 8.29 ppm (Figure 4.1). The ^{1}H NMR resonances were relatively sharp. Variable temperature experiments would be required to determine whether the isomers exist in dynamic equilibrium.

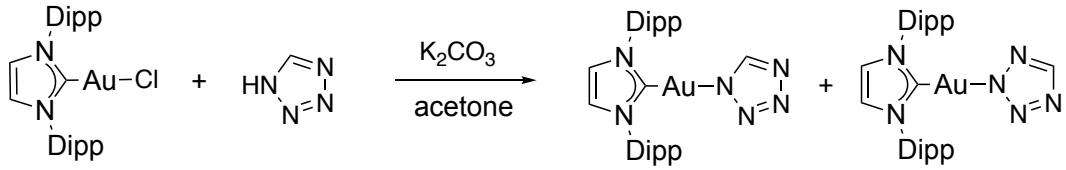

Scheme 4.1. Synthesis of an isomeric mixture of 1-[(IDipp)Au](CHN$_4$) and 2-[(IDipp)Au](CHN$_4$).

Addition of (IDipp)AuOTf to the mixture of 1-auro(tetrazolate) and 2-auoro(tetazolate) resulted in a single set of broad IDipp-derived resonances (Figure 4.2), suggesting formation of a fluxional *N-N'*-diauro(tetrazolate) cation $\{[(IDipp)Au]_2(CHN_4)\}^+$ (Scheme 4.2). Calculations suggest that for analogous organic tetrazolium ions, the 1,5,4-tautomer is the major species, and that it exists primarily in equilibrium with the 1,5,3-tautomer,

while the 1,5,2- and 2,5,3-tautomers were found to be *ca.* 15-20 kcal/mol less favorable.[21] Based on this analogy, I suspect the 1,4-diauro(tetrazolate) cation to be the major species present in the {[(IDipp)Au]$_2$(HCN$_4$)}OTf equilibrium mixture.

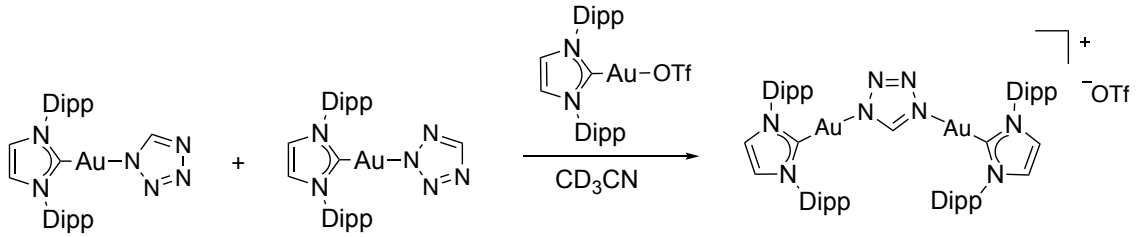

Scheme 4.2. Formation of the proposed major {[(IDipp)Au]$_2$(CHN$_4$)}OTf tautomer.

Addition of (IDipp)AuO*t*-Pent or (IDipp)AuN(*i*-Pr)$_2$ to the fluxional species, however, did not result in formation of the desired cationic *N,C,N'*-triauro(tetrazolylidene) cation. Instead, deauration occurred, regenerating the neutral N-monoaurated tetrazole (IDipp)Au(CHN$_4$) and the corresponding bridged digold species, {[(IDipp)Au]$_2$O*t*-Pent}OTf or {[(IDipp)Au]$_2$N(*i*-Pr)$_2$}OTf, as judged by ^{1}H NMR. Addition of LiN(*i*-Pr)$_2$ to the diaurated tetrazolyl cation similarly resulted in deauration (Scheme 4.3), producing the neutral *N*-monoaurated tetrazole (IDipp)Au(CHN$_4$) and (IDipp)AuN(*i*-Pr)$_2$ as judged by ^{1}H NMR.

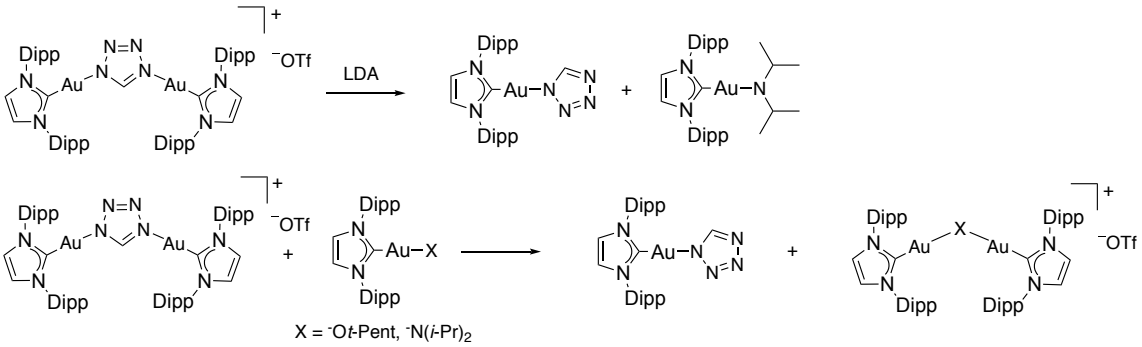

Scheme 4.3. Deauration as a result of attempted metalation of {[(IDipp)Au]$_2$(CHN$_4$)}OTf.

Reasoning that metalation might be inaccessible by the above route due to insufficient acidity of the tetrazole-derived CH proton relative to N-bound LAu^+, I devised an alternative approach toward synthesis of the *N,C,N'*-triauro(tetrazolylidene) cation. Instead of metalating the N-H and C-H bonds of the heterocycle to generate the 1,5-diaurated species, I envisioned that 1,3-dipolar cycloaddition of (IDipp)AuCN with (IDipp)AuN_3 would generate the neutral 1,5-diauro(tetrazolate) [(IDipp)Au]$_2$(CN_4). At room temperature in THF-d_8 solution, this reaction showed no progress over an extended period of time. Similarly, little evidence of reaction was observed when a CD_2Cl_2 solution of the gold azide and gold cyanide were heated at 120°C overnight. When a CD_3CN solution of the gold azide and gold cyanide were heated to 60°C overnight, however, reaction between (IDipp)AuN_3 and CD_3CN occurred, resulting in formation of the IDipp-supported 1-auro(5-methyltetrazolate)-d_3 (IDipp)Au(CD_3CN_4) (m/z = 669.4, $[M+H]^+$) instead of the desired product (Scheme 4.4). The unreacted (IDipp)AuCN in the product mixture served as an internal standard and indicated quantitative conversion of (IDipp)AuN_3 to (IDipp)Au(CD_3CN_4) (Figure 4.5). When the reaction was conducted in CH_3CN instead of CD_3CN, the 5-methyl group of the resulting tetrazolate was detected by ^{1}H NMR at δ 1.85 ppm in CD_3CN solution. When cycloaddition of (IDipp)AuN_3 with CD_3CN was carried out in the absence of (IDipp)AuCN, (IDipp)Au(CD_3CN_4) was isolated in 56% yield.

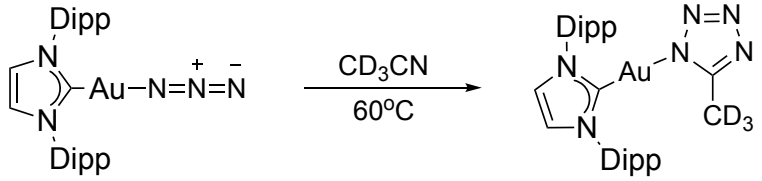

Scheme 4.4. 1,3-dipolar cycloaddition of CD_3CN and (IDipp)AuN_3.

4.3 Conclusion

An isomeric mixture of IDipp-supported 1-aurated and 2-aurated tetrazole (IDipp)Au(CHN_4) was prepared by metalation of 1*H*-tetrazole by (IDipp)AuCl in the presence of K_2CO_3 in acetone solution. Addition of (IDipp)AuOTf to this equilibrium mixture gave the fluxional cationic *N,N'*-diauro(tetrazolate) as the triflate salt {[(IDipp)Au]$_2$(CHN_4}OTf, as judged by ^{1}H NMR. Attempted metalation of {[(IDipp)Au]$_2$(CHN_4}OTf at the 5-position of the tetrazolyl moiety by LiN(*i*-Pr)$_2$, (IDipp)Au(O*t*-Pent), or (IDipp)AuN(*i*-Pr)$_2$ resulted in deauration. Attempted 1,3-dipolar cycloaddition of (IDipp)AuN_3 with (IDipp)AuCN in THF, DCM, and methanol resulted in no reaction, even at elevated temperature; however, in CD_3CN solution, (IDipp)AuN_3 underwent cycloaddition with the solvent to give the 1-auro(5-methyltetrazole)-*d$_3$* cation as the triflate salt [(IDipp)Au(CD_3CN_4)]OTf.

4.4 Experimental

4.4.1 General Considerations

Unless otherwise indicated, manipulations were performed in an MBraun glovebox under nitrogen atmosphere, or using standard Schlenk techniques under argon atmosphere. Glassware was dried in a ventilated oven at 160 °C or flame-dried and allowed to cool under vacuum. Molecular sieves (Alfa Aesar) and Celite (EMD 545) were dried under vacuum for at least twelve hours at 160°C. Dichloromethane (EMD Millipore Omnisolv), hexanes (EMD Millipore Omnisolv), toluene (EMD Millipore Omnisolv), and tetrahydrofuran (EMD Millipore Omnisolv) were sparged with ultra-high purity argon for 30 minutes and dried using an MBraun solvent purification system. DCM was then transferred onto calcium hydride and further dried for at least 12 hours. It was then degassed and vacuum-transferred to a resealable flask, and stored over 3Å molecular sieves in the

glovebox. THF, hexanes, and toluene were then transferred onto sodium benzophenone ketyl and further dried until a purple color was achieved. They were then degassed and vacuum-transferred to a resealable flask, and stored over molecular sieves in the glovebox. Pyridine (Sigma-Aldrich) and acetonitrile (EMD HPLC) were stirred over calcium hydride (Alfa Aesar) in sealed flasks for at least twelve hours. They were then degassed and vacuum-transferred to resealable flasks, and stored over 3Å molecular sieves in the glove box. Benzene (Alfa Aesar, ACS grade) was dried over sodium benzophenone ketyl in a sealed flask until a purple color was achieved. It was then degassed, vacuum-transferred to a resealable flask, and stored over 3Å molecular sieves in the glovebox. Methanol (BDH), acetone (BDH), and hexanes used in benchtop work (BDH) were used as received.

THF-d_8 (Cambridge Isotope Laboratories) was dried over sodium benzophenone ketyl, degassed by several freeze-pump-thaw cycles, and vacuum-transferred into a resealable flask. Dichloromethane-d_2 and acetonitrile-d_3 (Cambridge Isotope Laboratories) were dried over calcium hydride for at least twelve hours, degassed by several freeze-pump-thaw cycles, and vacuum-transferred into resealable flasks. Methanol-d_4 (Cambridge Isotope Laboratories) was used as received. Chloroform-d_3 (Cambridge Isotope Laboratories) was used as received.

Tetrachloroauric acid (Strem), dimethyl sulfide (Alfa Aesar), potassium carbonate (Alfa Aesar), calcium hydride (Alfa Aesar), silver acetate (Sigma-Aldrich), sodium metal (Alfa Aesar), benzophenone (Alfa Aesar), 4,4'-dimethylbiphenyl (Alfa Aesar), 1*H*-tetrazole (Alfa Aesar, 0.45 M in acetonitrile), trimethylsilyl cyanide (Aldrich), trimethylsilyl azide (Acros Organics), nitrogen (NexAir), and argon (both industrial and ultra-high purity grades, NexAir), were used as received. *N*,*N*′-Bis(2,6-diisopropylphenyl)imidazolium chloride,[22] (IDipp)AuCl, [23] (IDipp)AuN(*i*-Pr)$_2$,[24] (IDipp)Au(O*t*-Pent),[25] (IDipp)Au(OTf),[26] and

(IDipp)Au(OAc)[27] were prepared according to literature protocol and were characterized by ^{1}H NMR spectroscopy.

4.4.2 Analytical Measurements

^{1}H and ^{13}C spectra were obtained using a Varian Vx 400 MHz spectrometer, or Bruker Avance IIIHD 500 spectrometer. ^{1}H and ^{13}C NMR chemical shifts are referenced with respect to solvent signals and reported relative to tetramethylsilane. Infrared spectra were collected from neat solid samples using a Bruker Alpha-P infrared spectrometer equipped with an attenuated total reflection (ATR) attachment inside a glovebox. Elemental analyses were performed by Atlantic Microlab, Inc. in Norcross, Georgia.

4.4.3 Synthetic Procedures

4.4.3.1 (IDipp)Au(CHN_4)

A solution of 1*H*-tetrazole in acetonitrile (0.17 mL, 0.45 M) was rotary-evaporated to dryness in a 20-mL scintillation vial. Portions of (IDipp)AuCl (48 mg, 0.077 mmol) and K_2CO_3 (22.5 mg, 0.163 mmol) were added. The solids were suspended in acetone (10 mL) and stirred for 16 hours. The reaction mixture was then filtered through a plug of Celite and evaporated to dryness *in vacuo* (49 mg, 96%). ^{1}H NMR (400 MHz, CD_3CN): **1-[(IDipp)Au](CHN$_4$)** δ (ppm) 7.98 (s, 1H N_4CH), 7.62 (s, 2H, NC*H*), 7.57 (t, *J* = 7.8 Hz, 2H, *para*-CH), 7.41 (d, *J* = 7.8 Hz, 4H, *meta*-C*H*), 2.60 (sept, *J* = 6.9 Hz, 4H, $(CH_3)_2CH$), 1.34 (d, *J* = 6.9 Hz, 12H, $(CH_3)_2CH$), 1.25 (d, *J* = 6.9 Hz, 12H, $(CH_3)_2CH$). **2-[(IDipp)Au](CHN$_4$)** δ (ppm) 8.29 (s, 1H N_4CH), 7.62 (s, 2H, NC*H*), 7.58 (t, *J* = 7.8 Hz, 2H, *para*-CH), 7.41 (d, *J* = 7.8 Hz, 4H, *meta*-C*H*), 2.60 (sept, *J* = 6.9 Hz, 4H, $(CH_3)_2CH$), 1.34 (d, *J* = 6.9 Hz, 12H,

(CH_3)$_2$CH), 1.25 (d, *J* = 6.9 Hz, 12H, (CH_3)$_2$CH). Anal. Calcd for $C_{28}H_{37}AuN_6$: C, 51.38; H, 5.70; N, 12.84. Found C, 50.84; H, 5.78; N, 13.50.

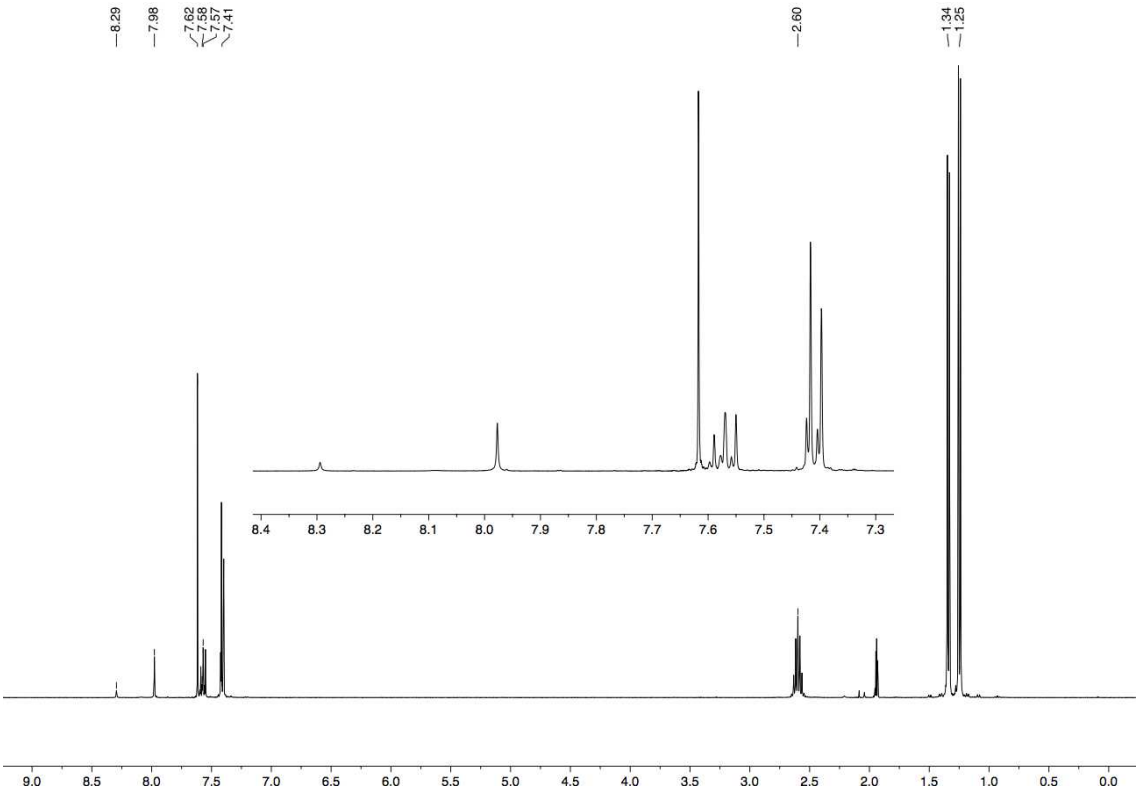

Figure 4.1. ^{1}H NMR (400 MHz, CD_3CN) spectrum of [(IDipp)Au](CHN_4).

4.4.3.2 {[(IDipp)Au]$_2$(CHN_4)}OTf

Portions of (IDipp)Au(CHN_4) (10 mg, 0.015 mmol) and (IDipp)AuOTf (11mg, 0.015 mmol) were combined in a 20-mL scintillation vial and dissolved in CD_3CN (1mL), and allowed to stand for 15 minutes before the acquisition of NMR data. ^{1}H NMR (400 MHz, CD_3CN): δ (ppm) 8.18 (s, 1H N_4CH), 7.60 (s, 4H, NC*H*), 7.54 (t, *J* = 7.7 Hz, 4H, *para*-CH), 7.37 (d, *J* = 7.8 Hz, 8H, *meta*-C*H*), 2.53 (sept, *J* = 6.8 Hz, 8H, (CH_3)$_2$C*H*), 1.25 (d, *J* = 6.8 Hz, 24H, (CH_3)$_2$CH), 1.25 (d, *J* = 6.8 Hz, 24H, (CH_3)$_2$CH).

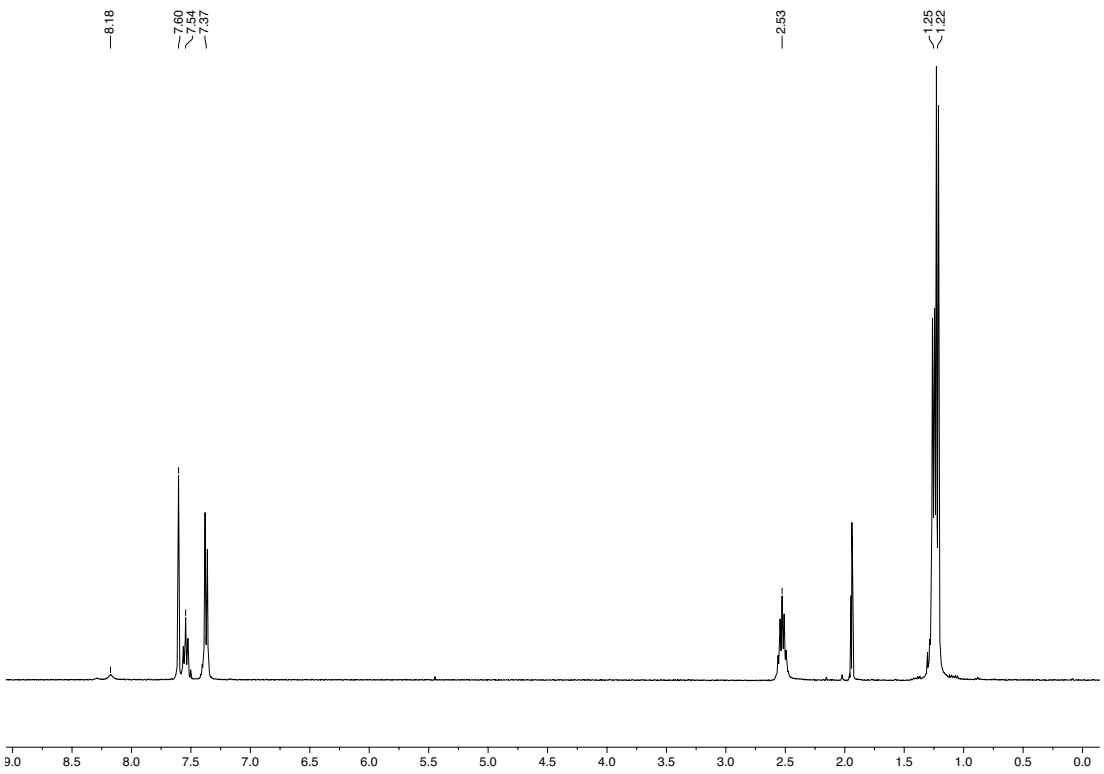

Figure 4.2. ^{1}H NMR (400 MHz, CD_3CN) spectrum of $[(IDipp)Au]_2(CHN_4)]OTf$.

4.4.3.3 (IDipp)AuCN

(IDipp)AuCN was prepared according to a modified literature procedure[27] and its purity was checked by ^{1}H NMR. A portion of (IDipp)AuOAc (135 mg, 0.21) was massed into a 25-mL Schlenk flask equipped with a stir bar. The solid was dissolved in THF (6 mL), the flask was fitted with a rubber septum, and trimethylsilyl cyanide (0.052 mL, 0.42 mmol) was added via syringe. The reaction mixture was stirred overnight. All volatiles were removed *in vacuo* to give the white solid. ^{1}H NMR (400 MHz, $CDCl_3$): δ (ppm) 7.52 (t, J = 7.8 Hz, 2H, *para*-C*H*), 7.30 (d, J = 7.8 Hz, 4H, *meta*-C*H*), 7.19 (s, 2H, NC*H*), 2.48 (sept, J = 6.8 Hz, 4H, $(CH_3)_2CH$), 1.31 (d, J = 6.9 Hz, 12H, $(CH_3)_2CH$), 1.22 (d, J = 6.9 Hz, 12H, $(CH_3)_2CH$).

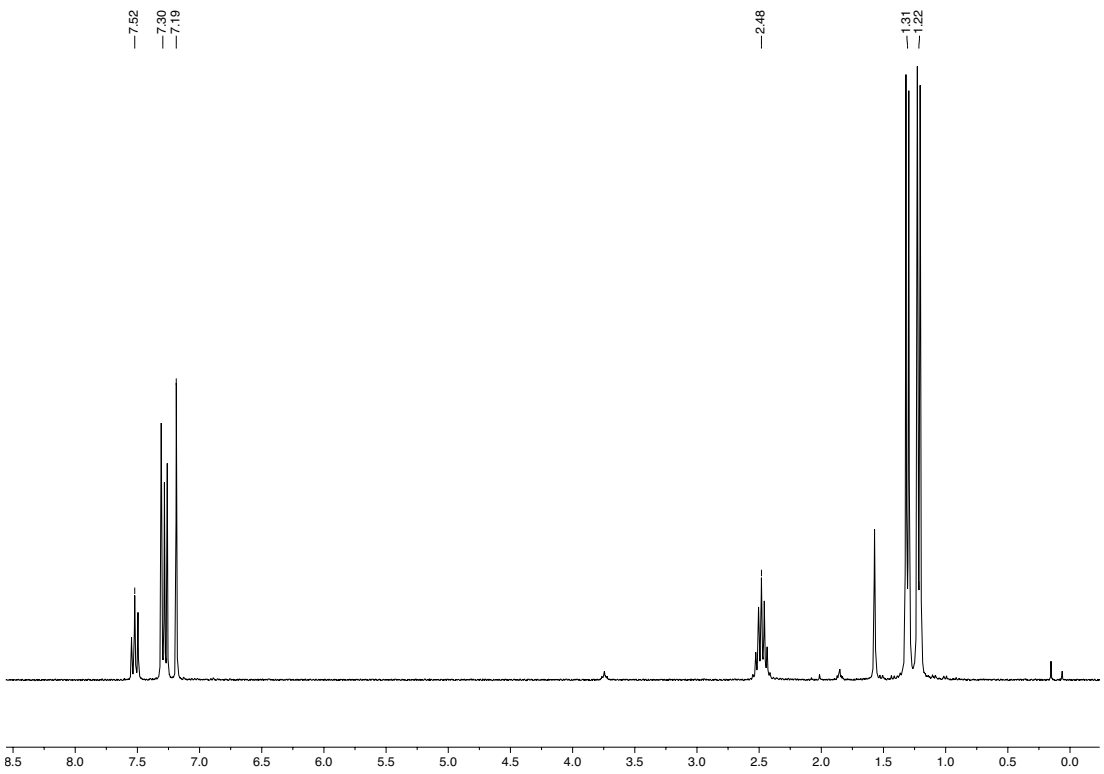

Figure 4.3. ^{1}H NMR (400 MHz, $CDCl_3$) spectrum of (IDipp)AuCN.

4.4.3.4 (IDipp)AuN_3

(IDipp)AuN_3 was prepared according to a modified literature procedure[7,28,29] and its purity was checked by ^{1}H NMR. A portion of (IDipp)AuOAc (130 mg, 0.20 mmol) was massed inside of a round-bottom flask equipped with a stir bar and dissolved in THF (6 mL). The round-bottom flask was fitted with a rubber septum and taken outside of the glove box. A portion of trimethylsilyl azide (0.045 mL, 0.41 mmol) was added via syringe and the reaction mixture was stirred for 15 hours, evaporated to dryness, triturated with hexanes, and collected by vacuum filtration. ^{1}H NMR (400 MHz, $CDCl_3$): δ (ppm) 7.52 (t, *J* = 7.8 Hz, 2H, *para*-C*H*), 7.30 (d, *J* = 7.8 Hz, 4H, *meta*-C*H*), 7.17 (s, 2H, NC*H*), 2.53 (sept, *J* = 6.8 Hz, 4H, $(CH_3)_2CH$), 1.33 (d, *J* = 6.9 Hz, 12H, $(CH_3)_2CH$), 1.22 (d, *J* = 6.9 Hz, 12H, $(CH_3)_2CH$).

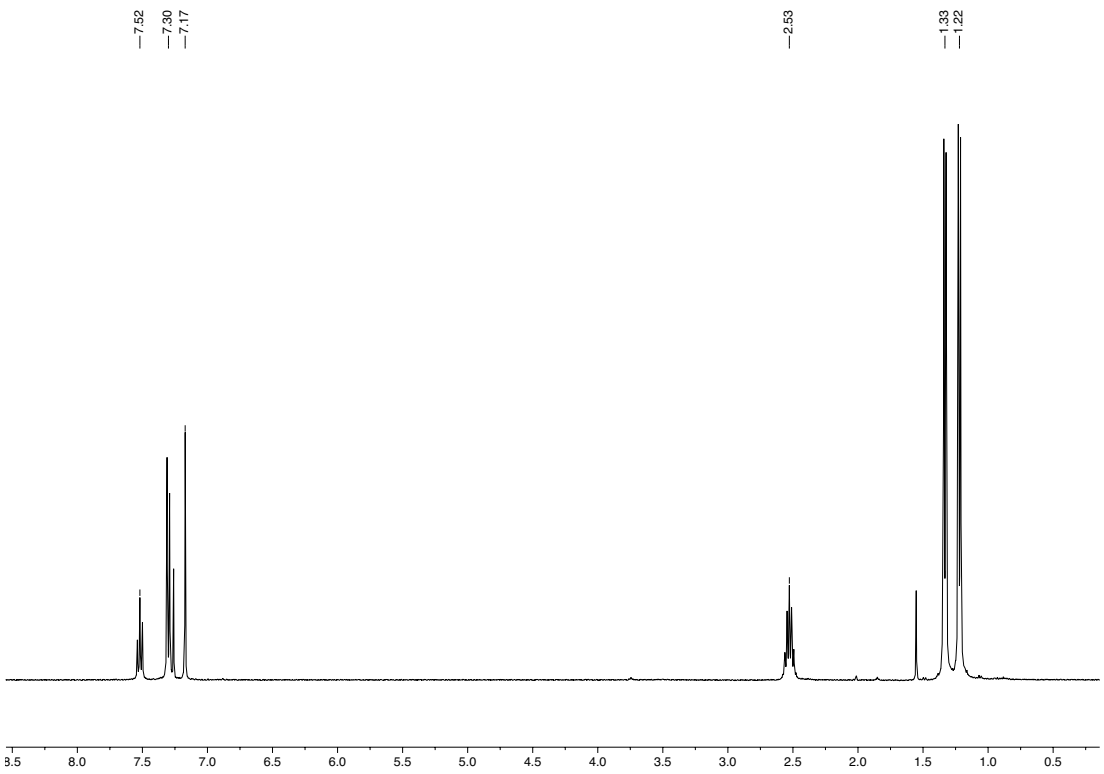

Figure 4.4. ^{1}H NMR (400 MHz, $CDCl_3$) spectrum of (IDipp)AuN_3.

4.4.3.5 (IDipp)Au(CD_3CN_4)

Method A. Portions of (IDipp)AuN_3 (10 mg, 0.016 mmol) and (IDipp)AuCN (10 mg, 0.016 mmol) were massed in a 20-mL scintillation vial and dissolved in CD_3CN (0.7 mL). The solution was quantitatively transferred to an NMR tube using additional portions of CD_3CN (0.3 mL). The NMR tube was capped and sealed with parafilm and heated to 60°C for 17.5 hours. The solution was then quantitatively transferred to a 20-mL scintillation vial and evaporated to dryness to give the white powder (20 mg, 100% NMR yield). ^{1}H NMR (500 MHz, CD_3CN): **(IDipp)Au(CD_3CN_4)** δ (ppm) 7.61 (s, 2H, NC*H*), 7.58 (t, *J* = 7.8 Hz, 2H, *para*-C*H*), 7.42 (d, *J* = 6.5 Hz, 4H, *meta*-C*H*), 2.60 (sept, *J* = 6.9 Hz, 4H, $(CH_3)_2CH$), 1.32 (d, *J* = 7.0 Hz, 12H, $(CH_3)_2CH$), 1.25 (d, *J* = 6.9 Hz, 12H, $(CH_3)_2CH$). **(IDipp)AuCN** δ (ppm) 7.59 (t, *J* = 7.8 Hz, 2H, *para*-C*H*), 7.53 (s, 2H, NC*H*), 7.41 (d, *J* = 6.5 Hz, 4H, *meta*-

C*H*), 2.51 (sept, *J* = 6.9 Hz, 4H, $(CH_3)_2CH$), 1.29 (d, *J* = 7.0 Hz, 12H, $(CH_3)_2CH$), 1.22 (d, *J* = 6.9 Hz, 12H, $(CH_3)_2CH$). ^{13}C NMR (126 MHz, CD_3CN): **(IDipp)Au(CD_3CN_4)** δ (ppm) 173.3 (NCAu), 146.99 (*ortho*-C), 134.91 (*ipso*-C), 131.83 (*para*-C), 125.5 (*meta*-C), 125.3(NCH), 29.70 ($CH(CH_3)_2$), 24.68 ($CH(CH_3)_2$), 24.08 ($CH(CH_3)_2$. **(IDipp)AuCN** δ (ppm) 186.0 (NCAu), 150.8 (CN), 146.91 (*ortho*-C), 134.73 (*ipso*-C), 131.78 (*para*-C), 125.4 (*meta*-C), 125.2 (NCH), 29.61 ($CH(CH_3)_2$), 24.74 ($CH(CH_3)_2$), 24.01 ($CH(CH_3)$. IR: ν (cm^{-1}) 2961, 2926, 2869, 2153, 2058, 1595, 1548, 1469, 1457, 1416, 1385, 1364, 1328, 1255, 1212, 1178, 1109, 1059, 976, 939, 936, 806, 760, 751, 710, 639, 549, 451. Anal. Calcd for $C_{57}H_{72}D_3Au_2N_9$: C, 53.35; H, 6.13; N, 9.82. Found C, 52.76; H, 5.73; N, 9.55.

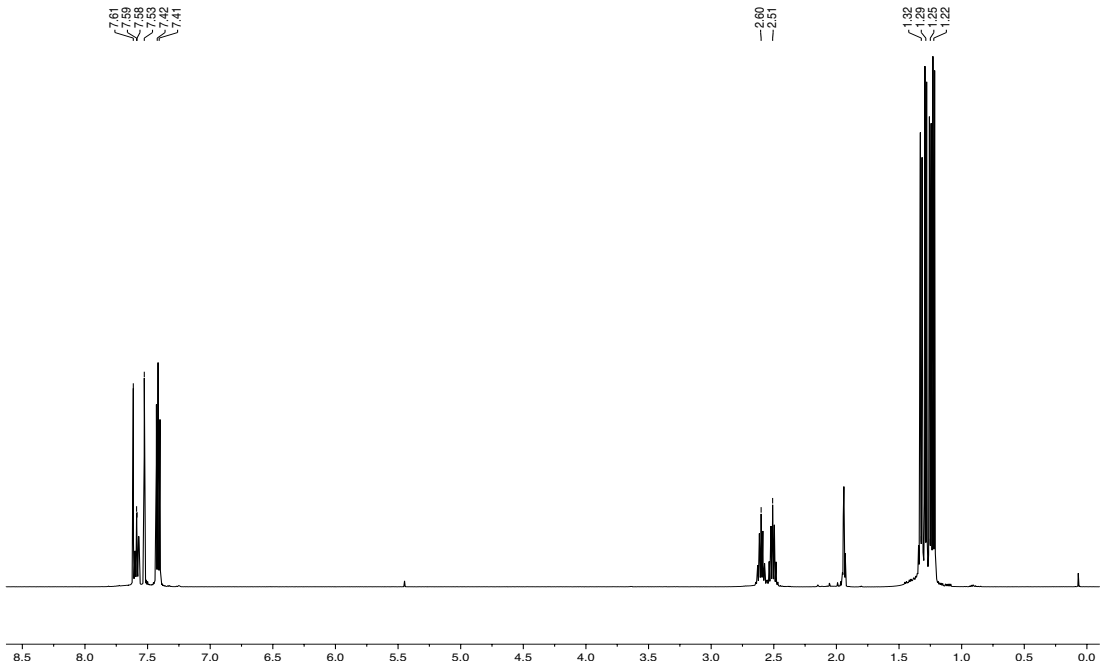

Figure 4.5. ^1H NMR (500 MHz, CD_3CN) spectrum of (IDipp)Au(CD_3CN_4) and (IDipp)AuCN.

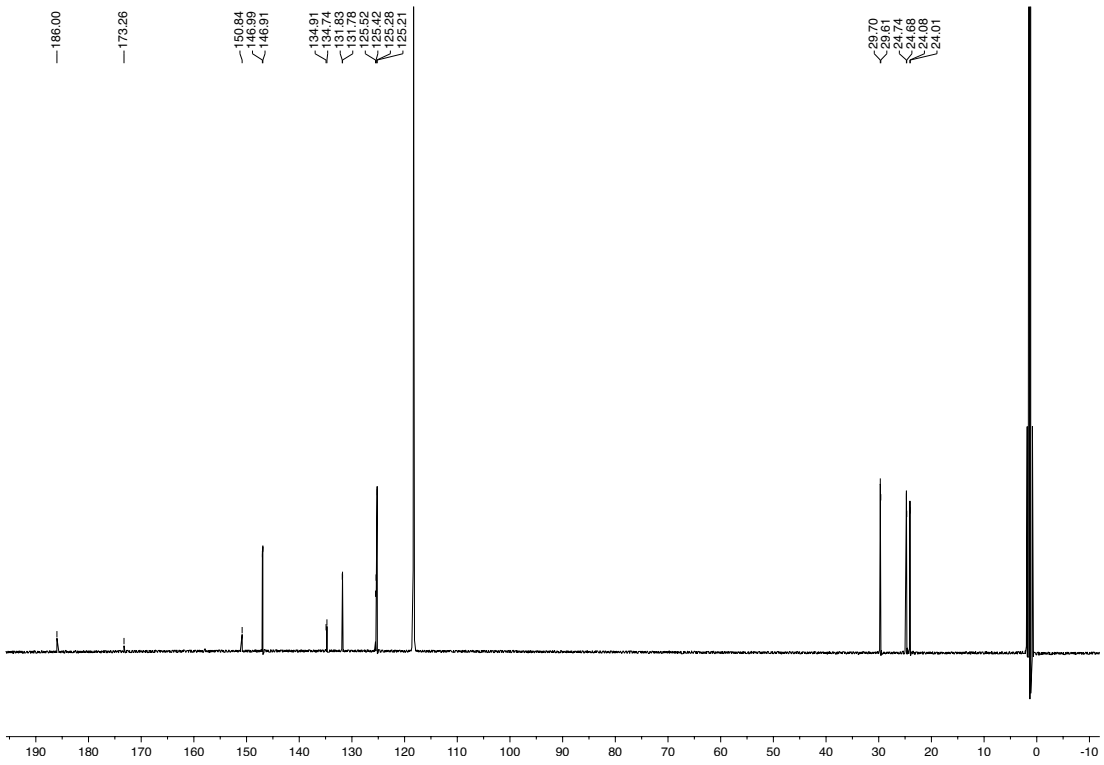

Figure 4.6. ^{13}C NMR (126 MHz, CD_3CN) spectrum of (IDipp)Au(CD_3CN_4) and (IDipp)AuCN. Methyltetrazolyl-d_3 derived resonances not observed.

Method B. A portion of (IDipp)AuN_3 (15 mg, 0.024 mmol) was dissolved in CD_3CN (1.2 mL) in a sealable NMR tube. The reaction mixture was heated to 60°C for 43 hours. The solvent was then removed *in vacuo* to afford the white solid (9 mg, 56%). ^1H NMR (500 MHz, CD_3CN): δ (ppm) 7.61 (s, 2H, NC*H*), 7.58 (t, *J* = 7.8 Hz, 2H, *para*-C*H*), 7.42 (d, *J* = 6.5 Hz, 4H, *meta*-C*H*), 2.60 (sept, *J* = 6.9 Hz, 4H, $(CH_3)_2CH$), 1.32 (d, *J* = 7.0 Hz, 12H, $(CH_3)_2CH$), 1.25 (d, *J* = 6.9 Hz, 12H, $(CH_3)_2CH$). ^{13}C NMR (126 MHz, CD_3CN): δ (ppm) 173.3 (NCAu), 147.01 (*ortho*-C), 134.92 (*ipso*-C), 131.84 (*para*-C), 125.53 (*meta*-C), 125.29 (NCH), 29.71 ($CH(CH_3)_2$), 24.68 ($CH(CH_3)_2$), 24.09 ($CH(CH_3)_2$ IR: ν (cm^{-1}) 3159, 3123, 3071, 2963, 2927, 2869, 1548, 1549, 1420, 1422, 1385, 1364, 1330, 1266, 1215, 1180, 1110, 1090, 1059, 1038, 978, 947, 805, 759, 734, 701, 640, 551, 452.

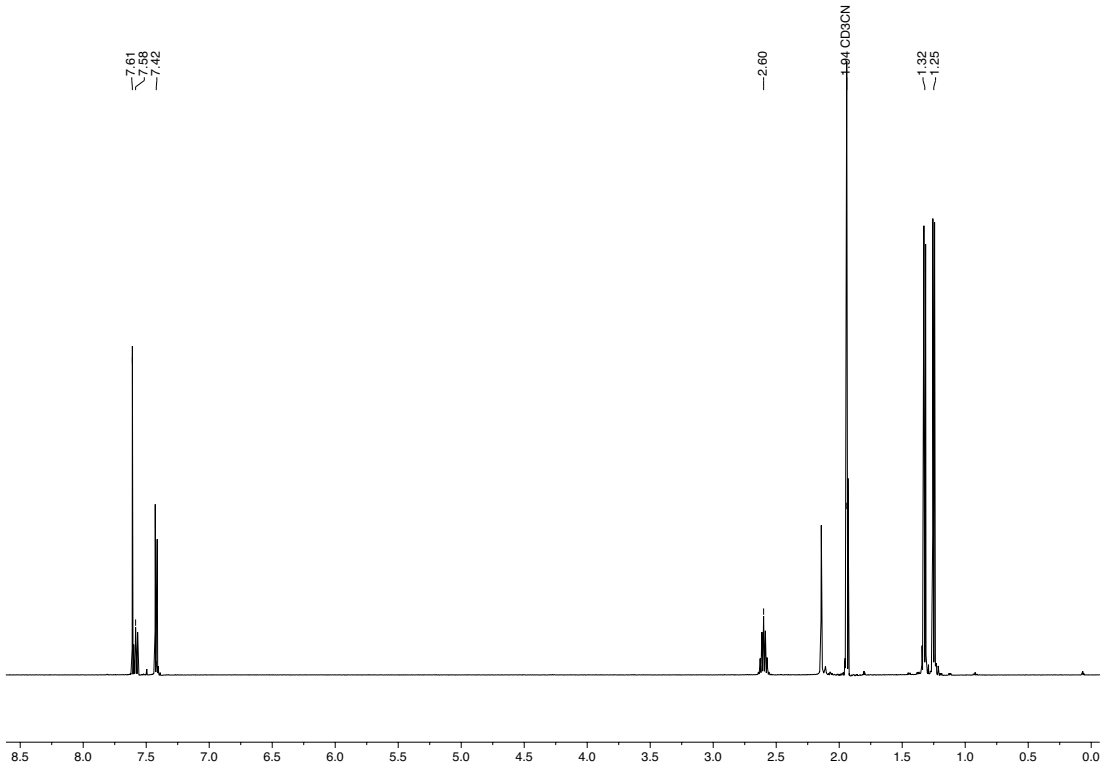

Figure 4.7. ^{1}H NMR (500 MHz, CD_3CN) spectrum of (IDipp)Au(CD_3CN_4). Impurity: H_2O (2.14 ppm).

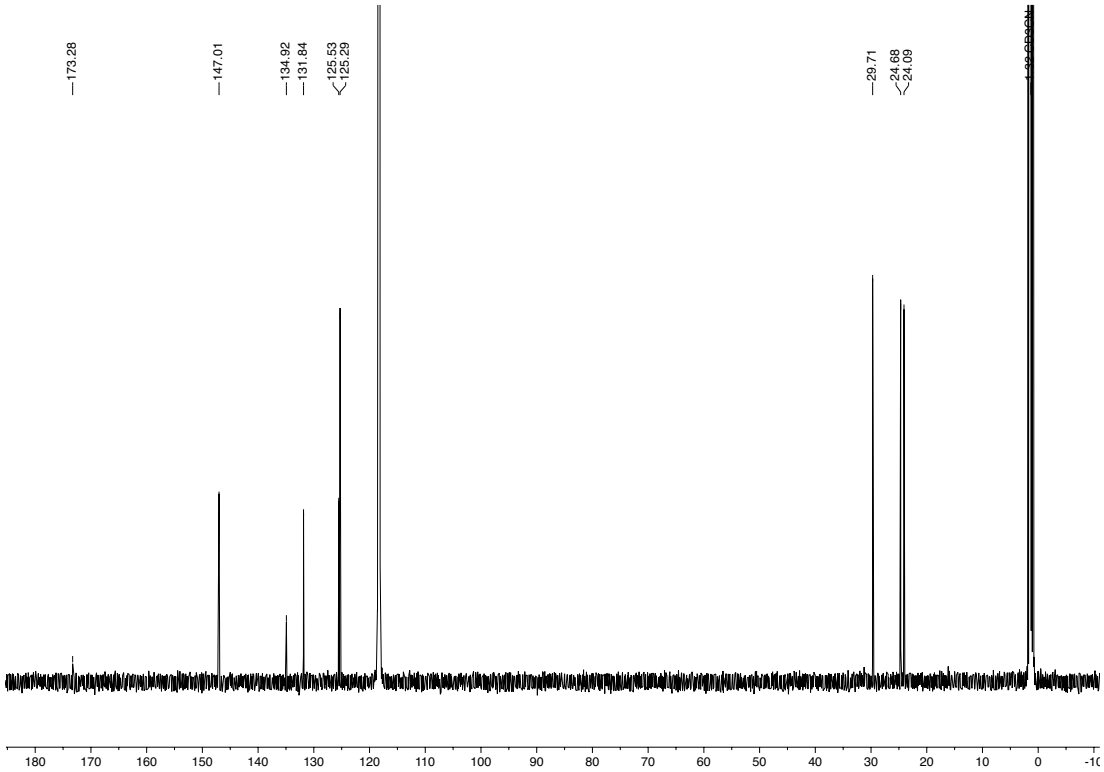

Figure 4.8. ^{13}C NMR (126 MHz, CD_3CN) spectrum of (IDipp)Au(CD_3CN_4). Methytetrazolyl-d_3 derived resonances are not observed.

4.5 Acknowledgements

We thank the U.S. National Science Foundation (CHE-1300659 to J.P.S.) and the Georgia Institute of Technology School of Chemistry and Biochemistry, and the College of Science for generous support of this research. Professor Jake D. Soper and Professor Henry S. La Pierre kindly allowed us the use of their groups' FT-IR spectrometers.

4.6 References

1. Huisgen, R.; Szeimes, G.; Moebius, L. 1.3-Dipolare Cycloadditionen, XXXII. Kinetik der Additionen Organishcer Azide an CC-Mehrfachbindungen. *Chem. Ber.* **1967**, *100*, 2494-2507.

2. Kolb, H. C.; Finn, M. G.; Sharpless, K. B. Click Chemistry: Diverse Chemical Function from a Few Good Reactions. *Angew. Chem. Int. Ed.* **2001**, *40*, 2004-2021.

3. Wang, Quian; Chan, T. R.; Hilgraf, R.; Fokin, V. V.; Sharpless, B.; Finn, M. G. Bioconjugation by Copper(I)-Catalyzed Azide-Alkyne [3+2] Cycloaddition. *J. Am. Chem. Soc.* **2003**, *125*, 3192-3193.

4. Himo, F.; Lovell, T.; Hilgraf, R.; Rostovtsev, V. V.; Noodleman, L.; Sharpless, K. B.; Fokin, V. V. Copper(I)-Catalyzed Synthesis of Azoles. DFT Study Predicts Unprecedented Reactivity and Intermediates. *J. Am. Chem. Soc.* **2005**, *127*, 210-216.

5. Worrell, B. T.; Malki, J. A.; Fokin, V. V. Direct Evidence of a Dinuclear Copper Intermediate in Cu(I)-Catalyzed Azide-Alkyne Cycloadditions. *Science*. **2013**, *340*, 457-460.

6. Partyka, D. V.; Updegraff, J. B. III; Zeller, M.; Hunter, A. D.; Gray, T. G. Carbon-Gold Bond Formation through [3+2] Cycloaddition Reaction of Gold(I) Azides and Terminal Alkynes. *Organometallics* **2007**, *26*, 183-186.

7. Robilotto, T. J.; Deligonul, N.; Updegraff, J. B. III, Gray, T. G. Azido, Triazolyl, and Alkynyl Complexes of Gold(I): Syntheses, Structures, and Ligand Effects. *Inorg. Chem.* **2013**, *52*, 9659-9668.

8. Robilotto, T. J.; Alt, D. S.; Recum, H. A.; Gray, T. G. Cytotoxic gold(I)-bearing dendrimers from alkyne precursors. *Dalton Trans.* **2011**, *40*, 8083-8085.

9. Demko, Z. P.; Sharpless, K. B. A Click Chemistry Approach to Tetrazoles by Huisgen 1,3-Dipolar Cycloaddition: Synthesis of 5-Acyltetrazoles from Azides and Acyl Cyanides. *Angew. Chem. Int. Ed.* **2002**, 41, 2113-2116.

10. Demko, Z. P.; Sharpless, K. B. An Expedient Route to the Tetrazole Analogues of α-Amino Acids. *Org. Lett.* **2002**, *4*, 2526-2527.

11. Aureggi, V.; Sedelmeier, G. 1,3-Dipolar Cycloaddition: Click Chemistry for the Synthesis of 5-Substituted Tetrazoles from Organoaluminum Azides and Nitriles. *Angew. Chem. Int. Ed.* **2007**, *46*, 8440-8444.

12. Jin, T.; Kitahara, F.; Kamijo, S.; Yamamoto, Y. Copper-catalyzed synthesis of 5-substituted 1*H*-tetrazoles via the [3+2] cycloaddition of nitriles and trimethylsilyl azide. *Tetrahedron Lett.* **2008**, *49*, 2824-2827.

13. Voitekhovich, S. V.; Gaponik, P. N.; Koldobskii, G. I. Organometallic Tetrazole Derivatives: Preparation and Application to Organic Synthesis. *Russ. J. Org. Chem.* **2005**, *41*, 1565-1582.

14. Beck, W.; Fehlhammer, W. P. Ligand Addition and Redox Reactions of Azido-Metal Complexes. *Angew. Chem. Int. Ed.* **1967**, *6*, 169-170.

15. Wehlan, M.; Thiel, R.; Fuchs, J.; Beck, W.; Fehlhammer, W. P. New *C*-tetrazolato complexes of rhodium(III), palladium(II), and gold(III). *J. Organomet. Chem.* **2000**, *613*, 159-169.

16. Gabrielli, W. F.; Nogia, S. D.; McKenzie, J. M.; Cronje, S.; Raubenheimer, H. G.; Tetrazolyl and tetrazolylidene complexes of gold: a synthetic and structural study. *New J. Chem.* **2009**, *33*, 2208-2218.

17. Kinzhalov, M. A.; Legkodukh, A. S.; Anisimova, T. B.; Novikov, A. S.; Suslonov, V. V.; Luzyanin, K. V.; Kukushkin, V. Y. Tetrazol-5-ylidene Gold(III) Complexes from Sequential [2 + 3] Cycloaddition of Azide to Metal-Bound Isocyanides and N4 Alkylation. *Organometallics* **2017**, *35*, 3974-3980.

18. Nomiya, K.; Noguchi, R.; Oda, M. Syntheses and crystal structure of coinage metal(I) complexes with tetrazole (Htetz) and triphenylphosphine ligand, and their antimicrobial activities. A helical polymer of silver(I) complex $[Ag(tetz)(PPh_3)_2]_n$ and a monomeric gold(I) complex $[Au(tetz)(PPh_3)]$. *Inorg. Chim. Acta.* **2000**, *298*, 24-32.

19. Gabrielli, W. F.; Nogai, S. D.; Nell, M.; Croje, S.; Raubenheimer, H. G. Neutral mononuclear and dinuclear complexes of gold(I) featuring azole ligands: Synthesis, structure and cytotoxicity. *Polyhedron* **2012**, *34*, 188-197.

20. Castillo, T. J. D.; Sarkar, S.; Abboud, K. A.; Veige, A. S. 1,3-Dipolar cycloaddition between metal-azide (Ph_3PAuN_3) and a metal acetylide ($Ph_3PAuC{\equiv}CPh$): an inorganic version of a click reaction. *Dalton Trans.* **2011**, *40*, 8140-8144.

21. Trifonov, R. E.; Ostrovskii, V. A. Protolytic Equilibria in Tetrazoles. *Russ. J. Org. Chem.* **2006**, *11*, 1585-1605.

22. Wang, H. M. J.; Chen, C. Y. L.; Ivan, J. B. L. Synthesis, Structure, and Spectroscopic Properties of Gold(I)-Carbene Complexes. *Organometallics* **1999**, 18, 1216-1223.

23. Collado, A.; Gomez-Suarez, A.; Martin, A. R.; Slawin, A. M. Z.; Nolan, S. P., Straightforward synthesis of [Au(NHC)X] (NHC = N-heterocyclic carbene, X = Cl, Br, I) complexes. *Chem. Commun.* **2013,** *49*, 5541-5543.

24. Johnson, M. W.; Toste, F. D.; Bergman, R. G. Preparation and reactivity of terminal gold(I) amides and phosphides. *Chem. Sci.* **2013**, *4*, 1023-1027.

25. Tsui, E. Y.; Müller, P.; Saidighi, J. P. Reactions of a Stable Monomeric Gold(I) Hydride Complex. *Angew Chem. Int. Ed.* **2008,** *47*, 8937-8940.

26. Iglesias, A.; Muñiz, K; Oxidative Interception of the Hydroamination Pathway: A Gold-Catalyzed Diamination of Alkenes. *Chem. Eur. J.* **2009**, *15*, 10563-10569.

27. Gaillard, S.; Slawin, A. M. Z.; Nolan, S. P. A *N*-heterocyclic carbene gold hydroxide complex: a golden synthon. *Chem. Commun.* **2010**, *46*, 2742-2744.

28. Partyka, D. V.; Deligonul, N. Phosphine- and Carbene-Ligated Silver Acetate: Easily-Accessed Synthons for Reactions with Silylated Nucleophiles. *Inorg. Chem.* **2009**, *48*, 9463-9475.

29. Partyka, D. V.; Robilotto, T. J.; Updegraff, J. B. III; Zeller, M.; Hungter, A.; Gray, T. G. Facile Synthesis of (Phosphine)- and (*N*-heterocyclic Carbene)Gold(I) and Silver(I) Azide Complexes. *Organometallics* **2009**, *28*, 795-801.

CHAPTER 5

CONCLUSION

This thesis describes the pursuit of an NHC-supported trigold(I) carbido cation. Three routes were explored towards the generation of such a species. These include decarbonylation of a trigold(I) ketenylidene cation (*see* Chapter 1), and two distinct approaches involving stepwise auration of (trimethylsilyl)diazomethane (*see* Chapter 3). Auration of (trimethylsilyl)diazomethane ultimately led to the pyridine adduct of the SIMes-supported trigold(I) carbido cation. Other relevant species were generated including an *N*-[diauro(trimethylsilyl)methyl]acetonitrilium cation, an *N*-[diauro(trimethylsilyl)methyl]-pyridinium cation, an *N*-(diauromethyl)pyridinium cation, and a gold(I) methoxymethyl complex.

The SIMes-supported trigold(I) ketenylidene cation was generated by reaction of the SIMes-supported gold(I) acetate with substoicheometric quantities of ketene generated by the equilibrium reaction of excess triethylamine and acetic anhydride. Formation of the triaurated species, rather than the digold(I) ketenyl complex, may be attributed in part to a moderate energetic contribution of about 20 kcal/mol resulting from closed-shell d^{10}-d^{10} attractions between gold centers.[1-5] The presence of these weak aurophilic interactions manifest as moderately close Au-Au contacts in the crystal structure of the trigold(I) ketenylidene tetrafluoroborate salt. The bond metrics of the ketenylidene moiety suggest net double bonding character for the C-C (1.318(8) Å) and C-O (1.183(7) Å) bonds, indicating that the description of this species as a triaurated acetylium ion is incorrect. This is corroborated by a weak carbonyl stretching frequency at 2013 cm^{-1}, which is lower in energy than that of ketene (2152 cm^{-1}) with a C-O double bond,[6] and much lower in energy than that of acetylium ion (2302 cm^{-1}) with a C-O triple bond.[7] This

observation is in alignment with the non-lability of the Au_3C-CO bond. Additionally, the trigold(I) ketenylidene cation exhibited no electrophilic behavior at its β-carbon, but was instead most reactive at the Au-C bonds. Reaction with nucleophiles such as sodium borohydride led to deauration rather than CH bond formation, giving (SIMes)AuH in 88% yield. Reaction with protic thiophenol also led to deauration to give (SIMes)AuSPh and the ketene transfer product, *S*-phenyl thioacetate, in greater than 95% yield.

Reaction of (trimethylsilyl)diazomethane with (IDipp)AuN(IPr)$_2$, (IDipp)AuO*t*-Pent, or (SIMes)AuO*t*-Pent led to deprotonation/auration of the substrate to give the corresponding gold(I) (trimethylsilyl)diazomethyl complexes.[8] Reaction of these complexes with electrophilic gold triflates including (IDipp)AuOTf and [(SIMes)Au(Py)]OTf in coordinating solvent (MeCN in the case of the former, pyridine in the case of the latter) gave the solvent adducts of the corresponding digold(I) (trimethylsilyl)methylidyne cations. Although the protonolyzed species {[(SIMes)Au]$_2$CH(Py)}OTf was cocrystallized with samples of {[(SIMes)Au]$_2$C(Py)SiMe$_3$}OTf prepared in this manner, it could not be intentionally generated by alcoholysis of {[(SIMes)Au]$_2$C(Py)SiMe$_3$}OTf. The {[(SIMes)Au]$_2$CH(Py)}OTf was generated independently, however, by reaction of (SIMes)AuOAc with (SIMes)AuC(N_2)SiMe$_3$. This reaction must involve an adventitious proton source, and suggests a basic intermediate is involved in generation of {[(SIMes)Au]$_2$CH(Py)}OTf. This intermediate is tentatively assigned as the diaurated pyridinium ylide {[(SIMes)Au]$_2$C(Py)}$^+$.

Reaction of (SIMes)AuC(N_2)SiMe$_3$ with the gold-nucleophile pair (SIMes)AuF was envisioned to result in desilylation/auration to give the neutral diaurated diazomethane [(SIMes)Au]$_2$C(N_2); however, the reaction proceeds instead in a 1:2 ratio, and is accompanied by dinitrogen loss to give the *N*-(triauromethyl)pyridinium cation as the bifluoride salt. This reactivity may be attributed in part to a modest energetic contribution due to closed-shell d^{10}-d^{10} attractions between gold centers.[1-5] Evidence of these

aurophilic attractions is observed as close Au-Au contacts in the solid state structure of the compound. Optimization of the reaction by including an equivalent of [(SIMes)Au(Py)]OTf resulted in generation of the cation as the more stable triflate salt. Description of this species as the pyridine adduct of an electrophilic trigold(I) carbido cation is supported by its reactivity with CO, which affords the trigold(I) ketenylidene cation.[9] Reaction of various (SIMes)AuX and $\{(SIMes)Au]_2X\}^+$ reagents, including (SIMes)AuF, (SIMes)AuF and (SIMes)AuOTf, as well as $\{(SIMes)Au]_2OAc\}^+$ with the SIMes-supported gold(I) (trimethylsilyl)diazomethyl complex at low temperature in non-coordinating solvent followed by addition of pyridine results in generation of the *N*-(triauromethyl)pyridinium cation. These experiments suggest the transient formation of a free trigold(I) carbido intermediate.

An *N,C,N′*-triauro(tetrazolylidene) cation was pursued by two separate routes. Initially, auration of 1*H*-tetrazole was carried out to give an isomeric mixture of IDipp-supported 1-aurated and 2-aurated tetrazole (IDipp)Au(CNH_4). Addition of (IDipp)AuOTf to the mixture led to the fluxional *N,N′*-diauro(tetrazolate) $\{[(IDipp)Au]_2(CHN_4\}OTf$. Attempted deprotonation of the tetrazole-derived CH led instead to deauration, regenerating the monoaurated tetrazole. Cycloaddition of (IDipp)AuN_3 and (IDipp)AuCN was attempted in various solvents with the intention of circumventing this problem, but no reaction was observed between the gold bound substrates. In CD_3CN solution at 60°C, however, (IDipp)AuN_3 underwent cycloaddition with the solvent to give (IDipp)Au(CD_3CN_4).

5.1 References

1. Pyykö, P.; Tamm, T. Theory of the d^{10}-d^{10} Closed-Shell Attraction: 4. $X(AuL)_n^{m+}$ Centered Systems. *Organometallics*. **1998**, 17, 4842.

2. Pyykö, P. Strong Closed-Shell Interactions in Inorganic Chemistry. *Chem. Rev.* **1997**, 97, 597.

3. Schmidbaur, H.; Schier, A. Aurophilic interactions as a subject of current research: an up-date. *Chem. Soc. Rev.,* **2012**, 41, 370-412.

4. Schmidbaur, H.; Schier, A. A Briefing on aurophilicity. *Chem. Soc. Rev.* **2008**, 37, 1931-1951.

5. Schmidbaur, H. The Aurophilicity Phenomenon: A Decade of Experimental Findings, Theoretical Concepts and Emerging Applications. *Gold Bull*. **2000**, 33, 3-10.

6. Duncan, J. L.; Munro, B., The ground state average structure of ketene. *J. Mol. Struct.* **1987,** *161*, 311-319.

7. Davlieva, M. G.; Lindeman, S. V.; Neretin, I. S.; Kochi, J. K., Structural effects of carbon monoxide coordination to carbon centers. π and σ bindings in aliphatic acyl versus aromatic aroyl cations. *New J. Chem.* **2004,** *28* (12), 1568-1574.

8. Tsui, E. Y.; Müller, P.; Sadighi, J. P., Reactions of a stable monomeric gold(I) hydride complex. *Angew. Chem., Int. Ed.* **2008,** *47* (46), 8937-8940.

APPENDIX A

COLLABORATOR CONTRIBUTIONS

Chapter 2: A Trigold(I) Ketenylidene Cations

John Bacsa of the Emory X-Ray Crystallography Center collected and solved X-ray diffraction data.

Chapter 3: An *N*-(triauoromethyl)pyridinium Cation and Related Species

John Bacsa of the Emory X-Ray Crystallography Center collected and solved X-ray diffraction data.

APPENDIX B

PERMISSIONS TO REPRODUCE PUBLISHED MATERIAL

Chapter 1: Introduction

Figure 1.6 is adapted from the following article with permission from the publisher and copyright holder, the Royal Society of Chemistry:

> Werlé, C.; Goddard, R.; Fürstner, A. The First Crystal Structure of a Reactive Dirhodium Carbene Complex and a Versatile Method for the Preparation of Gold Carbenes by Rhodium-to-Gold Transmetalation. *Angew. Chem. Int. Ed.* **2015**, 54, 15452-15456.

Scheme 1.7 is adapted from the following article with permission from the publisher and copyright holder, the Royal Society of Chemistry:

> Hussong, M. W.; Rominger, F.; Krämer, P.; Straub, B. F. Isolation of a Non-Heteroatom-Stabilized Gold-Carbene Complex. *Angew. Chem. Int. Ed.* **2014**, 53, 9372-9375.

Scheme 1.4 is adapted from the following article with permission from the publisher and Copyright holder, the Royal Society of Chemistry:

> Harris, R. J.; Widenhoefer, R. A. Gold carbenes, gold-stabilized carbocations, and cationic intermediates relevant to gold-catalyzed enyne cycloaddition. *Chem. Soc. Rev.* **2016**, 45, 4533.

Scheme 1.5 is adapted from the following article with permission from the publisher and Copyright holder, the Royal Society of Chemistry:

> Brooner, R. E. M.; Widenhoefer, R. A. Experimental evaluation of the electron donor ability of a gold phosphine fragment in a gold carbene complex. *Chem. Commun.* **2014**, 50, 2420.

Chapter 2: A Trigold(I) Ketenylidene Cation

This chapter is adapted from the following article with permission from the publisher and copyright holder, the American Chemical Society:

> Daugherty, N. T.; Bacsa, J.; Sadighi, J. P. A Trigold(I) Ketenylidene Cation. *Organometallics*. **2017**, 36, 3171-3174.